6-21-2021 1:30 PM

Characterization of the Ang/Tie2 Signaling Pathway in the Skeletal Muscle of DMD

Yiming Lin, *The University of Western Ontario*

Supervisor: Hoffman, Lisa M, *The University of Western Ontario*

A thesis submitted in partial fulfillment of the requirements for the Master of Science degree in Pathology and Laboratory Medicine

Abstract

In Duchenne muscular dystrophy (DMD), angiogenesis appears to be attenuated. Local administration of angiopoietin 1 (Ang1) has been shown to reduce inflammation, ischemia, and fibrosis in DMD mice. Ang1 is a vital vascular stabilizing factor that activates the endothelial cell receptor Tie2, leading to downstream pro-survival PI3K/Akt pathway activation and eNOS phosphorylation. In this study, we aim to characterize the Ang/Tie2 signaling pathway within the skeletal muscle of mouse models of DMD. Utilizing immunoblots and RT-qPCR, we show that Ang1 is downregulated, while the antagonist angiopoietin 2 (Ang2) is upregulated, leading to a decreased Ang1/Ang2 ratio. This correlates with a reduction in phosphorylated Tie2/total Tie2 ratio. Interestingly, no significant differences in Akt or eNOS phosphorylation were observed, although DMD murine models did have elevated total Akt protein concentrations. These observations suggest that Ang1/Tie2 signaling may be dysregulated in DMD and further investigations may lead to new therapeutic interventions for DMD.

Keywords

Duchenne muscular dystrophy (DMD), angiopoietin-1 (Ang1), angiopoietin-2 (Ang2), Tie2, protein kinase B (Akt), endothelial nitric oxide synthase (eNOS), vascular-targeted therapy

Summary for Lay Audience

Duchenne muscular dystrophy (DMD) is a fatal neuromuscular disease that affects 1 in every 3000 boys. The most common symptom of DMD is muscle cell death and tissue degeneration. The body will naturally attempt to repair the damages by triggering an inflammatory response to remove the cellular debris of cells that undergo apoptosis, also known as programmed cell death. Muscle stem cells, cells that can become muscle cells, will then be activated and undergo cell division to repair the damages. Additionally, nearby blood vessels will undergo angiogenesis, the process of forming new blood vessels from preexisting vessels, to supply the regenerating tissue with sufficient nutrients and oxygen that is needed for tissue repair. Unfortunately, angiogenesis appears to be impaired in DMD, leading to the formation of immature vessels that are incapable of functional perfusion (i.e. supplying the necessary nutrients and oxygen needed for repair). To treat this vascular defect, our lab has shown that the administration of angiopoietin-1 (Ang1) can stimulate the formation of new functional vessels that are capable of functional perfusion. Ang1 is a vascular stabilizing factor that binds to the Tie2 receptor on the surface of endothelial cells and triggers a cascade of signaling effects that help maintain vasculature integrity and help the maturation of angiogenic vessels. Although we have shown that Ang1 can help repair vascular defects, Ang1 signaling has not been previously characterized in DMD. In this study, we aimed to evaluate Ang1 signaling, including the expression of its antagonist angiopoietin-2 (Ang2), receptor Tie2 expression and activation, and further downstream targets protein kinase B (Akt) and endothelial nitric oxide synthase (eNOS) activation. From our results, we show that Ang1 is expressed less in DMD mouse models compared to healthy mice, while more Ang2 is being produced. This difference may shift the Ang1/Ang2 concentration ratio towards Ang2 and lead to the decrease in activated Tie2/total Tie2 ratio seen in this study. These findings suggest that Ang1 signaling is reduced in DMD and warrants further investigation that may need to development of new therapeutic options for DMD patients.

Co-Authorship Statement

Yiming Lin is the main author of this dissertation and performed the majority of the presented experimental work.

The contributions of other authors are highlighted below:

Andrew McClennan assisted with mouse care and handling and performed a portion of the genotyping.

Joanne Tang assisted with mouse euthanasia and skeletal tissue collection.

Caroline O'Neil performed the H&E and Masson's Trichrome staining.

Acknowledgments

Firstly, I would like to express my gratitude and appreciation to my supervisor, Dr. Lisa Hoffman, for your patience, support, and guidance since day one of my undergraduate honors thesis project and throughout my graduate degree. Your encouragement and mentorship have helped shape me into the budding scientist that I am today, and I will cherish your lessons on perseverance moving onto the next chapter of my career.

Secondly, I would like to thank my advisory committee, Dr. Zia Khan, Dr. Steven Kerfoot, and Dr. Krishna Singh for their advice and mentorship. Thank you, Dr. Khan, for your patience and mentorship whenever I needed advice. Thank you, Dr. Kerfoot, for your assistance and genuine interest in the multiphoton study. Thank you, Dr. Singh, for your input on the western blot analysis and for providing me with the necessary HUVEC samples.

To all past and present members of the Hoffman Lab: Patrick Murphy, Joanne Tang, Sarah Hakim, Andrew McClennan, Jonathan Wong, Yasmeen Shweiki, and Niharika Kashyap, thank you for supporting me and sharing this journey with me. Especial thanks to Andrew McClennan for his work on the breeding and handling of the mice.

I would also like to thank the following individuals for their contributions to my project. Thank you, Farzad Asadi Jomnani, for your patience and willingness to help whenever I had a question regarding any methodologies or analysis; you are truly the nicest person I have had the pleasure of meeting. Thank you, Ana Maria Pena Diaz, for tolerating all my endless questions regarding RT-qPCR analysis. Lastly, thank you, Caroline O'Neil, at Robarts Research Institute for performing our tissue embedding, sectioning, and H&E and Masson's Trichrome staining.

To all my friends and loved ones, thank you for having my back, making me laugh, and bringing joy to my life whenever we are together.

Finally, to my parents, I dedicate this work to both of you. Thank you for the love and support you have shown me and for always being there for me and believing in me. I have reached this achievement because you taught me what hard work and dedication can accomplish.

Table of Contents

List of Figures

List of Appendices

List of Abbreviations

°C	Degrees Celsius
ABIN2	TNFAIP3 interacting protein 2
ADAM12	ADAM metallopeptidase domain 12
aFGF	Acidic fibroblast growth factor
Akt	Protein kinase B
AP	Alkaline phosphatase
Ang1	Angiopoietin-1
Ang2	Angiopoietin-2
Ang3	Angiopoietin-3
Ang4	Angiopoietin-4
Ang/Tie	Angiopoietin-Tie
ANOVA	Analysis of variance
A.U.	Arbitrary Units
bFGF	Basic fibroblast growth factor
BMD	Becker's muscular dystrophy
Cav-1	Caveolin-1
CCAC	Canadian Council on Animal Care
cGMP	Cyclic guanosine monophosphate

CK	Creatine Kinase
CRISPR/Cas9	Clustered regularly interspaced short palindromic repeat/Cas9
Dll4	Notch delta ligand 4
DMD	Duchenne muscular dystrophy
Dok-R	Dok-related docking protein
DPC	Dystrophin-associated protein complex
ECM	Extracellular matrix
Egfl-7	Epidermal growth factor-like protein 7
ELISA	Enzyme-linked immunosorbent assay
eNOS	Endothelial nitric oxide synthase
EPHA7	EPH Receptor A7
ERK1/2	Extracellular signal-regulated protein kinase
ESC	Embryonic stem cells
FAK	Focal adhesion kinase
FAPs	Fibro/Adipogenic progenitors
FDA	US Food and Drug Administration
FOXO1	Forkhead transcription factor FKHR
GEF	Guanine nucleotide exchange factor
GFP	Green fluorescent protein
GSK3B	Glycogen synthase kinase 3 beta

H&E	Hematoxylin and eosin
HB-EGF	Heparin-binding epidermal-like growth factor
HGF	Hepatocyte growth factor
HIF-1α	Hypoxia-inducible factor-1
HSC	Hematopoietic stem cells
HUVECs	Human umbilical vein endothelial cells
ICAM1	Intercellular adhesion molecular 1
IGF-1	Insulin-like growth factor 1
KLF2	Kruppel-like factor 2
LECT2	Leukocyte cell-derived chemotaxin 2
LDH	Lactate dehydrogenase
LH2	Liquid nitrogen
mDia	mammalian diaphanous
mdx	Dystrophin-null
mdx/utrn$^{+/-}$	Dystrophin-null, utrophin hemi/heterozygous mouse
mdx/utrn$^{-/-}$	Dystrophin-null, utrophin-null mouse
MLPA	Multiplex ligation-dependent probe amplification
NCK2	Non-catalytic region of tyrosine kinase adapter protein 2
NF-κB	Nuclear factor kappa-light chain-enhancer of activated B cells
NG2	Neural-glia antigen 2

NO	Nitric Oxide
nNOS	Neuronal nitric oxide synthase
PAI-1	Plasminogen activator inhibitor type-1
pAkt	Phosphorylated Akt
PCR	Polymerase chain reaction
PDE-5	Phosphodiesterase-5
PDGFRα	Platelet-derived growth factor receptor alpha
PDGF-BB	Platelet-derived growth factor-BB
PDGFβ	Platelet-derived growth factor subunit B
PI3K	p85 subunit of phosphoinositide 3-kinase
PMA	Phorbol 12-myristate-13-acetate
PMO	Phosphorodiamidate morpholino oligomer
pTie2	Phosphorylated Tie2
ROS	Reactive oxygen species
RT-qPCR	Quantitative reverse transcription PCR
S1P	Sphingosine-1-phosphate
SJHC	St. Joseph's Health Care
TA	Tibialis anterior
TGFβ	Transforming growth factor beta
$Tie2^{PEKO}$	pericyte Tie2 knock out mice

TIMPs	Tissue inhibitors of metalloproteinases
TNF	Tumor necrosis factor
TNFα	Tumor necrosis factor alpha
VEGF	Vascular endothelial growth factor
WPB	Weibel-Palade bodies
WT	Wild type
VCAM1	Vascular cell adhesion protein 1
VE-cadherin	Vascular endothelial cadherin
VEPTP	Vascular endothelial protein tyrosine phosphatase
vSMC	Vascular smooth muscle cells
YAP	Hippo-YES-associated protein

1 Introduction

1.1 Duchenne Muscular Dystrophy (DMD)

Duchenne muscular dystrophy (DMD) is an X-linked recessive progressive neuromuscular disease. It affects 1 in 3000-5000 boys, making it the most severe and common form of male pediatric muscular dystrophy (Darras et al., 2014; Zellweger et al., 1975). DMD is typically diagnosed between three to five years of age (Ciafaloni et al., 2009). DMD occurs due to mutations in the dystrophin gene, leading to an absence of the dystrophin protein (Mercuri et al., 2013). Cardiac and respiratory muscles are severely affected, often resulting in cardiac failure or respiratory impairment that severely reduces life expectancy in patients (Bach et al., 2011; Passamano et al., 2012).

1.2 Diagnosis of DMD

Initial diagnosis of DMD is done through the evaluation of creatine kinase (CK) levels following the appearance of suggestive symptoms, including Gower's sign and weakness in the proximal lower limbs (Yiu et al., 2015). If CK levels are found to be elevated by 10-20 times the normal values, then genetic testing is conducted to evaluate for deletion or duplication of the dystrophin gene using multiplex ligation-dependent probe amplification (MLPA) or a comparative genomic hybridization array (del Gaudio et al., 2008; Stuppia et al., 2012). If genetic testing is inconclusive, a muscle biopsy sample must be obtained and evaluated for dystrophin expression by immunohistochemistry or western blot analysis (Belfall et al., 1988; Hoffman et al., 1988).

1.3 Pathology of DMD

DMD results from spontaneous or inherited mutations in the *DMD* gene coding for dystrophin (Abbs et al., 2010; Derek et al., 2002). *DMD* is the largest known gene in the human genome, with a length of over 2200 kb and containing 79 exons. The majority of mutations are deletions spanning from one to several exons resulting in a shift in the reading frame, with point mutations and exonic duplications accounting for the remaining types (Flanigan et al., 2009; Tuffery-Giraud et al., 2009). The result is the formation of mutated dystrophin transcripts that are subject to degradation by nonsense-mediated decay. In less

severe cases where the mutation results in the production of partially functional dystrophin, patients are diagnosed with Becker's muscular dystrophy (BMD). Patients with BMD have longer life spans and will experience milder symptoms compared to DMD patients (Bushby et al., 1993).

Dystrophin is a 427 kDa cytoplasmic protein predominantly expressed in cardiac, smooth, and skeletal muscles but its isoforms can also be found in endothelial cells, neurons of the brain, and Schwann cells. Structurally, dystrophin functions to link the myofiber cytoskeleton to the extracellular matrix via the dystrophin-associated protein complex (DPC) (Inna et al., 2000). The DPC is composed of proteins that can be categorized based on their cellular location within the DPC (Fig. 1). The cytoplasmic group consists of dystrophin, dystrobrevin, syntrophin, and neuronal nitric oxide synthase (nNOS). Here, dystrophin functions to link the intracellular actin network to the DPC while dystrobevin and syntrophin anchor nNOS to dystrophin. The transmembrane group consists of β-dystroglycan, sarcoglycan, and sarcospan. Here, the sarcoglycan subcomplex associates with β-dystroglycan which itself associates with dystrophin to form a connection to the extracellular proteins of the DPC. Lastly, the extracellular group of DPC consists solely of α-dystroglycan, which functions as a receptor for extracellular matrix ligands such as laminin, linking the DPC to the basal lamina (Campbell et al., 1992). Working in unison with several other proteins, the DPC provides a costamere scaffold for myocytes, dispelling contractile forces throughout the sarcolemma to the basal lamina during muscle contractions (Gao et al., 2015). Additionally, the DPC mediates mechanical signals between the intracellular and extracellular spaces.

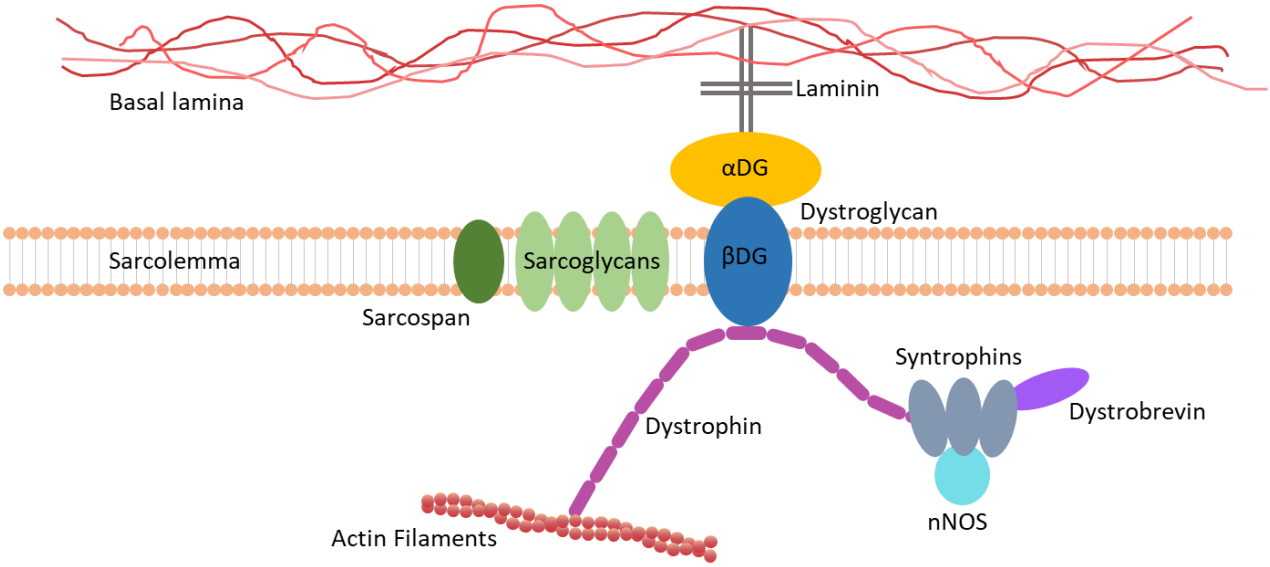

Figure 1. Dystrophin-associated protein complex (DPC)

Dystrophin links the actin cytoskeleton to the DPC which is connected to the extracellular matrix through laminin connections. This provides structural integrity to the muscle cell sarcolemma during muscle contractions. Dystrophin also recruits other proteins such as nNOS to the sarcolemma.

The absence of dystrophin results in the inability of myofibers to cope with mechanical stress. Hence during muscular contractions, the sarcolemma tears, resulting in an influx of extracellular components into the intracellular space. The influx of Ca^{2+} into the cytosolic space triggers the activation of cellular calpain proteases, ultimately resulting in plasma membrane protein cleavage and apoptosis. Necrosis ensues, leading to the expression of pro-inflammatory cytokines and producing a sustained innate immune response (Deconinck et al., 2007). Elevated levels of immunoglobulins IgA and IgG, as well as the release of CK and lactate dehydrogenase (LDH) from degenerating myofibers, have thus been used as markers of muscle damage. Tissue infiltration by inflammatory cells such as M1 (classically activated) and M2 (alternatively activated) macrophages and lymphocytes lead to cytokine secretion and subsequent effector cell activation and extracellular matrix production (Porter et al., 2002). The excess deposition of matrix proteins leads to tissue rigidity and fibrosis, which is compounded throughout the life of the patient, resulting in the replacement of functional skeletal muscle with fibrotic and adipose tissue (Mann et al., 2011; Rockey et al., 2015). As cycles of muscle degeneration and regeneration occur, the rate of regeneration diminishes over time, eventually leading to severe muscle atrophy and fibrosis within the dystrophic tissue.

1.4 Muscle Ischemia in DMD

Nitric oxide (NO) within the skeletal muscle mediates cell-cell interactions, muscle contraction, glucose metabolism, and importantly, vasodilation. The production of NO in skeletal muscles by neuronal nitric oxide synthase (nNOS) is mediated through signals exchanged between the physical interaction of nNOS and dystrophin as part of the DPC (Brenman et al., 1995; Shiao et al., 2004). In the absence of dystrophin and subsequent disruption of the DPC, nNOS dissociates from the sarcolemma to the cytosol and is downregulated (Brenman et al., 1995; Mikael et al., 2000). Functionally, through a process known as functional sympatholysis, nNOS-derived NO acts as a local paracrine signal and attenuates sympathetic vasoconstriction in response to increased metabolic loads (Tidball et al., 2014). Thus, reduced sarcolemmal nNOS-derived NO impedes the skeletal muscle's ability to regulate vasodilation and results in reduced blood flow and local functional muscle ischemia. Gail et al. found that the *mdx* mouse, a model of DMD, displayed an inability to

attenuate α-adrenergic vasoconstriction that is phenotypically similar to nNOS-deficient mice (Gail et al., 1998). Indeed, recovery of nNOS activity in a transgenic *mdx* mouse alleviates the functional muscle ischemia present in normal *mdx* mice (Wehling et al., 2001).

Endothelial nitric oxide synthase (eNOS) is another NOS isoform that is constitutively expressed in the vascular endothelium. It is activated by cytosolic increases in Ca^{+} and by phosphorylation at Ser-1177 mediated by upstream kinases (Fleming, 2010). eNOS-derived NO crucially regulates vascular tone and modulates the effects of numerous angiogenic factors. During angiogenesis, vascular endothelial growth factor (VEGF)-mediated, and eNOS-dependent NO production directly functions to increase vascular permeability and induce endothelial cell migration and proliferation (Namba et al., 2003). Although eNOS expression is found primarily in the arteries and decreases towards the microvessels, it assists in regulating microvessel circulation and helps facilitate angiopoietin-1 (Ang1) mediated capillary formation (Babaei et al., 2003). eNOS within endothelial cells forms a complex with dystrophin and caveolin-1 (Cav-1) at the caveolae. In the absence of dystrophin, eNOS is not localized to the caveolae, altering its activation (Feron et al., 2006; Ferruccio et al., 2000). Indeed, a reduction in NO production in endothelial cells isolated from *mdx* mice has been reported (Palladino et al., 2013). Attempts at increasing eNOS expression have resulted in beneficial effects in DMD (Dabiré et al., 2011).

1.5 Pre-clinical Mouse Models of DMD

Among the numerous animal models of DMD, the *mdx* mouse model is the most used and well-studied (McGreevy et al., 2015). The *mdx* mouse possesses a spontaneous nonsense point mutation in exon 23 resulting in a lack of functional dystrophin. However, despite the absence of functional dystrophin, *mdx* mice are spared of most clinical symptoms experienced by human individuals with DMD. The skeletal muscles of *mdx* mice are subject to several phases of degeneration and regeneration. In the first two weeks after birth, *mdx* skeletal muscle function and histology are indistinguishable from those of a healthy mouse. After the third week, the muscles will undergo necrosis and display histological features of myopathy such as centrally nucleated myofibers and inflammatory infiltrates. After 6 weeks, most of the degeneration in the skeletal muscles such as the hind limb muscles will plateau as levels of regeneration outpaces the level of degeneration. Up to this point, fibrosis, the

hallmark of DMD symptoms, is nearly absent from the skeletal muscles with the only exception being the diaphragm muscle (Desguerre et al., 2012; Stedman et al., 1991). However, even within the diaphragm tissue where levels of degeneration and fibrosis continuously progress, it is not significant enough to be life-threatening. Thus, *mdx* mice typically only have their lifespans reduced by up to 19% (Chamberlain et al., 2007). In DMD patients, fibrotic development and degeneration of the diaphragm is a major cause of death and patient lifespans are often reduced by as much as 75% (Passamano et al., 2012). This makes the *mdx* mice a sub-optimal model for studying the skeletal muscle degeneration associated with DMD.

Part of the difference in pathology between DMD patients and the *mdx* mouse model may be due to compensatory mechanisms, one of which is the upregulation of homologous proteins capable of compensating for the absence of dystrophin. Utrophin is a dystrophin homolog that also functions to strengthen the sarcolemma by linking the extracellular matrix (ECM) to the cytoskeleton. Normally, utrophin is predominantly expressed during embryonic development and regenerating muscles and is replaced by dystrophin upon myofiber maturation. In adults, its expression is limited to the vascular smooth muscles, nerves, endothelium, and neuromuscular junctions (Blake et al., 1996). However, within the *mdx* mouse, utrophin is upregulated in skeletal muscles independent of regeneration, and capable of compensating for the loss of dystrophin (Grady et al., 1997). Double knockout *mdx*/*utrn*$^{-/-}$ mice missing both dystrophin and utrophin exhibit severe muscle pathology like those of DMD patients and have a significantly shorter life span. The *mdx*/*utrn*$^{-/-}$ mouse displays muscular dystrophy at four weeks of age, develops profound fibrosis by eight weeks of age, and dies prematurely at approximately 20 weeks of age (Rafael et al., 1998). However, due to their severe disease pathology and reduced lifespan, they are difficult to breed and care for and are therefore unsuitable for long-term studies. Thus, the intermediate *mdx*/*utrn*$^{+/-}$ model is more manageable (Fig 2). *Mdx/utrn*$^{+/-}$ do not express dystrophin but have only one functional utrophin allele which results in a disease phenotype that is similar to that of a human DMD patient. Indeed, our lab has previously demonstrated that the *mdx/utrn*$^{+/-}$ mouse displays significant tissue degeneration and fibrosis in the diaphragm that is absent in the *mdx* mouse, but at a lower rate than the *mdx*/*utrn*$^{-/-}$ mouse (Gutpell et al., 2015). This makes the *mdx*/*utrn*$^{+/-}$ mouse model an ideal model for studying DMD disease progression.

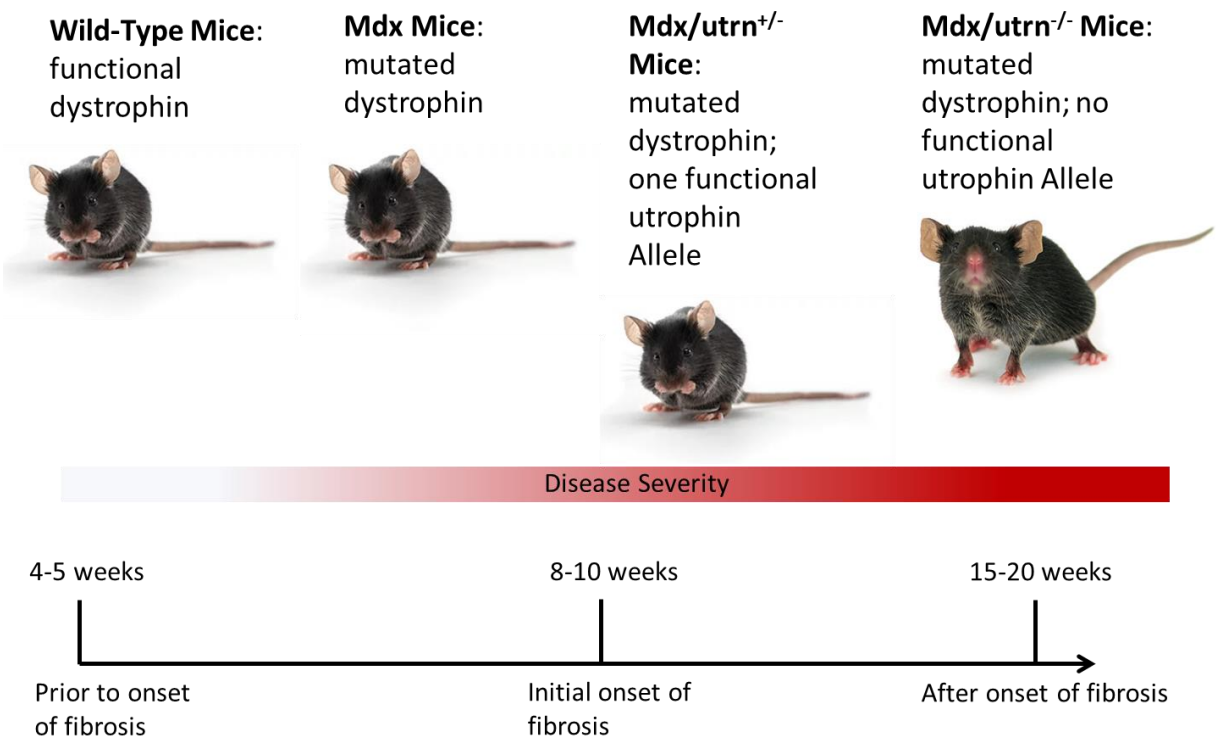

Figure 2. Mouse models of DMD

Wild-type (WT), *mdx*, *mdx/utrn*$^{+/-}$, and *mdx/utrn*$^{-/-}$ mice differ through their alterations in dystrophin and utrophin expression. Disease severity is greatest in the *mdx/utrn*$^{+/-}$, and *mdx/utrn*$^{-/-}$ mice due to their absence of both dystrophin and utrophin. Disease severity also increases in the *mdx/utrn*$^{+/-}$, and *mdx/utrn*$^{-/-}$ mice due to their progression of fibrosis which is absent in both WT and *mdx* mice.

1.6 Muscle Regeneration in DMD

Physiological skeletal muscle regeneration is a product of efficient collaboration between myogenesis and angiogenesis. Capillarization and the cross-sectional area of individual regenerating myofibers both increase during skeletal tissue regeneration as angiogenesis and myogenesis are seen to occur concomitantly (Latroche et al., 2017). Wound healing first begins after the activation of quiescent satellite cells, which are myogenic stem cells situated between the plasma membrane of the myofibers and the basal lamina (Fig. 3). After activation, myogenic satellite cells may undergo symmetrical cell division (producing two identical daughter stem cells) to replenish the stem cell pool, or asymmetrical cell division (producing a daughter stem cell and a committed progenitor daughter cell). The committed cell will subsequently differentiate into myoblasts and myocytes, capable of fusing with existing myofibers or fusing to form new myofibers to repair the damaged muscle fibers (Yin et al., 2013). Concurrently, transforming growth factor beta (TGFβ) expressed by inflammatory cells will signal effector cells such as fibroblasts and myofibroblasts to synthesize extracellular matrix proteins such as collagen I and collagen III, fibronectins, proteoglycans, and fibrinogen while inhibiting the production of ECM proteases such as collagenase and promoting protease inhibitors such as tissue inhibitors of metalloproteinases (TIMPs) and plasminogen activator inhibitor type-1 (PAI-1) to construct a temporary ECM (Delaney et al., 2017). This temporary ECM functions as a scaffold for regenerating myofibers and is crucial in guiding the formation of neuromuscular junctions. Likewise, the degradation of this ECM results in the formation of protein fragments that serve specific functions during the tissue repair process. The orchestrated formation and degradation of this temporary ECM is orchestrated by several cell types, proteases, and respective inhibitors upregulated during the initial tissue regeneration. An imbalance of these specific proteins can lead to aberrant ECM accumulation within the regenerating tissue, commonly known as fibrosis (Mann et al., 2011).

Of equal importance is the formation of new blood vessels for oxygen and metabolite delivery to sites of muscle regeneration. Development of new vascular networks are initiated upon stimulation by several angiogenic factors such as VEGF, acidic fibroblast growth factor (aFGF), basic fibroblast growth factor (bFGF), hepatocyte growth factor (HGF), hypoxia-

inducible factor-1 (HIF-1α), and angiopoietin 2 (Ang-2), released by satellite cells, inflammatory cells, and fibroblasts (Folkman et al., 1987). The angiogenic cascade then proceeds, leading to endothelial cell activation, proliferation and migration, and invasive capillary sprouting. The activated endothelial cells will differentiate into tip and stalk cells. Tip cells function to sense angiogenic factors and will invade toward the angiogenic stimulus while simultaneously expressing proteolytic enzymes to degrade the ECM to make way for new vessels. Stalk cells follow closely behind the tip cells, proliferating into organized 3D lumen structures as the new vessel elongates. As the tip cell approaches neighbouring sprouts, it will fuse with the encountered sprout in a process known as anastomosis to generate connecting vessel loops (Blanco et al., 2013). To complete the angiogenic process, endothelial cells will express platelet-derived growth factor BB (PDGF-BB) that leads to the recruitment of peri-endothelial support cells known as pericytes. Pericytes will then facilitate vessel maturation via induction of endothelial cell quiescence and endothelial tight junctions' stabilization (Stratman et al., 2010).

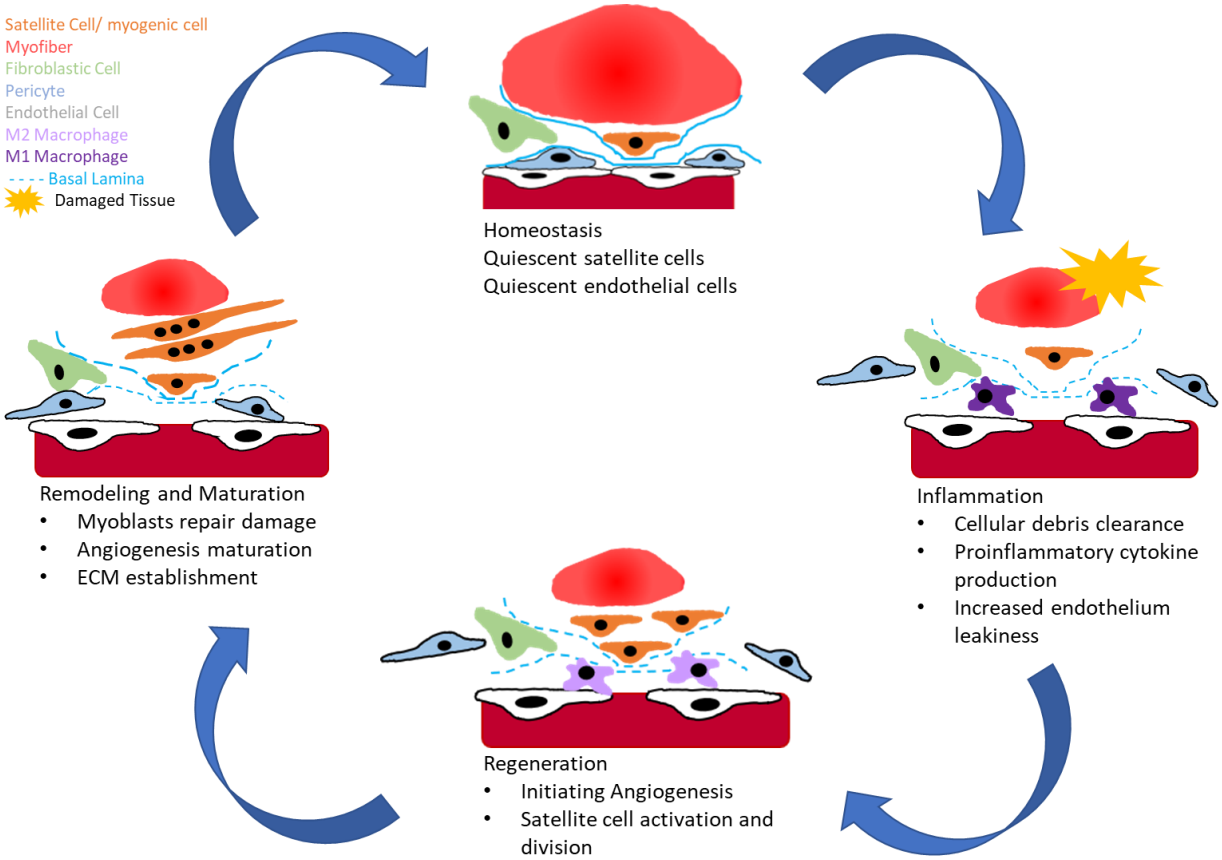

Figure 3. Physiological muscle regeneration

Tissue damage first activates an inflammatory response that leads to the emigration of inflammatory leukocytes into the damaged tissue for clearance of cellular debris. Muscle regeneration follows through the activation of satellite cells and the initiation of the angiogenic cascade. Remodeling and maturation of the regenerative phase are completed after myoblasts repair the tissue damage through the formation of new myofibers and new mature vessels.

Pericytes are a heterogenous population of mesenchymal cells that reside in the basement membrane of the microvasculature (Attwell et al., 2016). Primarily found to be associated with capillaries, their presence is also associated with higher-order vessels such as arterioles, venules, and veins, although they are notably absent from lymphatic vasculature. Distinctions between pericytes and other peri-endothelial cells such as vascular smooth muscle cells (vSMC) can be made through their anatomical location, round cell body morphology, and numerous finger-like projections that extend along the length of the vessels ending in physical contact with endothelial cells. Interestingly, lineage-tracing studies have shown that pericytes in different tissues originate from diverse sources, ranging from hematopoietic, endothelial, to macrophage origins, with evidence that pericytes from a single vessel having different developmental origins (Yamazaki et al., 2018; Yamazaki et al., 2017). Nonetheless, all pericytes, regardless of origin, play functional roles in the homeostasis of skeletal and cardiac muscles by regulating blood vessel permeability and angiogenesis. After activation of pericyte PDGFβ surface receptors via PDGF-BB released from endothelial cells, pericytes will stabilize the vessel walls through paracrine signalling via Ang1 secretion (Bergers et al., 2005; Fuxe et al., 2011). Ang1 will bind to Tie2 receptors on endothelial cells, inducing vessel quiescence and maturation (Brindle et al., 2006; Fukuhara et al., 2010; Young Koh et al., 2009). Pericyte density ranges between different tissue types. The brain has the highest pericyte to endothelial cell ratio between 1:1 and 1:3 (Armulik et al., 2010), while a ratio of 1:100 is found in the skeletal muscle vasculature (Armulik et al., 2011; Shepro et al., 1993). The difference in coverage appears to correlate with endothelial permeability properties, endothelial cell turnover, and orthostatic blood pressure. However, evidence has suggested that skeletal muscle pericyte density increases significantly in response to exercise-induced angiogenesis (Baum et al., 2015).

Besides regulating vessel stability, skeletal muscle pericytes have been also implicated as a potent tissue-resident progenitor with myogenic, fibrotic, and adipogenic potential (Fig. 4). A subpopulation of pericytes expressing alkaline phosphatase (AP) and neural-glia antigen 2 (NG2) was found to be capable of entering the satellite compartment and differentiating into myotubes following skeletal tissue injury (Dellavalle et al., 2011). Additionally, utilizing a Nestin-GFP/NG2-DsRed double transgenic mice, Birbrair et al. demonstrated that only type 2 ($Nestin^{+}/NG2^{+}$) pericytes were capable of myogenic potential and fusing with myotubes,

whereas type 1 ($Nestin^{-}/NG2^{+}$) pericytes were found to contribute to fibrosis and fat accumulation (Birbrair et al., 2013). Recent evidence has implicated another EPH Receptor A7 (EPHA7) positive subpopulation of pericyte capable of differentiating into both muscle fibers and micro vessels upon transplantation into a DMD mouse model (Yoshida et al., 2020). Further studies have shown that Noggin, expressed by newly formed muscle fibers, is capable of recruiting $NG2^{+}$ progenitors and promote their commitment to a myogenic fate (Ugarte et al., 2012). Conversely, exposure of myoblasts to Notch Delta ligand 4 (Dll4) and PDGF-BB downregulates myogenic genes, while promoting pericyte marker upregulation and migration of these myoblasts to a perivascular position (Cappellari et al., 2013). While this conversion was initially thought to only occur during embryonic development, recent work by Gerli et al. has shown this mechanism to be conserved in adult murine and human satellite cell-derived myoblasts (Gerli et al., 2019).

The relationship between satellite cells and pericytes, two central cells in myogenesis and angiogenesis, respectively, is thus crucial in maintaining muscle homeostasis and regulating muscle regeneration. As previously mentioned, satellite cells are located beneath the basement membrane of the myofibers, situating them directly adjacent to capillaries and in close proximity to pericytes. Skeletal muscle pericytes have been shown to directly promote the satellite cell niche, regulating satellite cell quiescence and myogenesis through Ang1 and insulin-like growth factor 1 (IGF-1) signalling, respectively (Kostallari et al., 2015). Pericyte ablation has been shown to result in myofiber hypotrophy and impaired satellite cell quiescence (Kostallari et al., 2015). Thus, both myogenesis and angiogenesis in DMD may be severely impaired.

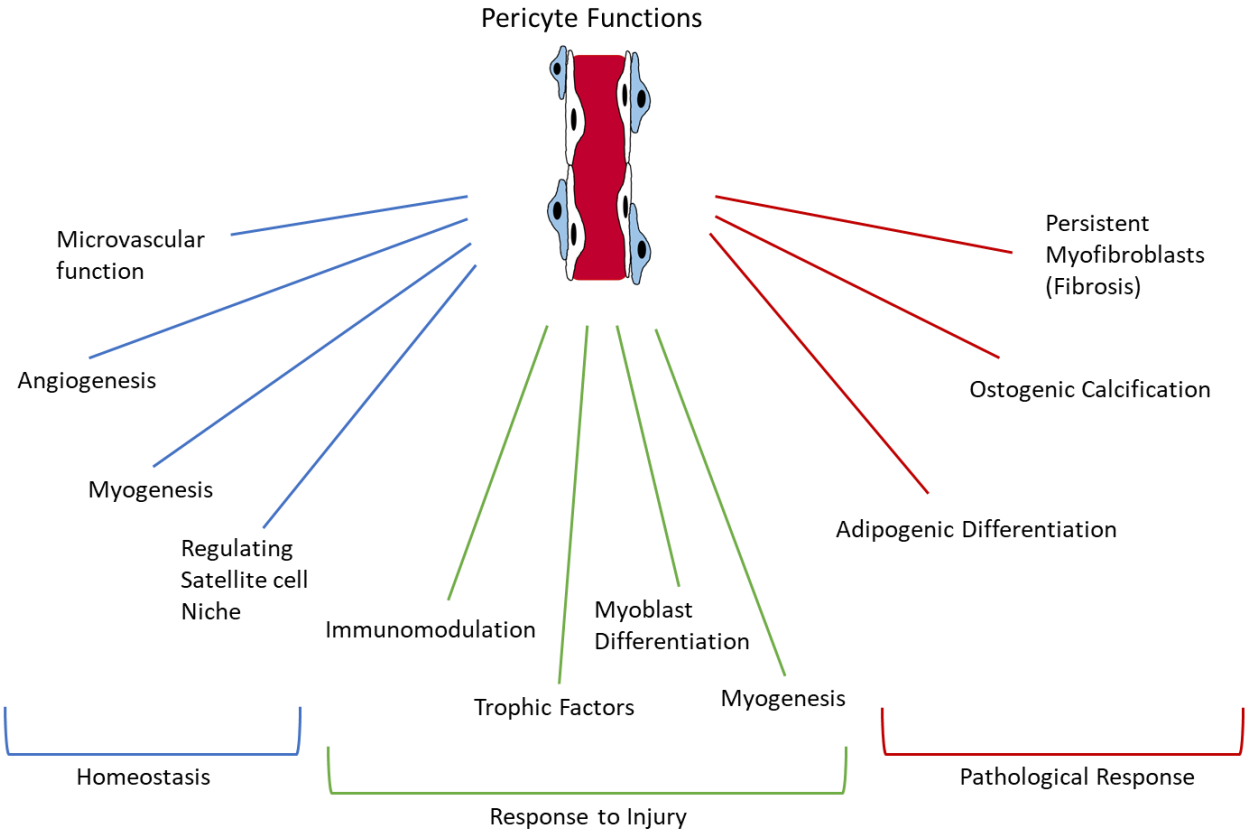

Figure 4. Pericyte functions in skeletal muscles

Pericytes are a population of mesenchymal cells capable of differentiating into several different cell types and capable of performing a multitude of functions to maintain homeostasis (blue), respond to injury (green), and amplification of pathological responses (red).

1.7 Myogenesis in DMD

Regenerative myogenesis following an acute injury stabilizes after the establishment of new myofibers and the conclusion of the inflammatory response. However, in DMD, as previously mentioned, the newly developed myofibers are susceptible to further damage, resulting in continuous cycles of muscle degeneration, chronic inflammation, regeneration, and ultimately, the depletion of the satellite cell pool over time (Fig. 5). Additionally, the absence of dystrophin within satellite cells results in a loss of cell polarity, aberrant asymmetric cell division, and altered myogenic commitment, resulting in reduced myogenic progenitor generation during tissue regeneration (Chang et al., 2016; Dumont et al., 2015). Myogenic pericytes populations, shown to contribute as much as 7% of the regenerated myofibers in diaphragm muscle tissues, had reduced myogenic capabilities within aged dystrophic mice and patients (Dellavalle et al., 2007). The decrease in pericyte and satellite cell populations is heavily associated with age, as both cell types are highly expressed within young patients but dwindle significantly in older individuals. Compounding on pathogenic myogenesis is the onset of fibrosis. The aberrant accumulation of ECM leads to a loss of tissue architecture and motile and contractile function of the skeletal muscle, while simultaneously reducing the regenerative capabilities of the tissue due to suboptimal fibrotic microenvironments characterized by profound chronic inflammation. Consequently, while fibro/adipocyte progenitor (FAPs) are a major source of myofibroblasts, ADAM metallopeptidase domain 12 (ADAM12) and platelet derived growth factor receptor alpha (PDGFRα) positive cells have been linked to muscle fibrosis (Dulauroy et al., 2012; Ieronimakis et al., 2016). Indeed, PDGFRα^+ pericytes have been shown to be fibrogenic *in vitro* when cultured with TGFβ (Chen et al., 2011). Lastly, through lineage tracing, ADAM12$^+$ and PDGFRβ^+ myofibroblast progenitors with pericyte characteristics were found to be responsible for a significant majority of differentiated myofibroblasts following cardiotoxin-induced muscle injury (Dulauroy et al., 2012). It is evident that myogenesis in DMD is dysregulated, severely hindering the endogenous regenerative capabilities of the tissue.

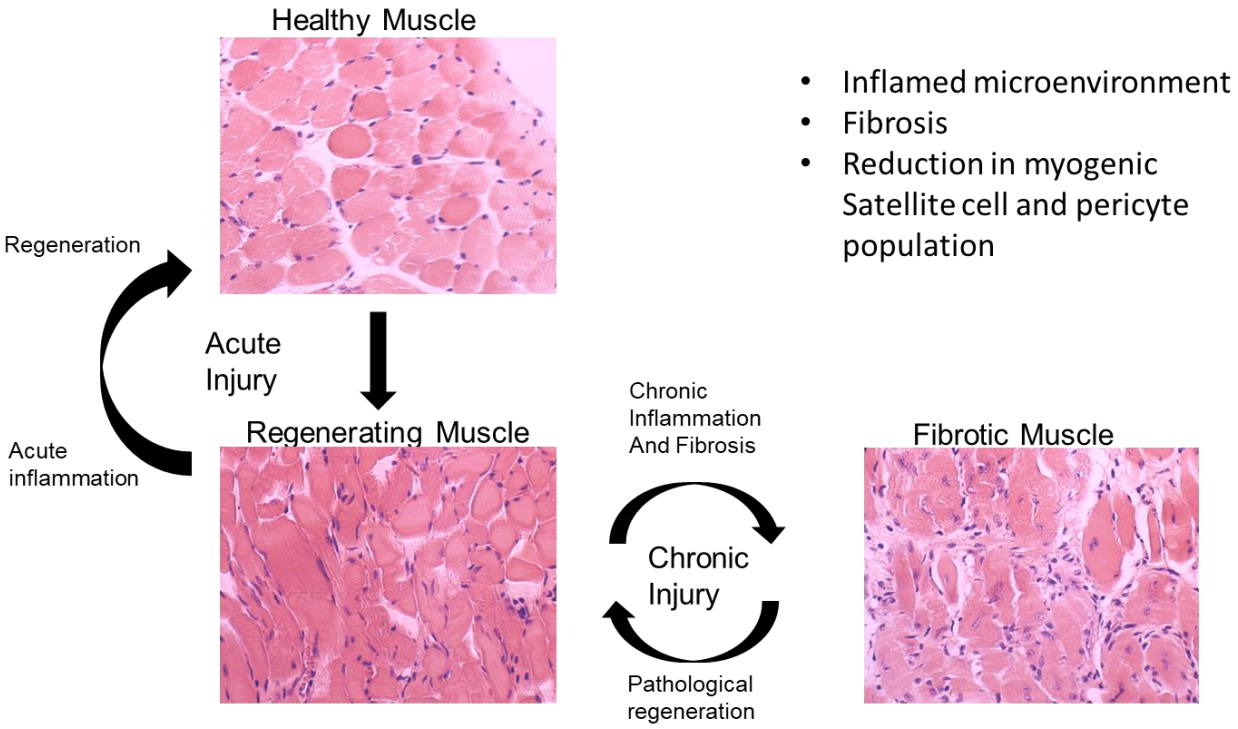

Figure 5. Pathological regeneration

Following an acute injury, an acute inflammatory response is triggered that precedes normal muscle regeneration. In DMD, chronic tissue degeneration triggers chronic inflammation in which physiological regeneration is unable to surpass the rate of degeneration resulting in pathological regeneration where inflammation and fibrosis are profound.

1.8 Angiogenesis in DMD

Dystrophin, although originally thought to be a myocyte-specific protein, is also expressed in endothelial cells (Loufrani et al., 2001). Several vascular abnormalities have been thus noted to affect DMD pathology. The absence of dystrophin impairs the endothelium's ability to perform flow-induced dilation. Evidence of grouped necrotic fibers within muscles of DMD patients was partially explained through the presence of ischemia denoted by lack of capillaries in the affected area. A decreased in vasculature density within the tibialis anterior (TA) and gracilis muscles of aged *mdx* mice compared to their wild-type counterparts has been observed (Palladino et al., 2013). Morphologically, capillary and endothelial cell areas were demonstrated to be much greater in muscle biopsies of DMD patients relative to control subjects (Miike et al., 1987). Like myogenesis, few angiogenic abnormalities are associated with early disease progression. For example, Straino et al. presented evidence for a normal angiogenic response within hindlimb muscles of *mdx* mice while Palladino et al. reported impaired angiogenic responses within *mdx* mice with a reduction in endothelial cell migration, proliferation, and tube formation (Palladino et al., 2013; Straino et al., 2004). Though initially thought to be contradicting evidence, the difference could be explained by the age of the animal models used within each respective study. Palladino et al. used mature 6-month-old *mdx* mice, while Straino et al. used young 2-month-old *mdx* mice that may still retain their potent regenerative capabilities. Utilizing a Flk-$1^{GFP/+}$ *mdx* mouse model, Latroche et al. demonstrate a significant decrease in muscle perfusion in 12-month-old dystrophic mice compared to their 3-month-old counterparts (Latroche et al., 2015).

Sprouting angiogenesis occurs in specific coordinated steps. Firstly, in response to a hypoxia environment, parenchymal cells will begin secreting the pro-angiogenic factor VEGF, forming an extracellular cytokine gradient that will act to guide migrating angiogenic cells (Gerhardt et al., 2003). The resulting VEGF signaling cascade leads to the degradation of the local basement membrane and the detachment of pericytes. Endothelial cells exposed to the highest levels of VEGF will then differentiate into endothelial tip cells, while its neighbouring endothelial cells differentiate into endothelial stalk cells. The tip cells form lamellipodia and filopodia that function to navigate and migrate the developing sprout towards the angiogenic stimulus gradient (De Smet et al., 2009). Following closely behind

the tip cells, stalk cells will begin to proliferate, elongate, and organize into pre-mature luminal structures. Upon contact with other capillaries or sprouts, the developing sprout will undergo anastomosis. Vascular remodeling that modulates vessel diameter and directional flow is then mediated by the expression of Ang1. Lastly, vascular maturation is achieved through Ang1-mediated pericyte recruitment and stabilization of the endothelial adheren junctions.

Both VEGF and HIF-1α are two prominent angiogenic factors expressed by satellite cells during muscle regeneration. Satellite cells isolated from aged, 12-month-old *mdx* mice demonstrated reduced expression of both VEGF and HIF-1α, leading to reduced angiogenic capabilities *in vitro* (Rhoads et al., 2013). Importantly, our lab has shown a significant reduction in VEGF and Ang1 concentration in fibrotic diaphragm tissue of *mdx/utrn*$^{+/-}$ mice, possibly resulting in deficiencies in both angiogenesis initiation and angiogenesis maturation (Gutpell et al., 2017). Thus, it is possible that with the absence of dystrophin in endothelial cells resulting in an impaired angiogenic response in combination with a lack of angiogenic factors, the vascular network in DMD is severely compromised and unable to support endogenous muscle repair.

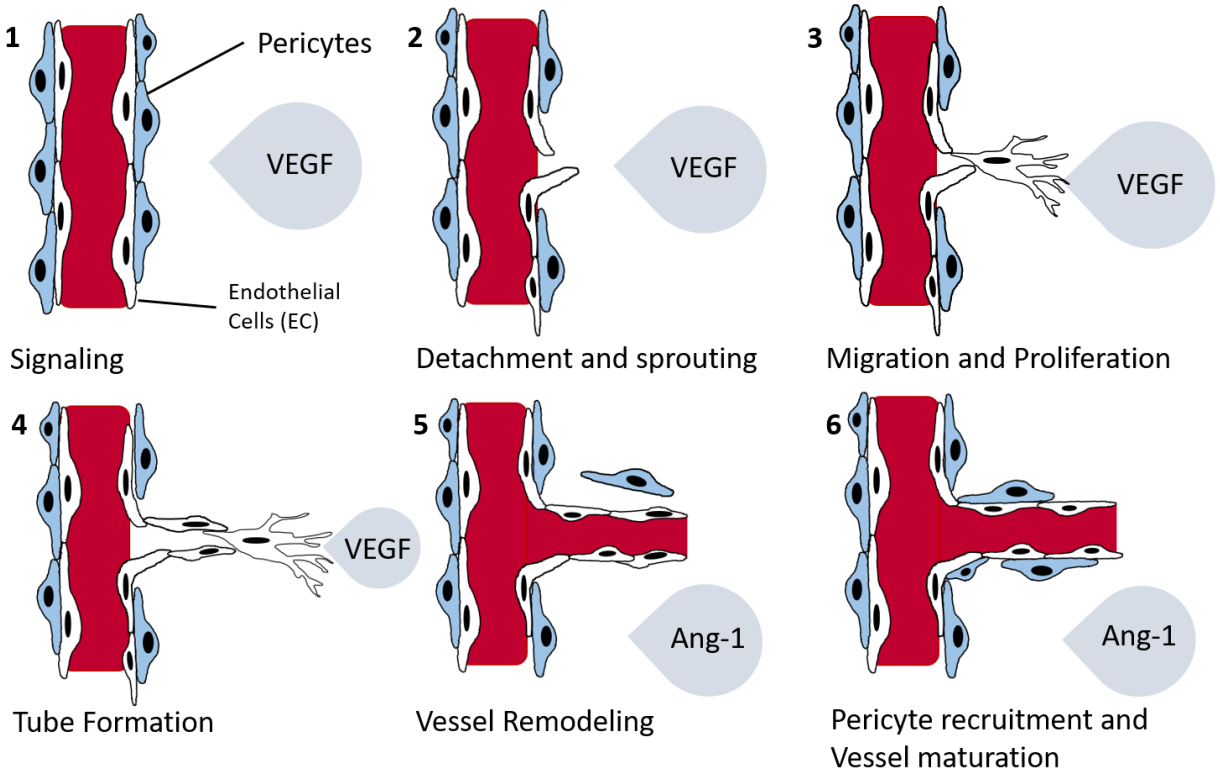

Figure 6. Sprouting Angiogenesis

Sprouting angiogenesis occurs in distinct steps. 1) Angiogenesis will begin upon the secretion of pro-angiogenic signals such as VEGF. 2) Endothelial cells will respond to the pro-angiogenic signals, resulting in detachment of pericytes and breakdown of the basement membrane. 3) Endothelial cells closest to the angiogenic signal will differentiate into tip cells that will migrate towards the signal. Neighbouring endothelial cells will differentiate into stalk cells that proliferate behind the tip cells. 4) The proliferating stalk cells will organize into pre-mature tubes. 5) The newly formed vessel will undergo remodeling upon signaling by Ang1. 6) Vessel maturation occurs through Ang1-mediated pericyte recruitment and stabilization of the adhesion junctions.

1.9 Current Therapies

Current treatments available for DMD only target the specific symptoms that DMD patients endure. Corticosteroid treatments are often started around the age of five, functioning to slow the rate of tissue degeneration and increase muscle strength (Darras et al., 2014; Passamano et al., 2012). Other complications such as respiratory infections and cardiac dysfunctions are treated with the use of antibiotics and angiotensin-converting enzyme inhibitors, respectively (Bach et al., 2011). While there are currently no commercially available cures, the restoration of dystrophin expression and subsequent DPC repair is seen as the definitive curative treatment for DMD. Recent advancements in gene therapy variants, exon skipping, and stem cell therapy to restore dystrophin production have been promising.

The use of recombinant adeno-associated viral vectors in the delivery of dystrophin gene fragments has resulted in the expression of functional dystrophin in animal models as well as in human patients. However, due to the large size of the dystrophin gene, these viral vectors are unable to carry the entire dystrophin gene. Instead, they carry a modified micro-dystrophin gene that lacks some dystrophin gene functions and results in reduced transduction efficiency (Duan, 2018; Kupatt et al., 2021). Two examples are the investigational gene therapy PF-06939926 developed by Pfizer (ClinicalTrials.gov Identifier: NCT04281485) and SRP-9001 developed by Sarepta (ClinicalTrials.gov Identifier: NCT03769116). PF-06939926 is currently undergoing Phase 1b trials in the United States and has recently entered Phase 3 trials at sites in Italy, Israel, and Spain with plans to expand to other countries, while SRP-9001 is expected to enter Phase 3 trials in the near future. Exon splicing has also been employed as a method of inducing functional dystrophin expression for individuals with mutations at specific vulnerable exons (Kupatt et al., 2021). Sarepta's Eteplirsen, a phosphorodiamidate morpholino oligomer (PMO), is the first exon-skipping drug approved by the US Food and Drug Administration (FDA) for the treatment of DMD for patients with specific exon 51 mutations. Another gene-editing strategy known as clustered regularly interspaced short palindromic repeat/Cas9 (CRISPR/Cas9) has shown to be effective in inducing dystrophin expression and improving muscle contractility in animal models of DMD. CRISPR-mediated exon skipping combines the two methods to utilize the

Cas9 protein and guide RNAs to target splicing regulatory sites, creating INDEL mutations and single-base changes that induce exon skipping (Zhang et al., 2020).

Stem cell therapy, in which mesenchymal or embryonic stem cells (ESC), derived either from donors or reprogrammed cells from the patient themselves, are implanted into patients to generate healthy dystrophin-expressing muscle fibers that fuse with the patient's dystrophic muscle fibers, has been met with complications. Goudenege et al. demonstrated that when MyoD expressing human ESC grown in myogenic culture mediums were transplanted into immunodeficient *mdx* mouse, they indeed participated in muscle regeneration and formed dystrophin expressing myofibers. However, their efficacy dropped significantly when transplanted into inflamed muscle fibers (Goudenege et al., 2012).

A significant obstacle that stem cell therapy and other regenerative treatments face is the inflamed and fibrotic microenvironment in which these therapies are introduced into. This microenvironment is not favourable for tissue regeneration, and thus, any myogenic approach designed to re-introduce dystrophin is unable to fulfill its purpose. In the case of stem cells, inflammation and fibrosis devastate a patient's stem cell niche, the microenvironment necessary for the stem cell's proliferation and differentiation (Lane et al., 2014). This reduces the engraftment, survival, proliferation, and function of the transplanted cells. Additionally, a decrease in oxygen and nutrient delivery to the tissues caused by the previously mentioned vascular defects cripples the tissue's endogenous repair process (Mikael et al., 2000). With reduced blood perfusion, the delivery of viral vectors and stem cells alike is severely hindered. Immunosuppressive agents such as tumor necrosis factor (TNF) inhibitors and nuclear factor kappa-light chain-enhancer of activated B cells (NF-κB) inhibitors administered in combination with the gene therapy are being tested (Miyatake et al., 2016). However, without addressing both muscle ischemia and the hostile microenvironment simultaneously, it is unlikely that these dystrophin restorative therapies will be completely effective. Thus, the addition of a vascular therapy to treat muscle ischemia and enhance endogenous muscle regeneration has been proposed (Ennen et al., 2013; Palladino et al., 2013; Podkalicka et al., 2019; Shimizu-Motohashi et al., 2014). Evidence has shown that increasing vasodilation and blood flow via phosphodiesterase-5 (PDE-5) inhibitors reduce myofiber damage in *mdx* mice and rescues functional muscle ischemia in patients (Batra et

al., 2019; Nelson et al., 2014). Lastly, induced VEGF overexpression results in significant increases in endogenous muscle regeneration evident by an increase in the number of myogenin-positive satellite cells and the number of regenerating myofibers (Messina et al., 2007). However, while VEGF treatment appears promising, the sole usage of VEGF in correcting the vascular defects of DMD has been challenged. One area of concern is the dosage of VEGF given to a patient considering evidence that long-term exposure to high VEGF dosages can lead to the formation of hemangiomas and vascular tumours (Carmeliet, 2000; Lee et al., 2000; Springer et al., 1998). Furthermore, our lab has shown that intramuscular administration of VEGF into the gastrocnemius muscle of *mdx/utrn*$^{+/-}$ mouse does not improve blood perfusion nor does it decrease collagen deposition (Gutpell et al., 2017). Interestingly, our lab has shown that administration of VEGF in combination with Ang1 improves blood flow and reduces fibrosis. Subsequent sole administration of Ang1 into gastrocnemius muscles of *mdx/utrn*$^{+/-}$ mice increased vascular density, vessel maturation, and decreased collagen deposition (Gutpell et al., 2017). Thus, is it vital to characterize the endogenous expression and activation of the Ang/Tie2 signalling pathway due to its role in vascular homeostasis and angiogenesis.

1.10 Angiopoietin-Tie Signalling Pathway

1.10.1 Overview

The angiopoietin-Tie (Ang/Tie) signalling pathway is a crucial pathway involved in modulating angiogenesis, blood and lymphatic vessel development, and vascular quiescence, permeability, and stability (Brindle et al., 2006; Fukuhara et al., 2010; Young Koh et al., 2009). Dysregulation of the Ang/Tie signalling pathway can lead to poor outcomes. In the cardiovascular system, vascular impairment, ischemia/reperfusion injury, development of atherosclerotic plaques, and peripheral arterial disease have all been linked to dysfunctional Ang/Tie signalling (Fujisawa et al., 2017; Yeboah et al., 2017). In diabetic macular edema, abnormal Ang/Tie signalling leads to vascular leakage and disrupted retinal and choroidal neovascularization (Whitehead et al., 2019). Ang/Tie2 signalling has also been heavily implicated in tumour angiogenesis and inflammation (U. Fiedler et al., 2006; Kobayashi et al., 2005; Metheny-Barlow et al., 2003).

The acronym Tie stands for tyrosine kinase with immunoglobulin and EGF homology domains. Originally identified as the second endothelial cell-specific receptor tyrosine kinase signalling system following the VEGF-VEGFR system, the Tie receptors, Tie1 and Tie2, are expressed on both blood and lymphatic endothelial cells (Fukuhara et al., 2010; Wong et al., 1997). Tie2 appears to be constitutively expressed on endothelial cells. Tie1 expression appears to be more heavily regulated and is found to be downregulated in the adult quiescent vasculature but upregulated in response to hypoxia, embryonic and adult angiogenesis, and malignant melanoma progression (McCarthy et al., 1998). Both have been found to be expressed on circulating hematopoietic cells including megakaryocytes, monocyte, satellite cells, hematopoietic stem cells in the bone marrow, and pericytes. Structurally, Tie1 and Tie2 share a 76% identity in their intracellular tyrosine kinase domains (Schnurch et al., 1993). Their extracellular domains are only 33% identical, leading to their different ligand associations. Tie1 binds to leukocyte cell-derived chemotaxin 2 (LECT2), primarily functioning to modulate Tie2 activation (Xu et al., 2019). Previous evidence has shown that Tie1/Tie2 heterodimer formation is necessary for Tie2 phosphorylation and downstream target activation. However, contradicting studies have shown that Tie1/Tie2 heterodimer disassociation and Tie2/Tie2 homodimer formation upon Ang1 ligand binding leads to Tie2 phosphorylation and vascular stability (Seegar et al., 2010). Recent computational modeling studies have shown that Tie2 activation is indeed sensitive to Tie1 expression, with higher Tie2 activation associated with lower Tie1 expression (Zhang et al., 2019). Interestingly, Tie1 functions to sustain Tie2 activation in remodeling stalk cells while negatively regulating Tie2 expression on tip cells during angiogenesis (Savant et al., 2015). Tie2 activation by either Ang1 or angiopoietin-2 (Ang2) leads to the release of ligands and Tie2 receptor phosphorylation, internalization, and subsequent degradation (Bogdanovic et al., 2006). Due to endocytosis of the Tie2 ligand which results in an overall decrease in available surface receptors, it has been hypothesized that Tie1's context-dependent modulation of Tie2 activation is enabled through its formation of Tie1/Tie2 heterodimers that prevents rapid Tie2 internalization and allows for sufficient Tie2 to perpetuate its downstream signalling. Thus, Tie1 indirectly mediates Ang1/Tie2's vascular stability and EC anti-apoptotic phenotype.

The angiopoietin family of proteins consists of Ang1, Ang2, angiopoietin-3 (Ang3), and angiopoietin-4 (Ang4) (Fagiani et al., 2013). Ang1 and Ang2 are the main ligands for Tie2

while Ang3 and Ang4 are respective mice and human orthologues. Ang1 is the primary Tie2 agonist. Ang1-Tie2 binding leads to the disassociation of the Tie1/Tie2 heterodimer and formation of Tie2 homodimers and downstream signal transduction (Seegar et al., 2010). Natively found in dimers, trimers, tetramers, and higher order multimers, only tetrameric or higher multimeric forms of Ang1 appear capable of activating Tie2 (Kyung-Tae et al., 2005). Ang1 is found to be constitutively expressed by pericytes, vSMCs, fibroblasts, osteoblasts, and tumour cells (Fagiani et al., 2013). Ang1 upregulation is associated with angiogenesis, while its downregulation is associated with TNF-α and IL-1B expression. After expression, Ang1 associates with the ECM through its linker peptide region. Ang1 deletion results in premature embryonic lethality with severe heart defects and an immature vasculature network lacking proper pericyte attachment and complexity (Jeansson et al., 2011). Conversely, transgenic expression of Ang1 leads to capillary diameter enlargement, increased endothelial cell proliferation, and increased pericyte coverage (Cho et al., 2005).

Ang2 primarily functions as the competitive antagonist to Ang1 and acts to inhibit Tie2 signalling. However, in experimental settings, Ang2 has been shown to be a weak Tie2 agonist in conditions where Tie1 is present and Ang1 is absent (Yuan et al., 2009). Unlike Ang1, Ang2 exists solely as lower-order multimers, such as dimers, trimers, and tetramers. Ang2 is primarily expressed by endothelial cells and is transcriptionally induced in response to hypoxia, high glucose concentration, shear stress, TNFα, and VEGF. Within quiescent endothelial cells, Ang2 is transcriptionally repressed by the transcription factor Kruppel-like factor 2 (KLF2) (Nayak et al., 2011). Endogenous and overexpressed Ang2 are stored within specialized endothelial storage granules called Weibel-Palade bodies (WPB). Stored Ang2 has a half-life of over 18 hours and can be rapidly released in seconds to minutes upon stimulation via WPB secretagogues such as phorbol 12-myristate-13-acetate (PMA), thrombin, and histamine (Fiedler et al., 2004). However, while Ang2 concentrations within WPB are detectable in quiescent vasculature, expression appears to vary dramatically depending on the tissue of origin. Prominent Ang2 expression and storage were found in the brain and within the female reproductive system while hardly detectable in skeletal and cardiac muscles (Akwii et al., 2019; Mofarrahi et al., 2011). Ang2-null mice develop chylous ascites shortly after birth and demonstrate an inability to fully initiate an inflammatory

response. Transgenic overexpression of Ang2 results in embryonic lethality mirroring Ang1-null and Tie2-null mice (Peter et al., 1997).

Ang3 and Ang4 are respectively mouse and human orthologues. Contextually, recombinant Ang3 has been shown to induce Tie2 phosphorylation in murine endothelial cells. However, when overexpressed, Ang3 may act as a Tie2 antagonist through inhibition of Ang1-Tie2 activation (Lee et al., 2004). Ang3 does not appear to induce Tie2 phosphorylation in human cells, however, Ang4 has been shown to be a potent Tie2 agonist in vitro with human umbilical vein endothelial cells (HUVECs). Both Ang3 and Ang4 induced angiogenesis *in vivo* in mouse corneal micropocket assays (Lee et al., 2004). Conversely, Ang3 and Ang4 have differing tissue expression distributions in their respective species. Significant Ang3 expression can be found in the heart, kidney, and testis tissue of mice while Ang4 expression is primarily isolated to human lung tissue. Both Ang3 and Ang4 expression are shown to be induced in response to hypoxia. However, no specific molecular mechanisms of expression for neither proteins have been well described. Neither protein is significantly expressed in skeletal muscle tissues.

Ang/Tie2 signalling can be modulated by several different endothelial and myocyte integrins to differing effects (Avraamides et al., 2008). Integrin α5β1 interacts with Tie2 in a fibronectin-dependent manner to facilitate increases in Ang1 mediated phosphorylation of Tie2, p85 subunit of phosphoinositide 3-kinase (PI3K)/protein kinase B (Akt) signalling, and support Tie2 localization and complex formation at the endothelial cell-endothelial cell junction (Ilaria et al., 2005; Pang et al., 2018). Conversely, α5β1 can also directly interact with Ang2 released by tip cells to mediate endothelial monolayer destabilization during angiogenesis (Felcht et al., 2012). In skeletal and cardiac myocytes, integrin-Ang1 interactions elicit activation of pro-survival pathways including the PI3K/Akt pathway and inhibited caspase-3 activation. Consequently, the opposing effects of Ang1 and Ang2 signalling also extend to integrin interactions. In diabetic retinopathy, retinal astrocyte αvβ5-Ang1 interactions facilitated the initiation of angiogenesis, inhibition of vascular leakage, and reduced neuronal dysfunction (Lee et al., 2013). In contrast, astrocyte αvβ1-Ang2 interactions induced astrocyte apoptosis (Yun et al., 2016). Similarly, α3β1-Ang2 interactions in diabetic retinopathy have been linked to pericyte apoptosis (Park et al., 2014).

Thus, Ang1 and Ang2 interaction whether it be with integrins or Tie2 helps facilitate the angiogenic response as well as maintain vascular homeostasis.

1.10.2 Ang/Tie Signalling in Endothelium Homeostasis

Tie2 will undergo specific subcellular localization upon angiopoietin activation. This localization helps differentiate the signalling outcomes between the quiescent and angiogenic endothelium (Kodama et al., 2008; Wong et al., 1997). In motile angiogenic endothelium, matrix-bound Ang1 binds to Tie2 and localizes it to cell-extracellular matrix contacts, and proceeds with cell migration and proliferation processes. In quiescent endothelium, Ang1/Tie2 signalling translocate Tie2 on confluent endothelial cells into clusters at the endothelial cell-endothelial cell junctions and induces pro-survival, endothelial tight junction stabilization, and anti-inflammatory signals. This is primarily achieved through downstream recruitment and activation of PI3K and subsequent Akt phosphorylation.

Akt signalling promotes endothelial cell survival though upregulation of pro-survival molecules including phosphorylated eNOS and survivin expression, while simultaneously suppressing apoptotic pathways such as caspase-9 and BAD (Shiojima et al., 2002; Somanath et al., 2006). Ang1-mediated Akt signalling additionally leads to phosphorylation and inhibition of the forkhead transcription factor FKHR (FOXO1) (Daly et al., 2004). FOXO1 activation has been heavily implicated in inducing endothelial cell apoptosis. Additionally, FOXO1 is a prominent Ang2 transcription factor, thus, Tie2 phosphorylation directly inhibits Ang2 expression and maintains Ang1/Tie2 signalling through a negative-feedback loop. Another important transcription factor is KLF2. It is a shear stress-regulated transcription factor that upregulates Tie2 expression while down-regulating Ang2 expression, thus promoting a resting endothelium phenotype (Nayak et al., 2011).

Ang1/Tie2 signalling also promotes endothelial cell tight junction stability and limits vessel permeability. Ang1 mediated activation of RhoGTPase Rac1 triggers the formation of lamellipodia protrusions that colocalize with vascular endothelial cadherin (VE-cadherin; also known as cadherin 5 (*cdh5*)) and stabilizes the endothelial cell-cell contact by promoting the reorganization of the actin cytoskeleton into a cortical arrangement (David et al., 2011). However, Rac1 is also capable of promoting the disassociation of the cell-cell contact

depending upon which guanine nucleotide exchange factor (GEF) forms the complex with Rac1. Similarly, the RhoGTPase RhoA, which normally signals the reorganization of the actin cytoskeleton into a stress-fiber arrangement that promotes endothelial contractions, exerts a different effect upon Ang1/Tie2 signalling. Ang1 mediated RhoA-GEF Syx complex formation activates mammalian diaphanous (mDia) leading to its sequestration of the non-receptor tyrosine kinase Src (Gavard et al., 2008; Ngok et al., 2012). This prevents Src mediated VE-cadherin phosphorylation-dependent redistribution and internalization, thus maintaining inter-endothelial cell stability. Indeed, *in vitro* administration of recombinant Ang1 was able to inhibit vascular leakage induced by inflammatory cytokines and growth factors such as VEGF, thrombin, and histamine (Gavard et al., 2008). VE-cadherin stability also directly regulates Hippo-YES-associated protein (YAP) phosphorylation and subsequent inhibition, another prominent Ang2 transcription factor critical to regulating vessel remodeling (Choi et al., 2015). Pharmacological inhibition of vascular endothelial protein tyrosine phosphatase (VEPTP), a prominent phosphatase inhibitor of Tie2, improved endothelial barrier function, even in mice lacking *cdh5* expression, through stabilization of the cortical actin cytoskeleton via RAP1 activation and decreased myosin light chain 2 phosphorylation (Frye et al., 2015). Lastly, Tie2 phosphorylation also leads to the recruitment of TNFAIP3 interacting protein 2 (ABIN2), which interferes with the NF-κB pathway and inhibits the expression of leukocyte adhesion molecules VAM1 and ICAM1 to promote an anti-inflammatory effect (Hughes et al., 2003; Tadros et al., 2003). Therefore, Ang1 bestows a protective effect on the endothelium, promoting vascular homeostasis and quiescence.

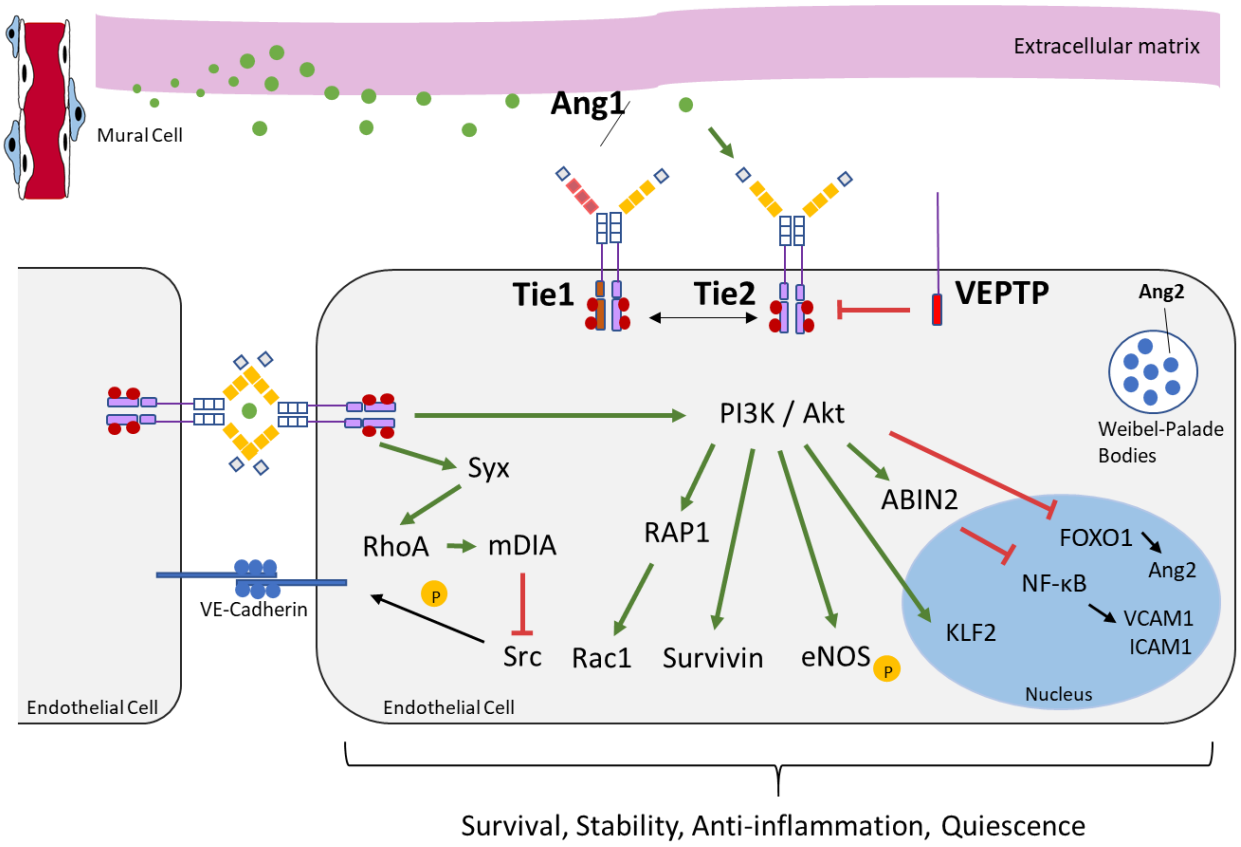

Figure 7. Ang/Tie2 signalling in quiescent endothelium

Angiopoietin 1 (Ang1) mediated localization of Tie2 at inter-endothelial cell junctions leads to Tie2 phosphorylation and activation of the p85 subunit of the phosphoinositide 3-kinase (PI3K) which in turn phosphorylates protein kinase B (Akt). Phosphorylated Akt contributes to enhancing cell-cell stability through activation of the RhoGTPase Rac1 via RAP1, resulting in reorganization of the actin cytoskeleton into a cortical arrangement. RhoGTPase RhoA also enhances inter-endothelial cell connections through activation of mammalian diaphanous (mDIA) which sequesters the non-receptor tyr kinase Src and preventing Src-mediated VE-cadherin phosphorylation and subsequent internalization and degradation. Akt signalling also confers endothelial cell pro-survival and anti-apoptotic effects through expression of suvivin and endothelial nitric oxide synthase (eNOS) phosphorylation. The anti-inflammatory effects of Ang1/Tie2 signalling are mediated through Akt directed inhibition of the FOXO1 transcription factor and A20-binding inhibitor of NF-κB (ABIN2) directed inhibition of NF-kB that inhibits expression of Angiopoietin 2 (Ang2), vascular cell adhesion protein 1 (VCAM1), and intercellular adhesion molecular 1 (ICAM1), respectively. Krupple-like factor 2 (KLF2) transcription factor upregulates Ang1 expression, ensuring endothelial cell quiescence. Adapted from Young Koh et al., 2009.

1.10.3 Ang/Tie2 in activated Endothelium and inflammation

Destabilization of the Ang1/Tie2 interaction and endothelium is necessary during various physiological and pathological conditions including angiogenesis, vascular remodeling, and when mounting an inflammatory response. In homeostatic endothelium, the Ang1/Ang2 ratio is heavily favored towards Ang1 due to it being constitutively expressed, while Ang2 is downregulated, allowing Ang1/Tie2 signalling to mediate vascular quiescence. However, upon endothelial activation, the secreted Ang2 shifts the Ang1/Ang2 ratio towards Ang2 (Wang et al., 2017). In the current model, endothelial cells will respond to stimuli within their microenvironment, secrete Ang2 from the WPB, which will sensitive the endothelial cells to inflammatory stimuli and initiate an inflammatory response (Fiedler et al., 2006; Scholz et al., 2011). Ang2 can act as a weak Tie2 agonist and has even been shown to enact a protective effect upon endothelial cells (Daly et al., 2006). However, Ang2 only appears to be a Tie2 agonist in the presence of Tie1 (Kim et al., 2016; Korhonen et al., 2016). In activated endothelium and during inflammation, surface Tie1 is cleaved, shifting Ang2 activity into a strictly Tie2 inhibitory role and inhibiting Ang1/Tie2 signalling (Mueller et al., 2016). The reduced Ang1/Tie2 signalling reduces RhoA activity, PI3K and Akt phosphorylation, and increases vessel permeability through Src mediated VE-cadherin phosphorylation and endocytosis and the detachment of pericytes from the basement membrane. The reduction in Akt signalling and internalization of VE-cadherin further perpetuates Ang2 signalling through FOXO1 and YAP mediated Ang2 transcription. Ang2 can also directly interact with β1-integrin to facilitate Tie2 independent destabilization of the endothelium through formations of actin stress fibers (Hakanpaa et al., 2015). Elevated Ang2 concentrations have also been shown to induce endothelial cell detachment from the endothelial monolayer and incite endothelial cell apoptosis (Scharpfenecker et al., 2005). These cumulative changes perpetuated through Ang2 primes the endothelium to respond to cytokine-mediated angiogenic and inflammatory signalling and allow for the infiltration of angiogenic myeloid cells, leukocytes, inflammatory cytokines, respectively.

In angiogenesis, the Ang/Tie2 system contributes to its initiation, migration, and proliferation of endothelial cells, the differentiation between tip and stalk cells, and maturation of the newly formed vessels. Ang2 does not directly promote angiogenesis other than in a specific

subpopulation of Tie2-negative endothelial cells, however, as previously mentioned, it prepares the endothelium for the subsequent angiogenic cascade in response to angiogenic factors such as VEGF and environmental cues like hypoxia. VEGF-stimulated sprouting angiogenesis is directly associated with lower Tie2 surface presentations, thus inhibiting vascular stabilization and promoting angiogenesis and vascular remodeling (Findley et al., 2007). Importantly, Ang2 upregulation in the absence of an external stimulus such as VEGF results in endothelial apoptosis and vessel regression (Holash et al., 1999; Ivan et al., 2002). This can be seen in the regressing ovarian corpus luteum during luteolysis (Fraser et al., 2003). Interestingly, evidence has shown that Ang2 appears to regulate VEGF expression at the transcriptional level through inhibition of HIF-1α expression and HIF-DNA-binding activity in Tie2 expressing cells, displaying a level of intrinsic coordination during angiogenesis (Lee et al., 2008). Following initiation, endothelial cells will begin to proliferate and migrate. Although Ang1 mediates endothelium quiescence and stability, it also contributes to endothelial cell migration. Activation of the PI3K pathway in non-resting endothelial cells leads to integrin-mediated signal transduction of focal adhesion kinase (FAK) and cell migration (Zhao et al., 2011). Additionally, Dok-related docking protein (Dok-R) can associate with Tie2 following Ang1 activation, recruit the Nck2 adapter protein, and control Ang1-mediated endothelial cell migration (Jones et al., 2003). Sprouting angiogenesis then proceeds through the differentiation of tip and stalk cells. Tip cells are characterized by low Tie2 expression and high Ang2 expression, while stalk cells are characterized through Tie2 expression (Savant et al., 2015). Transgenic inactivation of Ang2 reduces both the number of tip cells as well as resulting in fewer filopodia per tip cell. The low Tie2 expression on tip cells is not only transcriptionally mediated, but on the surface, upregulated Tie1 inhibits Tie2 surface presentation. However, in stalk cells, Tie1 functions to promote Tie2 activation. The difference in Tie2 expression and activation between tip cells and stalk cells can be similarly seen in the difference in Notch signalling. Specifically, Dll4 expressed by tip cells will activate Notch1 on stalk cells to induce a stabilization phenotype on the stalk cells and preserve differentiation between the two cell types. Consequently, Jag1 expressed by stalk cells antagonize Dll4/Notch signalling. Thus, the balance between Dll4 and Jag1, levels of Notch signalling, and Tie1-Tie2 interactions determine tip and stalk cell

specificity prevents peri-endothelial cell recruitment and maturation at the angiogenic sprout (Savant et al., 2015).

In stalk cells undergoing angiogenesis, Ang/Tie2 signalling mediated through paracrine Ang1 signalling from pericytes inhibits glycogen synthase kinase 3 beta (GSK3B) through PI3K/Akt activation. This in turn activates Wnt/B-catenin signalling which upregulates D114/Notch signalling, resulting in deposition of collagen IV to establish the basement layer of the developing endothelium and ultimately the maturation and quiescence of the newly developed vasculature (Zhang et al., 2011). Vessel lumen formation and subsequent pericyte recruitment are necessary for the maturation of the angiogenic process. Epidermal growth factor-like protein 7 (Egfl-7) is expressed in proliferating tissues and promotes vessel lumen formation. Conversely, TGFβ inhibits VEGF-mediated vessel lumen formation and prevents pericyte recruitment. Ang2 promotes the inhibitory actions of TGFβ while Ang1 signalling can overcome the suppressive effects of TGFβ and promote PI3K mediated tube formation in the presence of VEGF (Ramsauer et al., 2007; Saito et al., 2003). Lastly, Ang1 signalling promotes vessel maturation through mural cell recruitment. Endothelial heparin-binding epidermal-like growth factor (HB-EGF), hepatocyte growth factor (HGF), and PDGF-B have all been implicated as Ang-induced vSMC and pericyte recruitment factors (Aguilera et al., 2014; Iivanainen et al., 2003; Kobayashi et al., 2006). Furthermore, pericyte Ang1/Tie2 autocrine signaling assist in mediating endothelial cell-pericyte interactions, and Tie2 deletion in pericytes lead to dysregulated angiogenesis (Teichert et al., 2017). Lastly, both Ang1 and Ang2 bind to Tie2 with the same affinity. Thus, the delicate balance between Ang1/Ang2 ratios greatly contributes to determining whether new angiogenic sprouts remain sprouts or become mature vessels.

As previously mentioned, Ang2 is critical during inflammation as Ang2-deficient mice are incapable of eliciting an effective inflammatory response (Ulrike. Fiedler et al., 2006). This is in part due to Ang2-deficient mice’s inability to express endothelial cell adhesion molecules following TNFα signalling, resulting in impaired endothelial-leukocyte interactions. This prevents leukocyte infiltration into the damaged tissue. In chronic inflammation, blood capillaries are remodeled into venules to support vessel leakage and leukocyte infiltration. Ang2 appears to play a large role in this angiogenic process. In a

mouse model of chronic airway inflammation, Ang2 inhibition resulted in reduced remodeling of mucosal capillaries into venules, a reduction in leukocyte emigration, and decreased disease severity (Tabruyn et al., 2010). Indeed, numerous diseases and cancers characterized by endothelium activation, increased vascular leakage, and aberrant blood flow has shown elevated Ang2 concentrations and reduced Ang1 concentration and Tie2 phosphorylation (Fang et al., 2015; Hu et al., 2009; Ong et al., 2010; Yang et al., 2017). Several anti-Ang2 monoclonal antibodies have been developed for use in anti-angiogenic therapies in the treatment of solid tumors (Brown et al., 2010). Reduced Ang2 concentrations have been associated with a better disease prognosis. In models of sepsis, Ang2 heterozygous mice had reduced vascular leakage and inflammation, and milder kidney and lung injuries (David et al., 2012). In diabetic retinopathy, Ang2 concentrations have been shown to be elevated and appeared to mediate pericyte loss and endothelial cell apoptosis (Cai et al., 2008; Whitehead et al., 2019). In both disease models, administration of COMP-Ang1, an engineered variant of Ang-1, reduced injury and delayed fibrotic onset. Thus, is it necessary to evaluate the Ang1/Ang2 ratio in a DMD mouse model and determine the degree of Tie2 activation so that the inflammatory and ischemic microenvironment may be characterized and addressed.

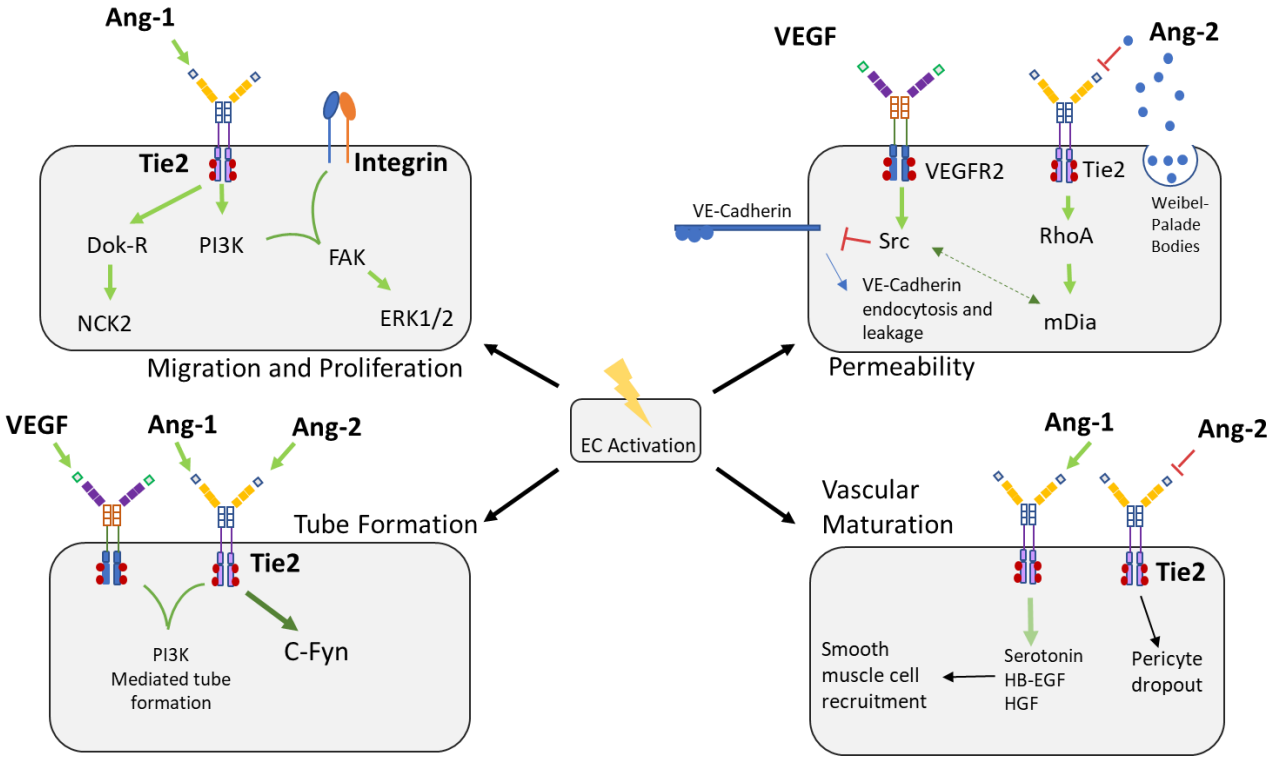

Figure 8. Ang/Tie2 signalling in activated endothelium

Ang1/Tie2 signalling enhances endothelial cell migration and proliferation through phosphoinositide 3-kinase (PI3K) and integrin-mediated activation of the focal adhesion kinase (FAK) which in turn activates the extracellular signal-regulated protein kinase (ERK1/2). Tie2 mediated recruitment of Dok-related docking protein (Dok-R) and non-catalytic region of tyrosine kinase adapter protein 2 (NCK2) also contributes to endothelial cell migration. Vascular permeability increases through decreased mDIa mediated Src sequestration caused by decreased Ang1/Tie2 signalling, allowing Src to phosphorylate VE-cadherin and mediate their internalization. Vascular tube formation via Ang1 signalling requires VEGF signalling and downstream PI3K signalling. Ang2 can also induce tube formation through activation of C-Fyn. Ang1/Tie2 signalling facilitates vascular maturation following the conclusion of angiogenesis through up-regulation of serotonin, heparin-binding EGF-like growth factor (HB-EGF), and hepatocyte growth factor (HGF), all known to contribute to smooth muscle cell recruitment. Conversely, elevated Ang2 concentration results in pericyte dropout. Adapted from Young Koh et al., 2009.

Ang 1 signalling is also prominent in other cell types (Fig 8). Within the bone marrow, osteoblasts derived Ang1 induces the adhesion of hematopoietic stem cells (HSCs) to osteoblasts and helps to maintain a quiescent and anti-apoptotic phenotype within the HSCs (Arai et al., 2004). Similarly, paracrine and autocrine Ang1/Tie2 signalling in satellite cells promotes their quiescence and self-renewal through the ERK1/2 pathway resulting in decreased differentiation and proliferation, entry into G_0, and increased activation of anti-apoptotic signalling pathways (Abou-Khalil et al., 2009). Ang1 treatment also increased ESE-1, NERF-2, and ELF-1 transcription factor expression in quiescent satellite cells, all three of which promote either Ang1 or Tie2 expression, thus, inducing a positive Ang/Tie2 expression feedback loop (Abou-Khalil et al., 2009). Importantly, despite the absence of Tie2 receptors, Ang1 has been found to be capable of binding to myoblasts through N-cadherin and initiate the expression of myogenin to promote myoblast differentiation and muscle regeneration (Youn et al., 2018). Lastly, pericytes express functional Tie2 that mediate downstream signalling of pro-survival and migration pathways through Akt activation and FOXO3 inhibition (Teichert et al., 2017). However, Tie2 expressing pericyte also appear to regulate angiogenesis initiation. Sprouting assays of co-culture spheroids of HUVEC and Tie2-silenced pericytes performed by Teichert et al. showed significant decreases in endothelial cell sprouting compared to HUVEC cultured with wild-type pericytes (Teichert et al., 2017). In another experiment, Teichert et al. compared the perfusion and permeability of tumour vessels in pericyte Tie2 knockout ($Tie2^{PEKO}$) mice compared to wild type and found that $Tie2^{PEKO}$ vessels were significantly leakier compared to wild type, revealing the vessel maturation impact of pericyte Tie2. Taken together, this provides strong evidence that Ang/Tie2 signalling in pericytes is an important regulator of angiogenesis. Lastly, our lab has shown that Ang1/Tie2 signalling, independent of other contributing but not crucial factors, is capable of inducing vessel maturation and stabilization and may hold therapeutic potential in several diseases that displays immature vascular phenotypes (Gutpell et al., 2017). Ultimately, without addressing the potential vascular and microenvironment defects, future curative treatments will not be able to reach their full therapeutic potential.

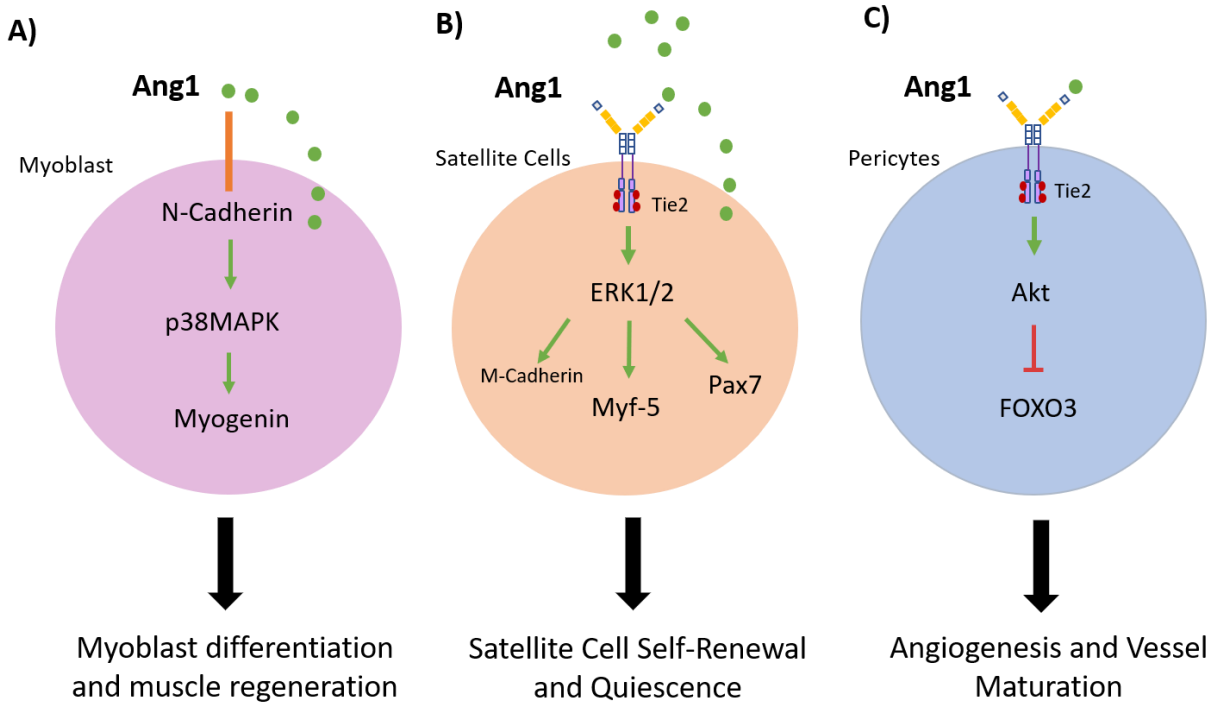

Figure 9. Ang1 signalling in myoblast, satellite cells, and pericytes

A) Ang1 interacts with N-cadherin on the surface of myoblasts to induce myogenin expression via p38MAPK that supports myoblast differentiation and muscle regeneration. **B**) Ang1/Tie2 signalling on satellite cells activate the extracellular signal-regulated protein kinase (ERK1/2) pathway to induce expression of quiescent satellite cell markers Pax7, Myf-5, and M-cadherin. **C**) Ang1/Tie2 signalling in pericytes can directly affect the initiation as well as the maturation phases of angiogenesis.

2 Hypothesis and Objectives

2.1 Rationale

Our lab has now shown that localized administration of Ang1 is sufficient in inducing increased muscle perfusion, reducing inflammation, and reducing the deposition of fibrotic tissue in hind limb muscle of *mdx/utrophin*$^{+/-}$ mice. Ang1 is a critical vascular stabilizing factor that is involved in both maintaining vessel quiescence and angiogenesis maturation. Any alterations to Ang1/Tie2 signaling mediated by changes in Ang1 concentration or elevated Ang2 concentrations can lead to hindered angiogenic responses and suboptimal endogenous muscle repair. It is hence vital to characterize the Ang1/Ang2 ratio in DMD and determine whether any of the downstream targets of the Ang/Tie2 pathways such as Akt activation and eNOS phosphorylation are disrupted, so that future therapeutics can be introduced to correct any abnormalities.

2.2 Hypothesis

We hypothesize that Ang1/Tie2 signalling is dysregulated through elevated Ang2 concentrations in DMD skeletal muscles leading to reduced AKT phosphorylation and eNOS phosphorylation.

2.3 Specific Aims/ Research Objectives

Aim 1: Characterize the expression of Ang1, Ang2, Tie2, phosphorylated Tie2, and VEPTP to evaluate changes in Ang1/Ang2 ratio and Tie2 activation in DMD mouse models relative to normal controls.

Aim 2: Evaluate changes in levels of AKT, phosphorylated-AKT, eNOS, and phosphorylated-eNOS to observe select downstream targets associated with Tie2 signalling.

3 Materials and Methods

3.1 Animal Care and Genotyping

All animal protocols were conducted in strict accordance with the Canadian Council on Animal Care (CCAC) and were approved by the Animal Use Subcommittee (Western University, London, ON, Canada). All experiments were performed at The Lawson Health Research Institute at St. Joseph's Health Care (SJHC) in London Ontario. C57BL/10 mice (Jax Laboratories), *mdx* mice (C57BL/10ScSn-Dmdmdx/J, Jax Laboratories, spontaneous nonsense mutation), *mdx/utrn*$^{+/-}$ (originally generated by Dr.'s Mark Grady and Josh Sanes (Washington University, St. Louis), were purchased from the Jackson Laboratory (Bar Harbor, ME) and maintained at the Animal Care Facility at SJHC. Additional wild-type mice were obtained from Charles River and additional *mdx*/*utrn*$^{+/-}$ mice were provided by Dr. Robert Grange (Virginia Polytechnic and State University). Colonies were maintained under controlled conditions (19-23˚C, 12-hour light/dark cycles) and allowed water and food ad libitum. Mice of three age ranges, either 4-5 weeks old, 8-10 weeks old, or 15-20 weeks wild type, *mdx,* and *mdx*/*utrn*$^{+/-}$ (n=3 for all groups) of either sex were used in this study.

Genotyping was conducted using tail snips or ear notch tissues by polymerase chain reaction (PCR) with platinum *Taq* polymerase (Thermofisher), using the following set of utrophin gene primers (Sigma): 5'-TGCAGTGTCTCCAATAAGGTATGAAC-3', 5'- 45 TGCCAAGTTCTAATTCCATCAGAAGCTG -3' (forward primers) and 5'-CTGAGTCAAACAGCTTGGAAGCCTCC-3' (reverse primer). Gel electrophoresis was used to determine the molecular weight of the amplified DNA.

3.2 Tissue Preparation

Mice were sacrificed via gas euthanasia and cervical dislocation upon reaching the desired age. Diaphragm tissue used for hematoxylin and eosin (H&E) and Masson's Trichrome staining were immediately dissected, fixed in 10% formalin for 24-48hrs, and embedded in paraffin. Section slides were produced from 5µm thick slices taken from every 5th serial section. Diaphragm and lung tissues used for western blot, enzyme-linked immunosorbent assay (ELISA), and qPCR analysis were dissected and immediately flash frozen in dry ice and stored in -80°C.

3.3 Microscopy and Image Analysis

Tissue slides were sent to Molecular Pathology at Robarts Research Institute, London, ON, for H&E and Masson's Trichrome Staining. Histological images were taken on a Zeiss Axioskop 50Fluorescence ERGO Trinoc microscope using a 20x objective using Northern Eclipse Image software. A minimum of five images were taken of each section. Qualitative analysis assessing the presence of centrally nucleated myofibers and inflammatory infiltrate (H&E) and collagen (Masson's Trichrome) was performed as representations of inflammation and fibrosis in the tissue.

3.4 RNA Extraction and cDNA Preparation

Frozen diaphragm tissue was cut and weighted, producing 10-20mg of tissue. Samples were subjected to 3 freeze-thaw cycles using liquid nitrogen (LH2), then homogenized in Trizol Reagent (Ambion), using polypropylene pestles (Fisher Scientific) and an Eppendorf tube. RNA purification was performed using Direct-zol™ RNA miniprep kit (Zymo) per the manufacturer's instructions. An in-solution DNase I treatment was performed post-purification using <10ug of RNA sample, DNase I (Zymo), DNA Digestion Buffer (Zymo), and water and incubated at room temperature for 15 minutes. Three volumes of Trizol to one volume of the treated sample were added. RNA purification using Direct-zol™ RNA miniprep kit was then repeated and suspended in 40ul of RNAase-free water. RNA concentration and quality were quantified using a DeNovix DS-11 spectrophotometer. All samples were verified to have a 260/280 ratio above 1.9 and a 260/230 ratio between 2.0-2.2.

cDNA was produced using 1µg of total RNA using the High Capacity cDNA Reverse Transcription Kit (Applied Biosystems) per the manufacturer's instructions.

3.5 RT-qPCR

Taqman Gene Expression Assays were used to assay *Tek* (Tie2) (Mm004432343_m1), *Angpt1* (Mm00456503_m1), *Angpt2* (Mm00545822_m1), *ActB* (Mm02619580_g1), *AP3D1* (Mm00475961_m1), and *GusB* (Mm01197698_m1). qPCR products were performed on the QuantStudio™ 5 system with Taqman Fast Advanced Master Mix (Applied Biosystems). Quantification was performed using Design & Analysis Software 2.4.3 (Thermofisher). Total

Tek, *Angpt1*, and *Angpt2* expressions were normalized to the geometric mean of control genes: *ActB*, *AP3D1*, and *GusB*.

3.6 Protein Extraction

Tissue were weighed and then homogenized in lysis buffer [20 mM Tris (pH 7.8), 17 mM NaCl, 2.7 mM KCl, 1mM MgCl2, 1% Triton X-100, 10% (w/v) glycerol, 1mM EDTA, supplemented with protease inhibitor (Roche) and phosphatase inhibitor (Abcam)] (tissue weight(mg): lysis buffer volume (µL) = 1:10) and incubated for 4hr at 4°C with continuous agitation. Samples were then centrifuged at 13 000rpm for 15 minutes and the supernatants were collected. Total protein was quantified using the bicinchoninic acid assay (Pierce). All samples were run in duplicates and absorbance was measured at 575nm with an iMark™ Microplate Absorbance Reader.

3.7 Western Blot

40µg of protein was combined in 1:1 ratio with Laemmli sample buffer with 2-mercaptoethanol, heat denatured at 70°C for 10 minutes, and loaded onto mini-PROTEAN TGX Stain-Free™ Precast Gels (Bio-Rad). 15 µl of PageRuler Plus Prestained Protein ladder was loaded onto the gel. Protein separation vis gel electrophoresis was run at 80 V for 30 minutes followed by 60 minutes at 120 V. The gel was cut and then activated via UV light using the Bio-Rad Gel Doc system. Protein was transferred onto a PVDF membrane using the Transblot Turbo machine (Bio-Rad) running for 10 minutes at 1.3 A constant; up to 25 V. Membrane was blocked with 5% bovine serum albumin (BSA) in tris-buffered saline containing 0.1% tween 20 (TBS-T) or 5% skim milk in 0.1% TBS-T for 1 hour with constant agitation. Membranes were incubated with primary anti-Ang1 (Abcam, ab8451, 1:1000), Ang2 (Invitrogen, PA5-27297, 1:1000), AKT (Cell Signalling, #9272, 1:2000), pAKT ser473 (Cell Signalling, #9271S, 1:500), eNOS (Abcam, ab76198), or Phospho-eNOS ser1177 (Mybiosource, MBS9601018, 1:1000) antibodies in 5% BSA TBS-T or 5% skim milk in 5% TBS-T at 4°C overnight and incubated with anti-rabbit HRP secondary antibody (Abcam, ab6721, 1:5000) or anti-mouse HRP secondary antibody (Abcam, ab97023, 1:5000) for 1 hour. Membranes were again thoroughly washed three times for five minutes with TBS-T. Total protein was visualized and imaged on the Bio-Rad Gel Doc

system. Chemiluminescent detection was performed using a one-minute incubation with SuperSignal West Pico PLUS chemiluminescent substrate (ThermoFisher). Bands were visualized via chemiluminescence using ImageLab (Bio-Rad) on the Bio-Rad Gel Doc. Signal was normalized to total protein signal from the stain-free blots (Taylor et al. 2013).

3.8 Enzyme-linked Immunosorbent Assay

To quantify levels of Ang1, Ang2, Tie2, and pTie2 in diaphragm tissue lysates, Mouse Angiopoietin 1 Elisa Kit (Develop), Quantikine Mouse Angiopoietin-2 (R&D Systems), Quantikine Mouse Tie2 (R&D Systems), Mouse Phosphorylated Tie 2 Duoset IC Elisa Kit (R&D Systems), and Mouse VE-PTP Elisa Kit (Blue gene) were used. Samples underwent ½ dilutions and all samples were run in duplicates. Each kit was performed using the manufacture's recommended instructions. Samples were measured with an iMark™ Microplate Absorbance Reader at 450nm and subtracted by absorbance at 570nm. A standard curve was generated using the mean absorbance and concentration of each standard in GraphPad Prism version 8.00 for Windows (GraphPad Software, La Jolla California USA).

3.9 Statistical Analysis

Ordinary one-way ANOVA followed by Tukey's honest significance test was performed comparing the difference between groups using GraphPad Prism version 8.00 for Windows (GraphPad Software, La Jolla California USA). Differences between groups were considered significant at a p-value of <0.05.

4 Results

4.1 Ang1/Ang2 ratio is skewed towards Ang2 in mature mdx/utrn+/- mice relative to age-matched wild-type.

Ang1 and Ang2 both play an important role in mediating Tie2 receptor signalling pathways and regulating endothelium homeostasis and activation. Due to Ang2 being the competitive inhibitor of Ang1, the ratio between Ang1 and Ang2 can dictate Tie2 signalling and any changes in the expression of either protein can lead to a shift in ratio and an alteration in receptor activation and downstream signalling pathway (Wang et al., 2017). To assess the expression of Ang1 and Ang2 in diaphragm tissue of 8-10 weeks-old and 15-20 weeks-old WT, *mdx*, and *mdx/utrn*$^{+/-}$ mice, *ANGPT1* and *ANGPT2* mRNA expression were first assessed using RT-qPCR. Young (8-10 weeks old) *mdx/utrn*$^{+/-}$ mice had significantly lower relative *ANGPT1* expression compared to young *mdx* mice (p=0.0098) and young WT (p=0.0022). No significant differences in *ANGPT2* mRNA expression were observed between the different genotypes (Fig 9). Interestingly, the subsequent protein data did not reflect the mRNA data. Using ELISA to quantify protein concentrations, young *mdx/utrn*$^{+/+}$ mice (1534.756±518.994 pg/mL) and young *mdx/utrn*$^{+/-}$ mice (1829.437±1369.454 pg/mL) had lower Ang1 protein concentration compared to young WT mice (2774.798±1908.568) but were not significantly different (p=0.3075). In contrast, both young *mdx/utrn*$^{+/+}$ mice (1198.470±300.132 pg/mL)(p=0.0255) and young *mdx/utrn*$^{+/-}$ mice (1226.882±658.067 pg/mL)(p=0.0123) had significantly higher Ang2 protein concentrations compared to young WT (346.888±137.783 pg/mL) (Fig 10).

H&E and Masson's Trichrome staining were performed to validate the inflammatory and fibrotic nature of the diaphragm tissues respectively. Centrally nucleated myofibers were visible in young *mdx/utrn*$^{+/+}$ and young *mdx/utrn*$^{+/-}$ diaphragm, indicating the occurrence of muscle regeneration (Fig 11). Inflammatory infiltrates were present in young *mdx/utrn*$^{+/-}$ and young *mdx* mice. Young and mature *mdx/utrn*$^{+/-}$ mice diaphragm had profound collagen deposition, evident of fibrosis. Mature mdx/utrn$^{+/-}$ also displayed collagen deposition, comparable to mdx/utrn+/- mice (Fig 12).

In the 15-20 weeks old age group, mature *mdx/utrn*$^{+/-}$ mice *ANGPT1* and *ANGPT2* mRNA expression did not significantly differ relative to mature WT mice. In contrast, mature *mdx/utrn*$^{+/+}$ mice had a significant decrease in *ANGPT2* mRNA expression (p=0.013) but not ANGPT1 mRNA expression) (p=0.9869) relative to the WT mice (Fig 9). However, the subsequent ELISA protein concentration analysis showed a significant decrease in Ang1 protein concentration in *mdx/utrn*$^{+/-}$ mice (965.069±473.061 pg/mL)(p=0.0032) compared to mature WT mice (3163.722±713.035) that was not reflected in the *ANGPT1* mRNA expression data. Additionally, mature *mdx/utrn*$^{+/-}$ mice did not have a significantly higher Ang2 protein concentration (1493.863±325.298 pg/mL)(p=0.4078) compared to the mature WT mice (1101.879±375.764 pg/mL) despite the increase in mRNA concentration (Fig 10). Mature *mdx/utrn*$^{+/+}$ did not have significantly different Ang1 protein concentrations (2033.553±1023.982 pg/mL) (p=0.1472) nor Ang2 protein concentrations (1861.551±761.507 pg/mL) (p=0.1113) compared to the WT.

The changes in Ang1 and Ang2 protein concentrations when analyzed as a function of age revealed an age-dependent decrease in Ang1 protein concentrations in *mdx/utrn*$^{+/-}$ in contrast to an age-dependent increase of Ang1 protein concentrations in both *mdx/utrn*$^{+/+}$ and WT mice (Fig 13). All three genotypes had an age-dependent increase in Ang2 protein concentrations. Western blot analysis was subsequently performed to confirm the ELISA data (Fig 14). Upon analysis of relative fold expression ratios between Ang1 and Ang2 mRNA, young *mdx/utrn*$^{+/-}$ mice had significantly lower *ANGPT1*/*ANGPT2* relative mRNA expression compared to *mdx/utrn*$^{+/+}$ mice (p=0.0398) but not significantly different from young WT mice (Fig 15). In mature 15-20 weeks-old mice, *mdx/utrn*$^{+/+}$ mice had double the relative Ang1/Ang2 mRNA expression ratios compared to both WT (p=0.0433) and *mdx/utrn*$^{+/-}$ (p=0.0452) mice. However, Ang1/Ang2 protein ratio quantification revealed a significantly lower Ang1/Ang2 ratio in both young (p<0.0001) and mature (p<0.0044) *mdx/utrn*$^{+/-}$ mice and young *mdx* mice (p=0.0027) compared to their WT counterparts (Fig 15). When analyzed as a function of age, the Ang1/Ang2 protein ratio in all three genotypes decreased as age increased with *mdx/utrn*$^{+/-}$ mice having the lowest ratio in both age groups. Altogether, these findings point to a highly skewed Ang1/Ang2 ratio in favour of Ang2 signalling in the skeletal muscle of *mdx* and *mdx/utrn*$^{+/-}$ mice that may result in Tie2 inactivation and downstream inhibition.

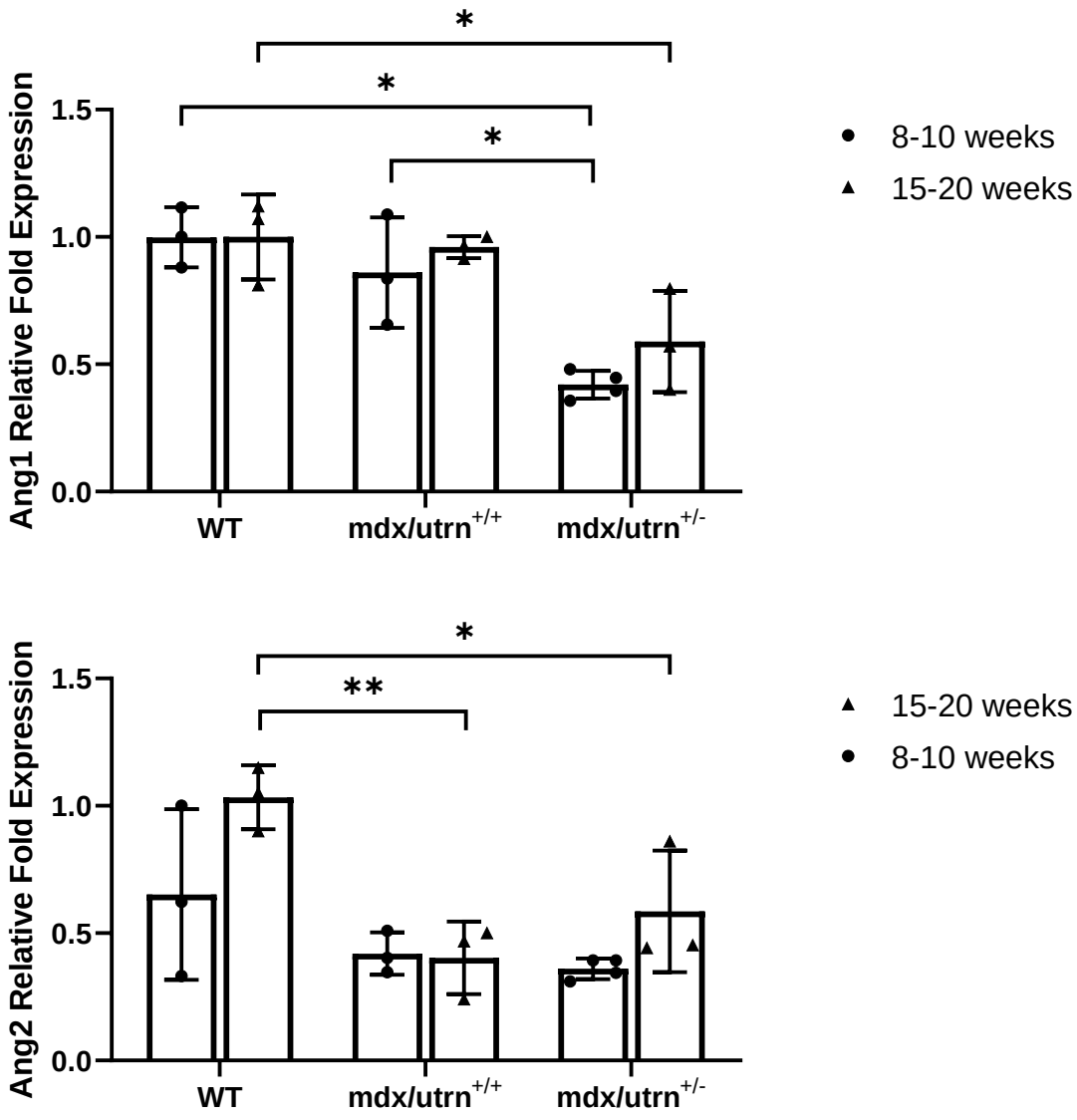

Figure 10. Rt-qPCR analysis of Ang1 and Ang2 gene expression.

RT-qPCR analysis of *ANGPT1* (Ang1) and *ANGPT2* (Ang2*)* relative fold expression in young (8-10 weeks-old) and mature (15-20 weeks-old) WT, *mdx/utrn*$^{+/+}$, and *mdx/utrn*$^{+/-}$ mice (*n*=3-5); reference genes: *ActB*, *AP3D1*, and *GusB*. Data are shown as individual values and mean±s.d. Statistics were performed using one-way ANOVA followed by Tukey's Test. *p<0.05, **p<0.01.

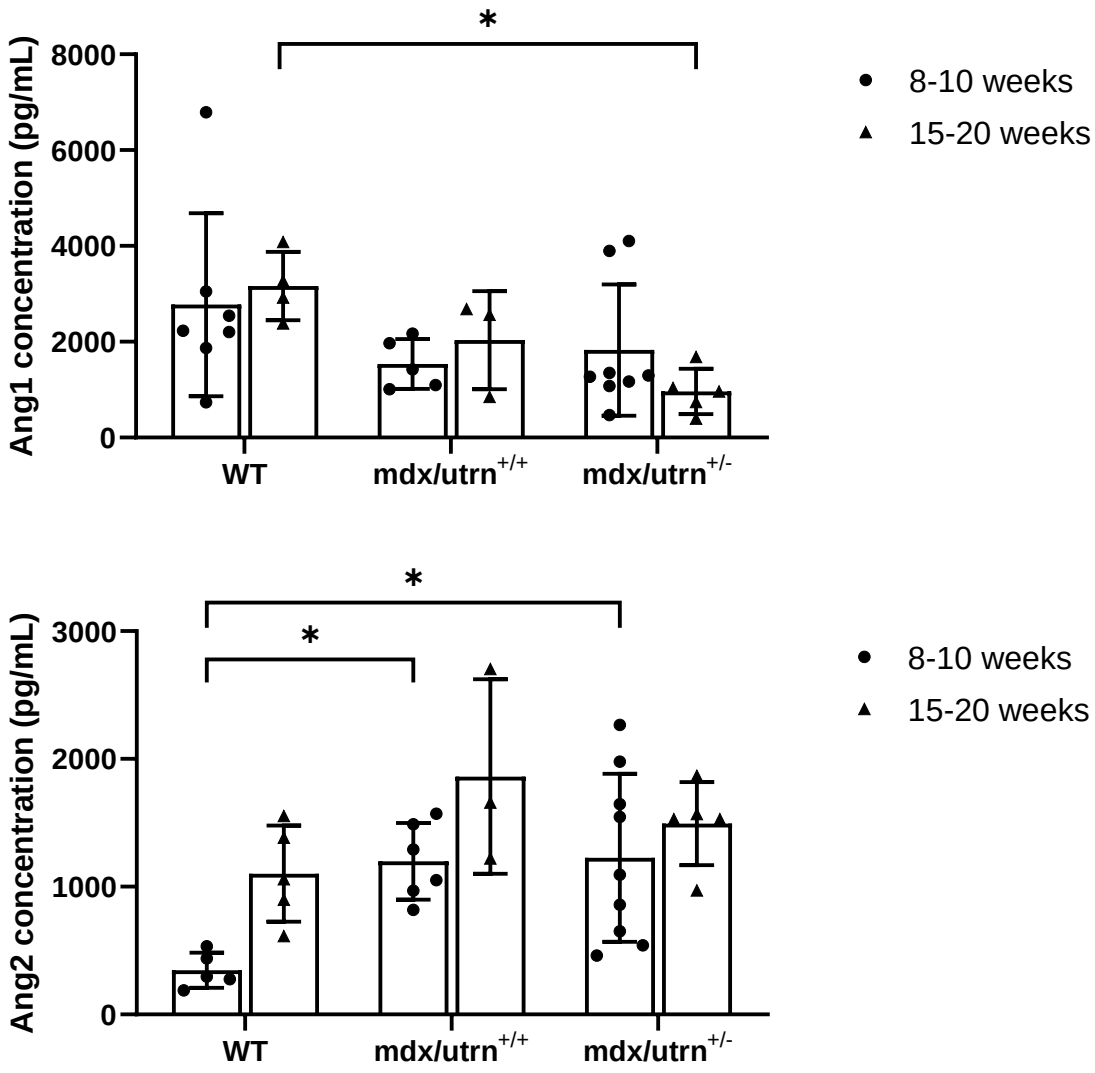

Figure 11. ELISA analysis of Ang1 and Ang2 gene expression and protein expression.

ELISA quantification of Ang1 and Ang2 concentration in diaphragm tissues lysates of young and mature WT, *mdx*, and *mdx/utrn*$^{+/-}$ mice (n=3). Data are shown as individual values and mean±s.d. Statistics were performed using one-way ANOVA followed by Tukey's Test. *p<0.05.

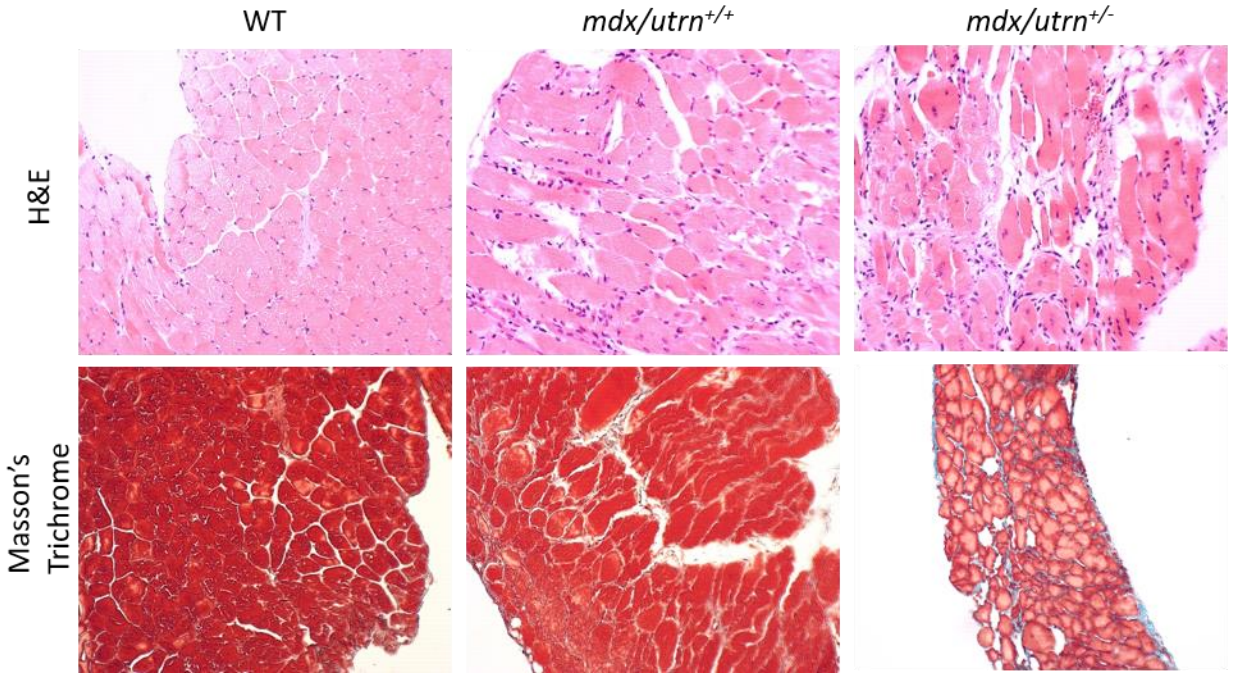

Figure 12. Muscle pathology in 8-10 weeks-old diaphragm muscle of wild-type, mdx, and mdx/utrn+/-.

Comparison of collagen deposition as an indicator of fibrosis, centrally nucleated myofibers as an indicator of tissue regeneration, and increased cellularity and polymorphonuclear cells as an indicator of inflammatory infiltrate.

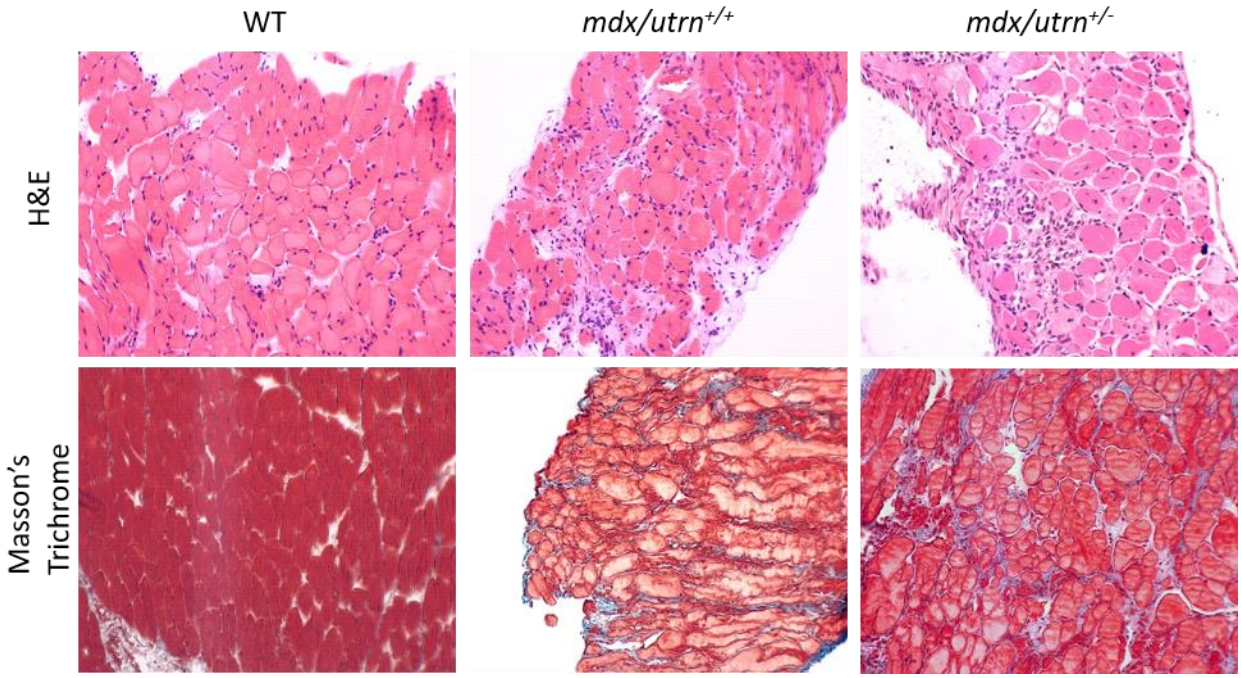

Figure 13. Muscle pathology in 15-20 weeks-old diaphragm muscle of wild-type, *mdx*, and *mdx/utrn*+/- mice.

Comparison of collagen deposition as an indicator of fibrosis, centrally nucleated myofibers as an indicator of tissue regeneration, and increased cellularity and polymorphonuclear cells as an indicator of inflammatory infiltrate.

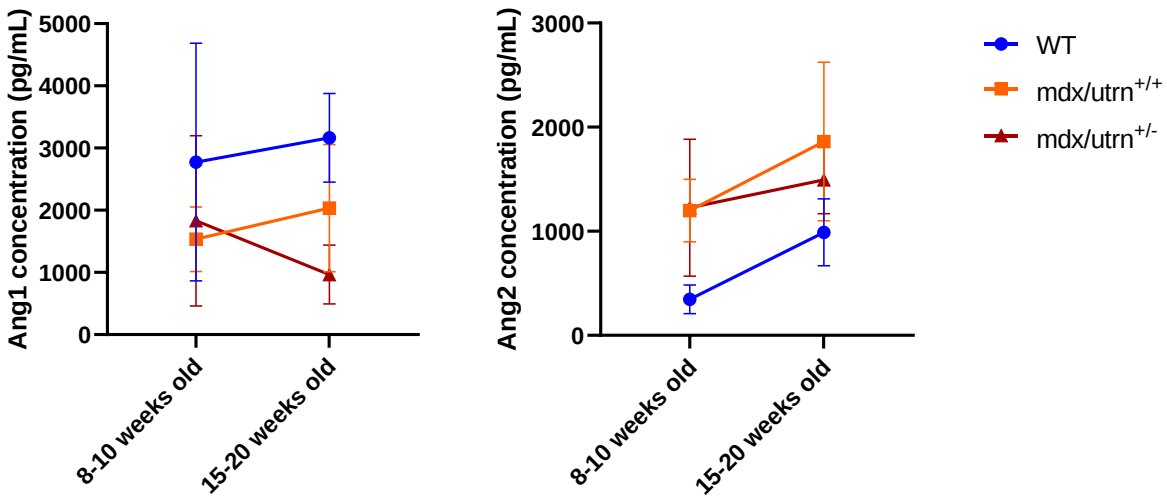

Figure 14. Function of age analysis for Ang1 and Ang2 protein expression.

Visualization of changes in Ang1 and Ang2 protein concentration between diaphragm tissue of 8-10 weeks of age mice and 15-20 weeks of age mice. Data are shown as mean±s.d.

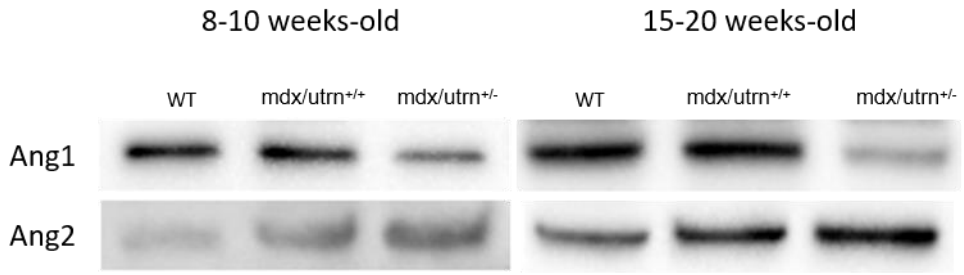

Figure 15. Western Blot Analysis of Ang1 and Ang2.

Representative image of Western blot analysis of Ang1 and Ang2 in diaphragm tissues lysates of young and mature WT, *mdx*, and *mdx/utrn*$^{+/-}$ mice.

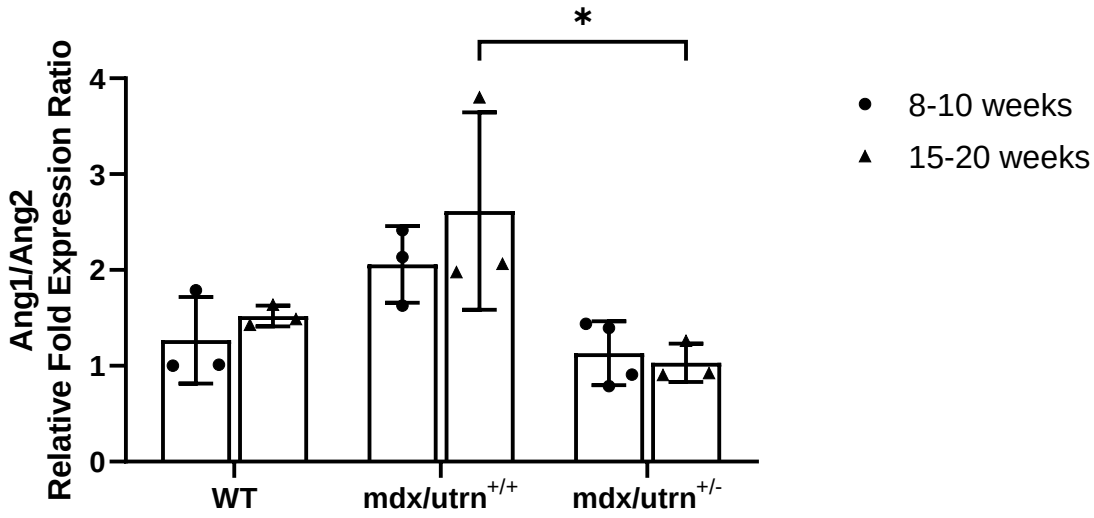
*
Ang1/Ang2
Relative Fold Expression Ratio
4
3
2
1
0
WT
mdx/utrn+/+
mdx/utrn+/-
8-10 weeks
15-20 weeks

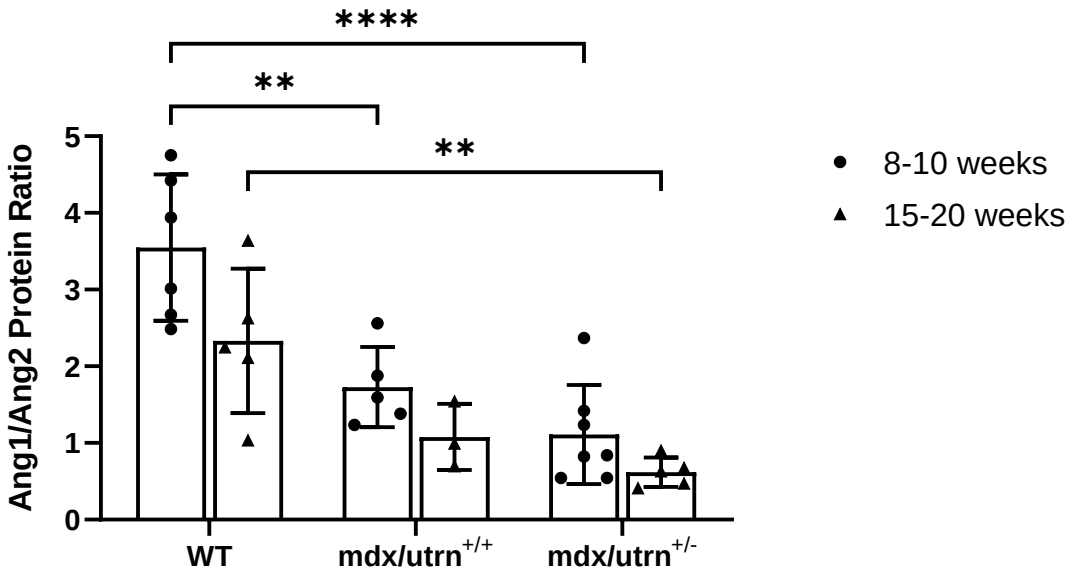
****
**
**
Ang1/Ang2 Protein Ratio
5
4
3
2
1
0
WT
mdx/utrn+/+
mdx/utrn+/-
8-10 weeks
15-20 weeks

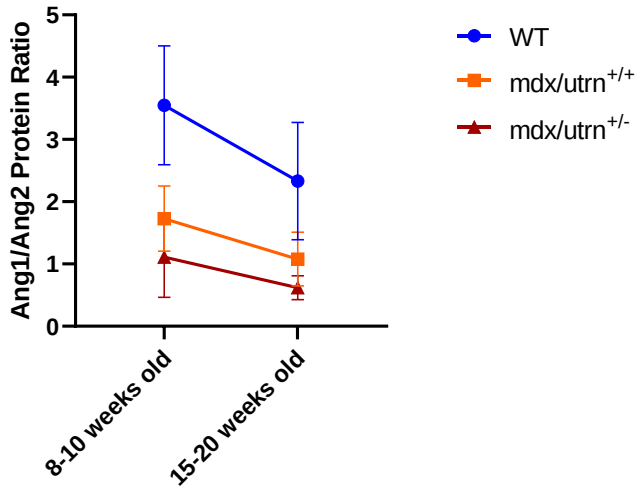
Ang1/Ang2 Protein Ratio
5
4
3
2
1
0
8-10 weeks old
15-20 weeks old
WT
mdx/utrn+/+
mdx/utrn+/-

Figure 16. Ang1/Ang2 Ratio Analysis.

Quantification of the ratio of Ang1 relative to Ang2 protein concentration in diaphragm tissues lysates of young and mature *WT*, *mdx*, and *mdx/utrn*$^{+/-}$ mice (n=3-9). Function of age analysis for changes in Ang1/Ang2 ratio between 8-10 weeks of age and 15-20 weeks of age. Data are shown as individual values and mean±s.d. Statistics were performed using one-way ANOVA followed by Tukey's Test. **p*<0.05, ***p*<0.01, ****p<0.0001.

4.2 pTie2/Tie2 ratio is decreased in mature mdx/utrn+/- mice compared to age-matched wildtype mice

Next, to determine the effects of the change in Ang1/Ang2 ratio on Tie2 expression and signalling in the diaphragm tissue of of 8-10 weeks-old and 15-20 weeks-old WT, *mdx*, and *mdx/utrn*$^{+/-}$ mice, *Tek* (Tie2) mRNA was first assessed via RT-qPCR. Neither young 8-10 weeks-old *mdx/utrn*$^{+/+}$ mice nor young *mdx/utrn*$^{+/-}$ mice had significantly different Tie2 mRNA expression relative to young WT mice (p=0.093) (Fig. 16). Protein concentration analysis via ELISA revealed elevated Tie2 expression in young *mdx/utrn*$^{+/-}$ mice (4542.796±613.177 pg/mL), albeit, not significantly higher than WT (3612.270±238.670 pg/mL) or *mdx* (3802.629± 615.762 pg/mL)(p=0.266). Tie2 mRNA expression in mature 15-20 weeks-old mice similarly did not significantly differ between each genotype (p=0.1665). Tie2 protein concentrations in both mature *mdx/utrn*$^{+/+}$ mice (3438.781±2137.56 pg/mL) and mature *mdx/utrn*$^{+/-}$ (3230.151±1449.219 pg/mL) were elevated compared to mature WT (2261.032±1646.605 pg/mL), but were not significant (p=0.6999).

Phosphorylated Tie2 (pTie2) protein analysis via ELISA was then used to evaluate levels of Tie2 activation and revealed a slight non-significant decrease in pTie2 protein concentration in young *mdx/utrn*$^{+/+}$ mice (1320.922±297.046 pg/mL) and young *mdx/utrn*$^{+/-}$ mice (1078.286±388.538 pg/mL) compared to young WT mice (1597.999±532.224 pg/mL). Similar to the mRNA data, no significant differences in pTie2 protein concentrations was detected between mature *mdx/utrn*$^{+/+}$ (1005.549±619.562 pg/mL), *mdx/utrn*$^{+/-}$ (908.122±477.387 pg/mL), and WT mice (990.652±663.280 pg/mL) (Fig 15). Function of age analysis showed a similar trend in decreases in both Tie2 and pTie2 concentrations in all three genotypes (Fig 17).

Interestingly, quantification of the ratio between pTie2 protein concentration and total Tie2 protein concentration showed a significant decrease in pTie2/Tie2 ratio in young *mdx/utrn*$^{+/-}$ mice (0.235±0.065 pTie2/Tie2) and young WT mice (0.437±0.119 pTie2/Tie2)(p=0.0383). Similarly, this significant difference was seen between mature *mdx/utrn*$^{+/-}$ (0.259±0.066 pTie2/Tie2) compared to mature WT mice (0.498±0.14 pTie2/Tie2) (p=0.0364). No significant differences were found between the pTie2/Tie2 ratio of mature *mdx/utrn*$^{+/+}$ and

WT,nor mature *mdx/utrn*$^{+/-}$ mice (. No significant age dependent changes in ratio were observed when pTie2/Tie2 ratio was analyzed as a function of time (Fig 18).

To determine whether the changes in pTie2/Tie2 ratio may be due to changes in the Tie2 regulatory protein VE-PTP (Frye et al., 2015), ELISA was performed to determine VE-PTP protein concentration. No significant differences in VE-PTP protein concentrations were seen between young *mdx/utrn*$^{+/+}$ mice (2100.521±717.907 pg/mL) and young *mdx/utrn*$^{+/-}$ mice (2095.981±625.203 pg/mL) compared to young WT mice (1888.470±719.714 pg/mL)(p=0.8486) (Fig 19). Similarly, no significant differences in VE-PTP protein concentrations were seen between mature *mdx/utrn*$^{+/+}$ mice (5593.717±2575.376 pg/mL) and young *mdx/utrn*$^{+/-}$ mice (2995±1870.149 pg/mL) compared to young WT mice (3252.685±1255.981 pg/mL) (p=0.2124), although concentrations were elevated in mature mice compared to young mice in each genotype. Taken together, this data shows that severely diseased mature mice have a lower pTie2/Tie2 ratio compared to WT mice.

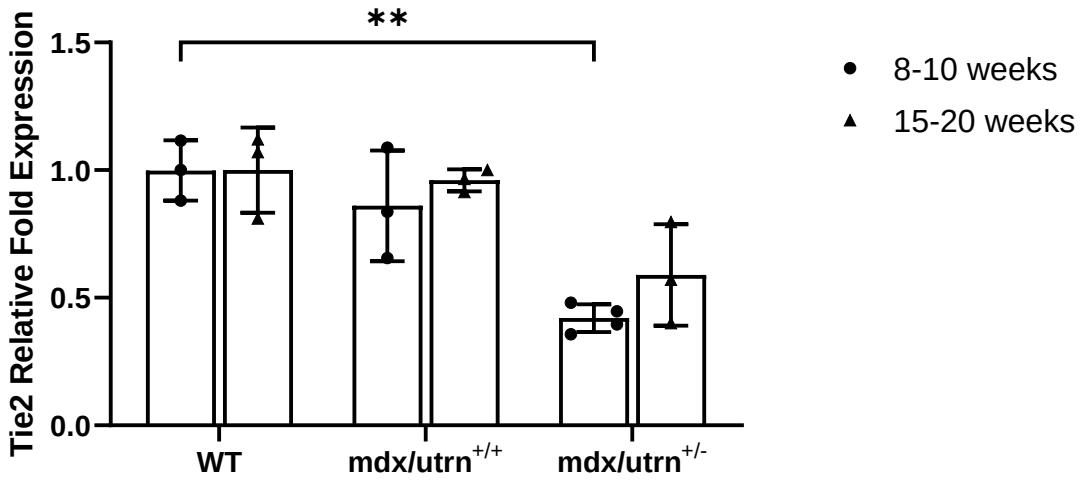

Figure 17. RT-qPCR analysis of Tie2 expression and phosphorylated Tie2 concentrations

RT-qPCR analysis of *TEK* (Tie2) relative fold expression in young (8-10 weeks-old) and mature (15-20 weeks-old) WT, *mdx,* and *mdx/utrn*$^{+/-}$ mice (*n*=3-4); reference genes: *ActB, AP3D1,* and *GusB.* Data are shown as individual values and mean±s.d. Statistics were performed using one-way ANOVA followed by Tukey's test. ***p*<0.01.

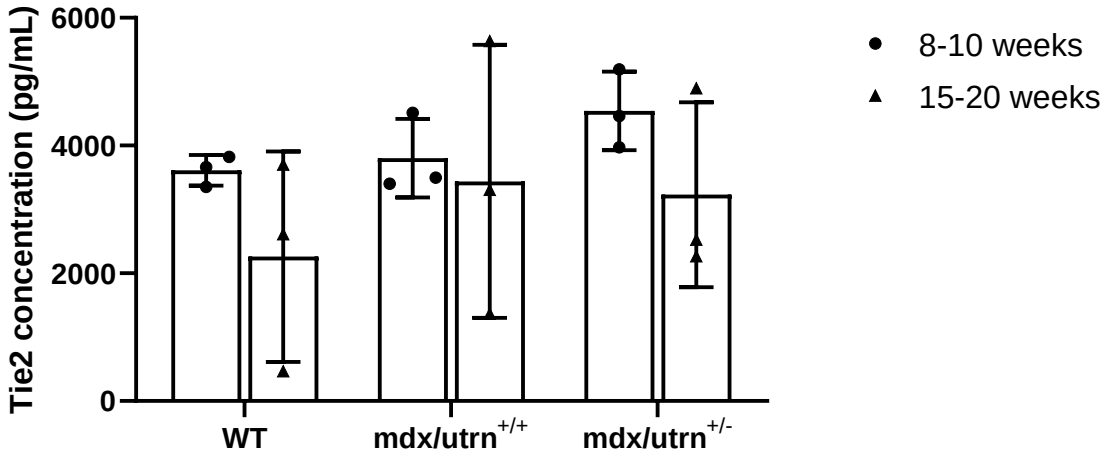
Tie2 concentration (pg/mL)
6000
4000
2000
0
WT
mdx/utrn+/+
mdx/utrn+/-
8-10 weeks
15-20 weeks

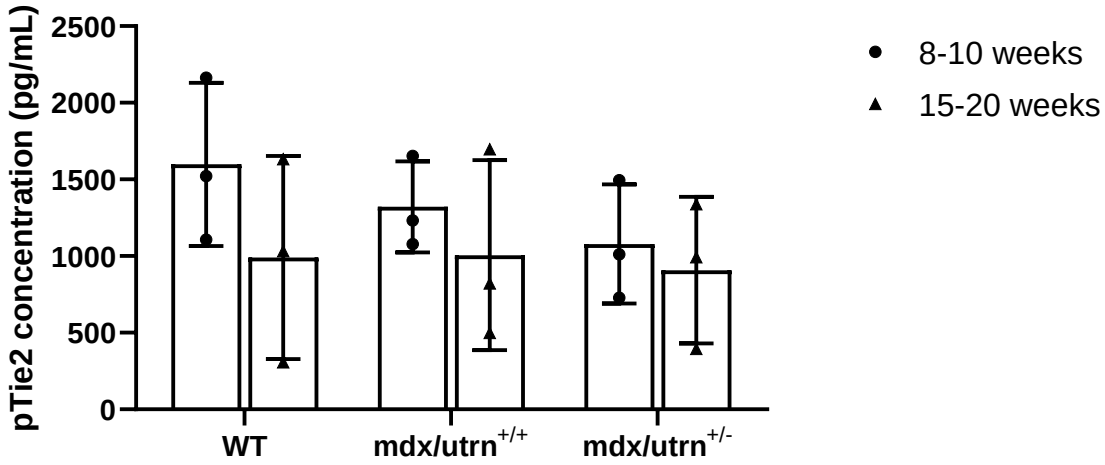
pTie2 concentration (pg/mL)
2500
2000
1500
1000
500
0
WT
mdx/utrn+/+
mdx/utrn+/-
8-10 weeks
15-20 weeks

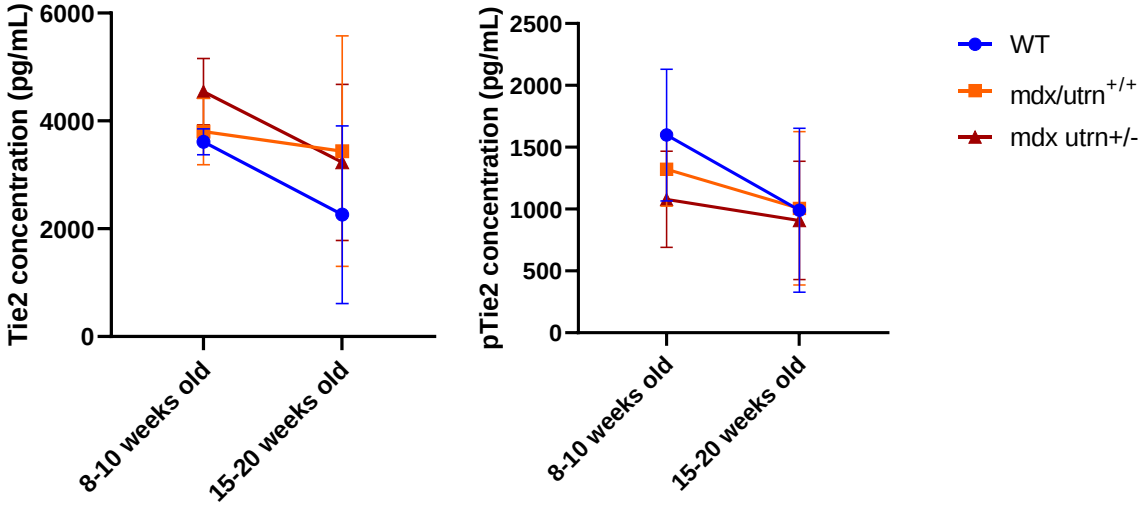
Tie2 concentration (pg/mL)
6000
4000
2000
0
8-10 weeks old
15-20 weeks old
pTie2 concentration (pg/mL)
2500
2000
1500
1000
500
0
8-10 weeks old
15-20 weeks old
WT
mdx/utrn+/+
mdx utrn+/-

Figure 18. ELISA analysis of Tie2 expression and phosphorylated Tie2 concentrations.

ELISA quantification of Tie2 and phosphorylated-Tie2 concentration in diaphragm tissues lysates of young and mature WT, *mdx*, *mdx/utrn*$^{+/-}$ mice (*n*=3). Data are shown as individual values and mean±s.d. Statistics were performed using one-way ANOVA followed by Tukey's test.

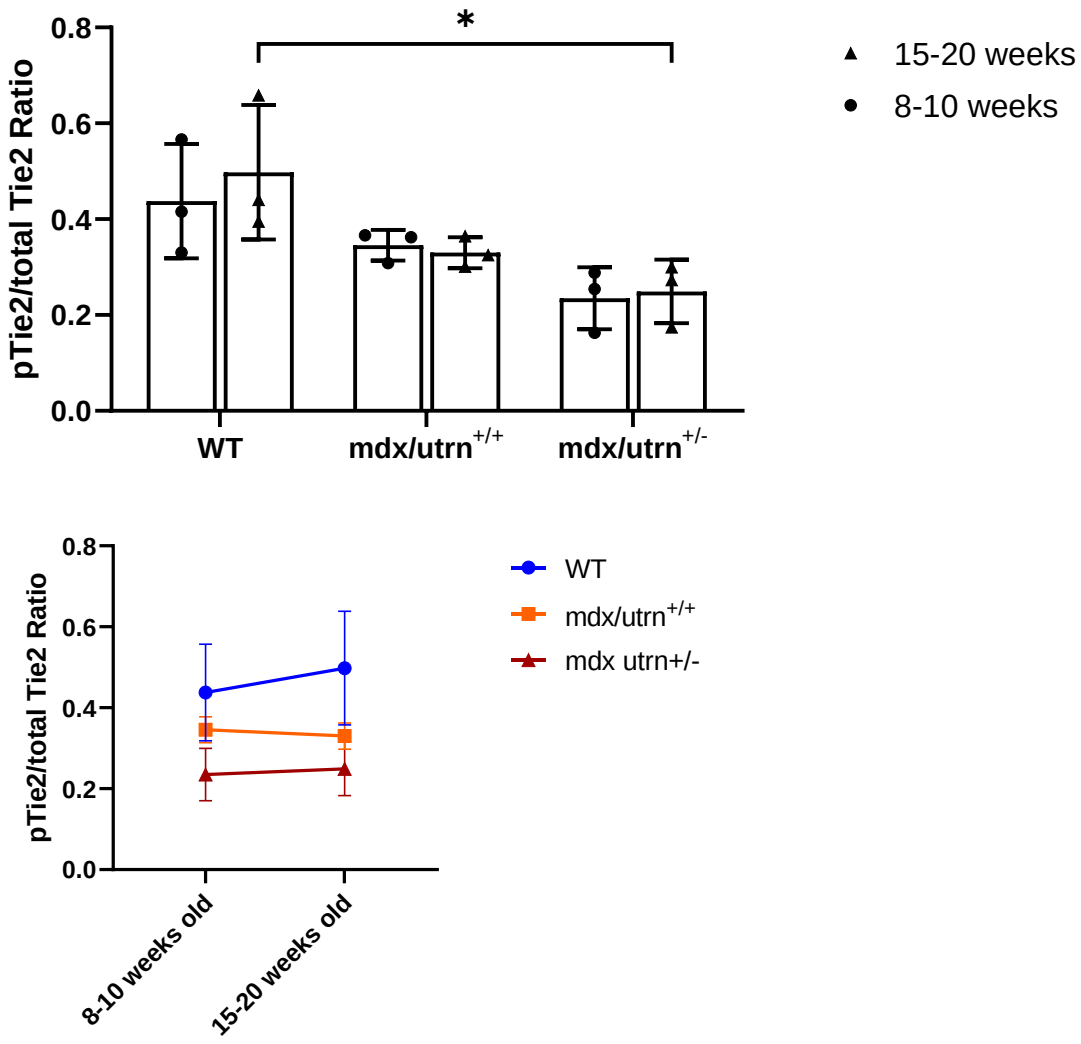

Figure 19. pTie2/Tie2 Ratio Analysis.

Ratio analysis of phosphorylated Tie2 (pTie2) relative to total Tie2 protein concentration in diaphragm tissues lysates of young and mature *WT*, *mdx*, and *mdx/utrn*$^{+/-}$ mice (n=3). Data are shown as mean±s.d. Statistics were performed using one-way ANOVA followed by Tukey's test. *p<0.05, **p<0.01.

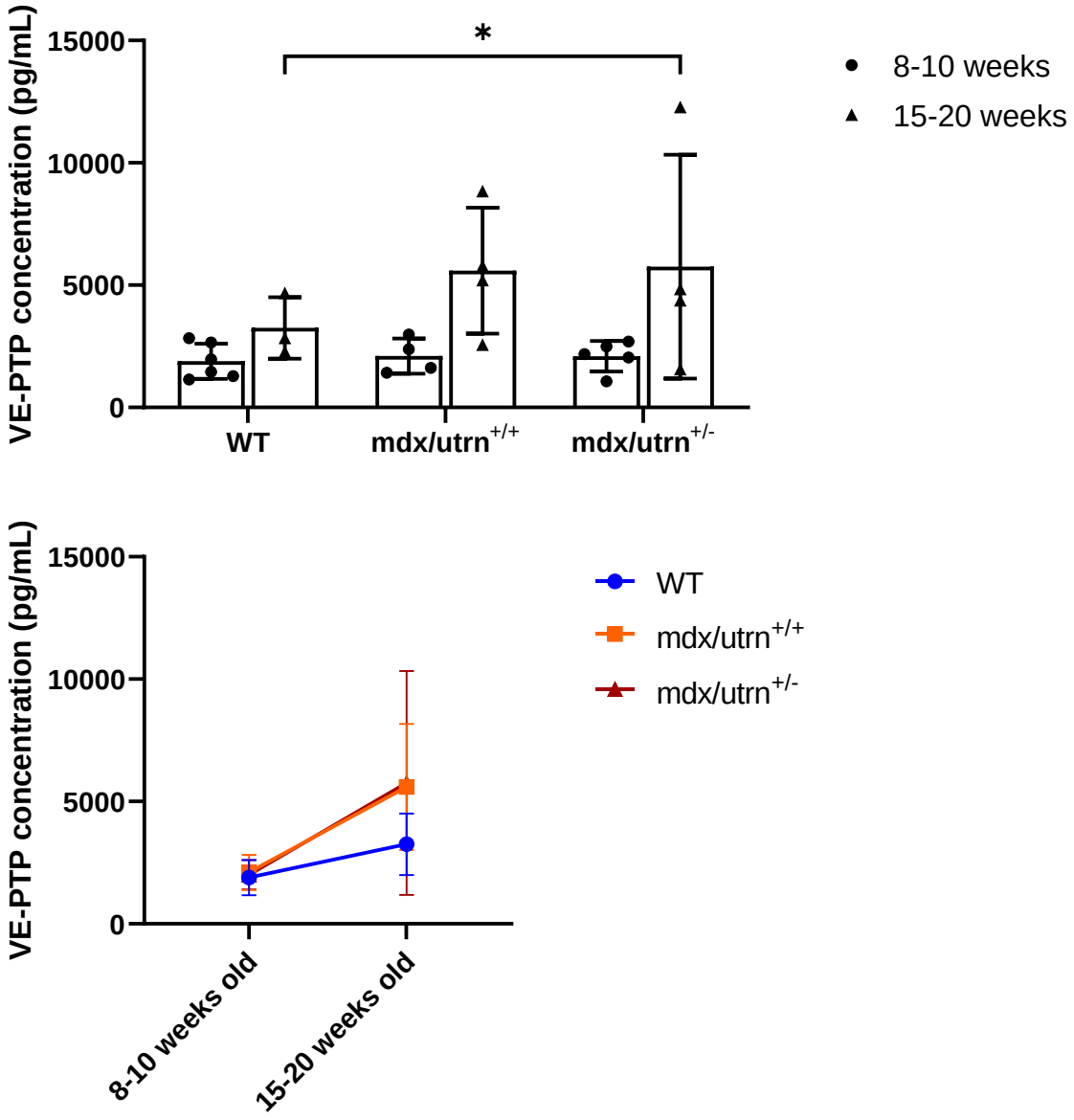

Figure 20. ELISA analysis of VEPTP expression.

Elisa quantification of VE-PTP protein concentration in young *WT*, *mdx*, and *mdx/utrn*$^{+/-}$ mice (n=3-6). Data are shown individual values and mean±s.d. Statistics were performed using one-way ANOVA followed by Tukey's test. *p<0.05, **p<0.01.

4.3 No significant differences in eNOS phosphorylation or Akt phosphorylation in mdx/utrn+/- mice.

Endothelium homeostasis is partially preserved through Tie2 mediated Akt phosphorylation leading to eNOS phosphorylation (Babaei et al., 2003). Thus, we wanted to assess whether the change in pTie2/Tie2 ratio affected Akt phosphorylation and subsequent eNOS phosphorylation in the diaphragm tissue of 8-10 weeks-old and 15-20 weeks-old WT, *mdx*, and *mdx/utrn*$^{+/-}$ mice. Semi-quantitative western blot analysis normalized to total protein was used to quantify Akt and eNOS phosphorylation (Fig 20A). In young 8-10 weeks old mice, phosphorylated Akt protein levels were not significantly different between young *mdx/utrn*$^{+/+}$ mice (0.889±0.376 A.U.), young *mdx/utrn*$^{+/-}$ mice, and young WT mice. Phosphorylated Akt levels in the mature 15-20 weeks-old age group similarly did not differ between mature *mdx/utrn*$^{+/+}$, *mdx/utrn*$^{+/-}$ mice, and mature WTs. The indifference in phosphorylated Akt levels was reflected in similarly unremarkable phosphorylated eNOS levels. Phosphorylated eNOS levels remained relatively similar between the disease model and WT in both young and mature mice (Fig 20B).

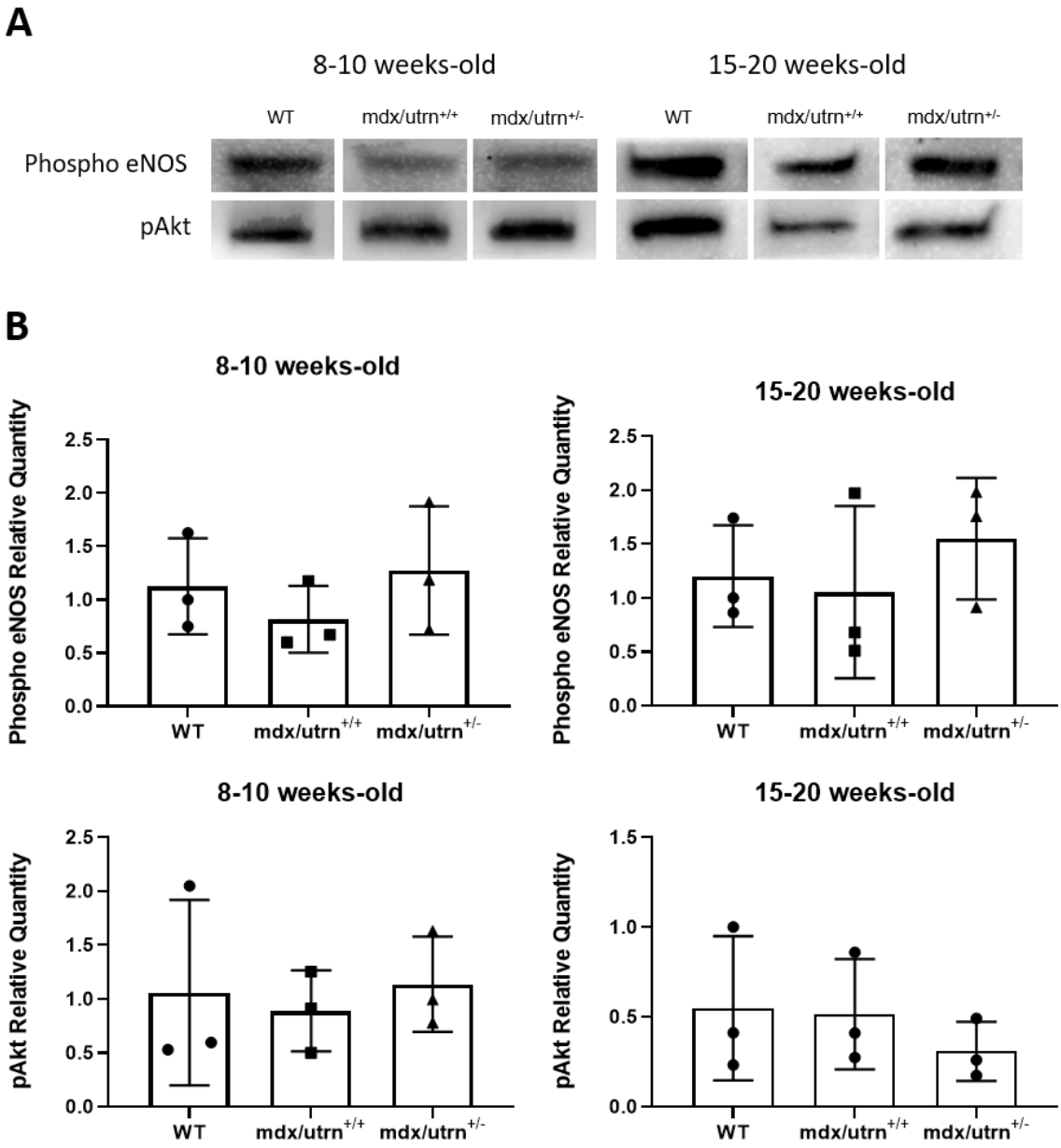

Figure 21. Western Blot analysis of phosphorylated eNOS and pAkt concentration in diaphragm tissue of WT, *mdx*, *mdx/utrn*$^{+/-}$ mice

(**A**) Representative images of western blot of phosphorylated AKT (*Ser473*) and phosphorylated eNOS (*Tyr1177*) in diaphragm tissues lysates of young and mature WT, *mdx*, and *mdx/utrn*$^{+/-}$ mice. (**B**) Western blot semi-quantitative analysis of phosphorylated AKT and phosphorylated eNOS in diaphragm tissues lysates of young and mature WT, *mdx*, and *mdx/utrn*$^{+/-}$ mice; normalized to total protein (n=3). Data are shown as individual values and mean±s.d. Statistics were performed using one-way ANOVA followed by Tukey's Test.

4.4 Total Akt is upregulated in mature mdx/utrn+/- mice

Although no changes in eNOS phosphorylation nor Akt phosphorylation were observed, total eNOS and Akt protein levels were also evaluated to rule out any changes in endogenous protein concentration as a cause for observed results. Western blot analysis was performed using the same tissue lysates as the eNOS and Akt phosphorylation experiments (Fig 21A). eNOS levels in the disease model were not significantly different from the WT in either young or mature mice. Akt protein levels were increased in both young *mdx* and young *mdx/utrn*$^{+/-}$ mice but were not significant. Akt was also elevated in both mature *mdx* and *mdx/utrn*$^{+/-}$ mice, but only *mdx/utrn*$^{+/-}$ was significant (Fig 21B). This may suggest that the overall pAkt/Akt ratio is decreased in mature *mdx/utrn*$^{+/-}$ mice.

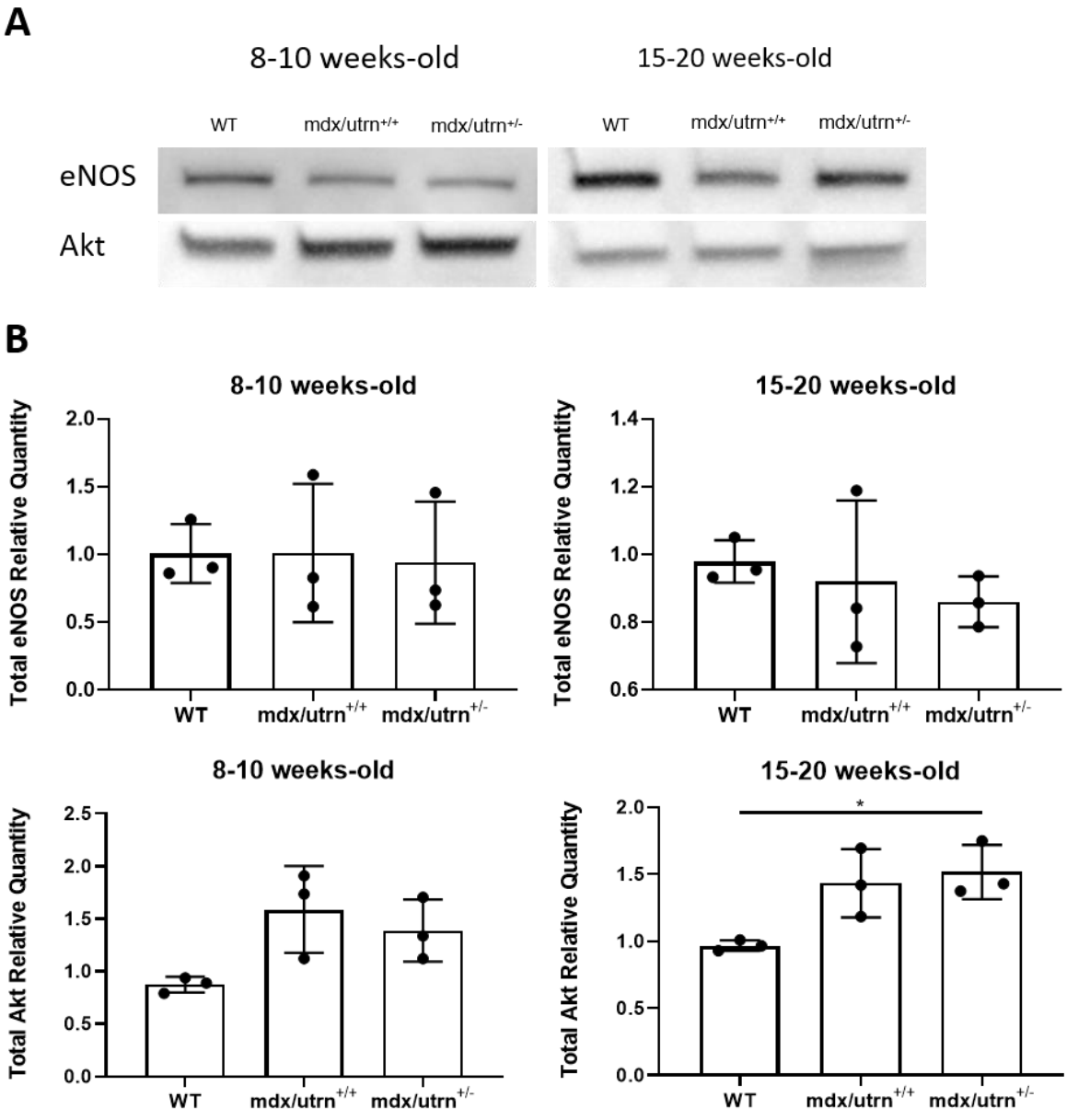

Figure 22. Western blot analysis of total eNOS and Akt protein in diaphragm tissue lysates

(**A**) Representative images of western blot of eNOS and Akt in diaphragm tissues lysates of young and mature WT, *mdx*, and *mdx/utrn*$^{+/-}$ mice. (**B**) Semi-quantitative analysis of total eNOS and Akt protein in diaphragm tissues lysates of young and mature WT, *mdx*, and *mdx/utrn*$^{+/-}$ mice; normalized to total protein (n=3). Data are shown as individual values and mean±s.d. Statistics were performed using one-way ANOVA followed by Tukey's test. *p<0.05.

5 Summary, Discussions, Limitations, and Future Directions

5.1 Summary of Results

Vascular therapy for DMD has been predominantly focused on the idea of utilizing VEGF to stimulate angiogenesis. However, our lab has shown that administration of VEGF alone cannot correct for the angiogenic defects within DMD, but rather, results in the formation of leaky vessels that are insufficient for functional perfusion. Subsequent administration of the vascular stabilizing factor Ang1 in combination with VEGF produced fully mature and functional vasculature and resulted in marked reductions in inflammation and fibrosis within the tissue (Gutpell et al., 2017). Ang1/Tie2 signalling in the endothelium is critical for survival, quiescence, and stability (Brindle et al., 2006; Young Koh et al., 2009). The importance of Tie2 signalling via Ang1 and Ang2 is perhaps an overlooked area of research in DMD because of the insufficient characterization data of this signalling pathway in muscular dystrophies. Thus, the first aim of this study was to characterize Ang1 and Ang2 expression, Tie2 expression and phosphorylation in the dystrophic diaphragm tissue of *mdx/utrn*$^{+/+}$ and *mdx/utrn*$^{+/-}$ mouse at two timepoints that represented tissue conditions prior to the onset of fibrosis (8-10 weeks-old) and after fibrosis (15-20 weeks-old). Upon finding decreased Ang1 expression and increased Ang2 expression that shifted the Ang1/Ang2 ratio towards Ang2 within the fibrotic *mdx/utrn*$^{+/-}$ mouse diaphragm, quantification of the angiopoietin receptor Tie2 was performed. Separately, no significant differences in Tie2 expression nor Tie2 phosphorylation were found. However, upon analysis of pTie2/Tie2 ratios, fibrotic *mdx/utrn*$^{+/-}$ had a significantly lower pTie/Tie2 ratio relative to the WT. VEPTP expression was also evaluated and found to be non-significant between groups. This prompted the question of whether the change in Tie2 activation affected downstream targets of Tie2 signaling. Thus, aim two of this study was to examine Tie2 downstream Akt and eNOS expression and phosphorylation. Akt and eNOS were then chosen based on their contribution to maintaining vascular stability and angiogenesis. Although Akt and eNOS phosphorylation were not significantly different between the genotypes, total Akt protein levels were elevated in diaphragm tissue of mature *mdx/utrn*$^{+/-}$ mice.

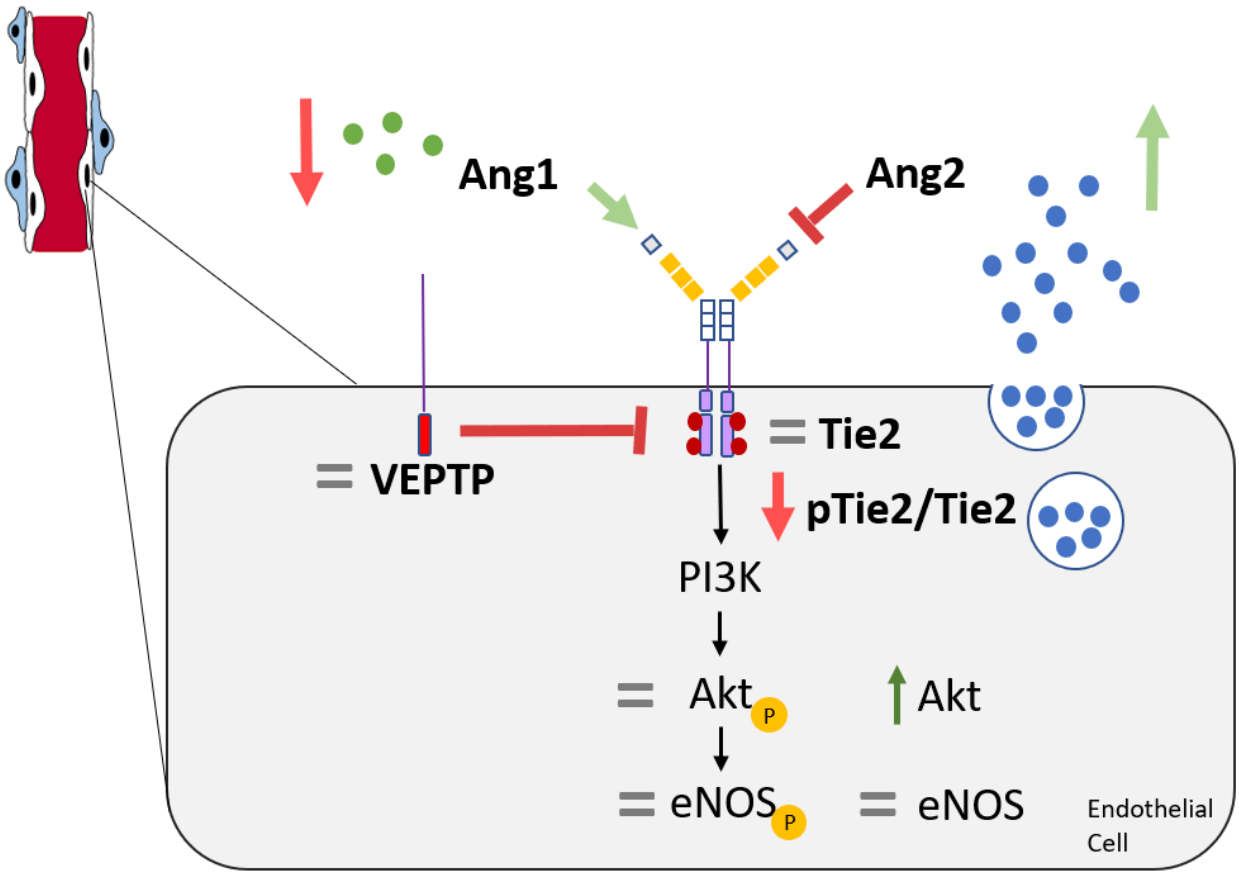

Figure 23. Graphical interpretation of results within mature 15-20 weeks-old *mdx/utrn*$^{+/-}$ mice compared to WT mice.

Ang1 protein concentrations were downregulated while Ang2 protein concentrations were upregulated, resulted in a decreased Ang1/Ang2 ratio. Total Tie2 protein concentration and pTie2 concentration were not significantly different relative to WT, however, pTie2/Tie2 ratio was significantly lower in the *mdx/utrn*$^{+/-}$ mice. Phosphorylated Akt, phosphorylated eNOS, and total eNOS levels were consistent between groups. Total Akt protein levels were elevated within *mdx/utrn*$^{+/-}$ mice.

5.2 Ang1 protein concentration is decreased in mature mdx/urn+/- mice

Upon Ang1-mediated activation, Tie2 will undergo auto-phosphorylation (pTie2) and downstream signal transduction. It is clear that Ang1 plays an important role in mediating vascular stability and contributes to the positive angiogenic effects of VEGF that are not observed for VEGF alone, and that impairments in Ang1 may contribute to vascular defects in DMD including increased vascular permeability and decreased functional perfusion. However, Ang1 also plays an important role in mediating myogenesis during muscle regeneration. Injection of COMP-Ang1, a potent derivative of native Ang1, can rescue ischemic muscle injury and induce muscle fiber regeneration through N-cadherin-mediated myogenin expression in myoblasts (Youn et al., 2018). Here, in line with our hypothesis of Ang1 deficiency, we show that Ang1 mRNA and protein concentrations are indeed reduced in the diaphragm tissue of mature *mdx/utrn*$^{+/-}$ mice. Downregulation of Ang1 is required for an effective inflammatory response due to Ang1's anti-inflammation and vascular stability effects. However, within the chronically inflamed microenvironment of the dystrophic diaphragm tissue, Ang1 expression may be insufficient, leading to a persistently de-stabilized vasculature. Evidence has shown that Ang1's antileakage action in the context of chronic inflammation is dependent on the presence of pericytes (Fuxe et al., 2011). Pericytes have been shown to contribute to muscle regeneration through their differentiation into myoblasts. Pericytes are also fibro/adipogenic progenitors, capable of differentiating into collagen-producing myofibroblasts that contribute to fibrosis in DMD (Dulauroy et al., 2012). Depletion of the pericyte population due to their differentiation into other cell types may directly perturb vascular stability. Ang1 in addition to being constitutively expressed by peri-endothelial cells such as pericytes and vascular smooth muscle cells is also expressed by other cells including satellite cells (Abou-Khalil et al., 2009). Satellite cells in DMD are severely hindered in their ability to self-renew due to impairments in asymmetrical cell division caused by the lack of dystrophin (Chang et al., 2016; Dumont et al., 2015). The decrease in Ang1 expression shown in this study may further contribute to a diminished satellite cell population through reductions in Ang1-mediated satellite cell self-renewal. Evidence of Ang1 deficiency presented in this study may thus be indirect evidence for

decreases in both satellite cells and pericytes populations that correlate with cycles of tissue regeneration and degeneration within the dystrophic skeletal muscles of DMD.

Interestingly, this significant decrease in Ang1 concentration was not seen in the *mdx/utrn*$^{+/+}$ diaphragm. Despite the similar levels of fibrosis and regeneration previously reported between mdx diaphragm and *mdx/utrn*$^{+/-}$ diaphragm (Gutpell et al., 2015), the difference in Ang1 expression between the *mdx/utrn*$^{+/+}$ and *mdx/utrn*$^{+/-}$ mice found in this study provides evidence for pathological differences between the two genotypes that have previously not been studied. Indeed, one of the major advantages in utilizing the *mdx/utrn*$^{+/-}$ mouse model over the traditionally used *mdx* mouse model is that *mdx/utrn*$^{+/-}$ mice present clinical symptoms experienced by DMD patients, compared to the mild pathology seen in *mdx/utrn*$^{+/+}$ mice. Additionally, Ang1 concentrations in both WT and mdx mouse diaphragms increased over time, whereas it decreased in the *mdx/utrn*$^{+/-}$ mouse. Again, the expression of utrophin in mdx mice may assist in its tissue regeneration. Whereas in the *mdx/utrn*$^{+/-}$, tissue regeneration may degrade into pathological regeneration over time that is dominated by fibrosis and chronic inflammation in the absence of both dystrophin and utrophin. In situations of inflammation, Ang1 signalling is heavily impeded by the expression of Ang2, which acts as the competitive antagonist to Ang1.

5.3 Ang2 protein expression is increased in young DMD murine models

Ang2 is released from the WPB in endothelial cells and act as autocrine signals that compete with Ang1 for Tie2 binding during the initiation of inflammation. Ang2-mediated inhibition of Tie2 signaling is necessary for the priming of the endothelial cells to receive inflammatory signals (Ulrike. Fiedler et al., 2006). The resulting Ang1/Ang2 ratio influences Tie2 receptor signaling and modulates endothelium quiescence and activation. In several pathological conditions, severely elevated Ang2 concentrations have been associated with a worse disease prognosis, often due to aberrant vascular leakage as a function of deficiencies in Tie2 downstream signaling products such as NO (David et al., 2012; Yeo et al., 2008). Given the observed detrimental effects of impaired Ang2 expression seen in other disease pathologies, and the importance of Ang1/Ang2 interactions in Tie2 signalling, we sought to evaluate Ang2 expression within DMD.

Our results show that in young mice, there were no significant differences in relative Ang2 mRNA expression. However, Ang2 protein concentrations were significantly elevated in young *mdx/utrn*$^{+/+}$ and young *mdx/utrn*$^{+/-}$ mice relative to the WT. The discrepancy between the observed mRNA and protein data may be explained by differences in post-transcription processes and energy abundance (Liu et al., 2016). The initial upregulation of Ang2 protein, prior to the onset of fibrosis, may help to facilitate the inflammatory response and initiate angiogenesis within the ischemic tissue, a crucial step in tissue regeneration. In the absence of Ang2, Tie2-active endothelial cells are unable to elicit an effective inflammatory response due to the inability to express cell adhesion molecules, thus impairing leukocyte infiltration (Ulrike. Fiedler et al., 2006; Hughes et al., 2003). Ang2-mediated inactivation of Tie2 indirectly activates NFκβ as well as the transcription factor FOXO1 which upregulates Ang2, thereby forming a positive feedback loop. This increase in Ang2 protein concentration seen within *mdx/utrn*$^{+/-}$ mice also correlates with a proteome profiling analysis of young 4-10-year-old human DMD patients which reported elevated Ang2 protein levels in patient serums (Hathout et al., 2019). Ang2 is also known to be capable of directly mediating endothelial cell differentiation and sprouting angiogenesis through interactions with integrin β1 on Tie2-negative endothelial cells in the presence of VEGF (Hakanpaa et al., 2015). In the absence of VEGF however, Ang2 induces endothelial cell apoptosis and vessel regression (Ivan et al., 2002). VEGF expression is downregulated in dystrophic satellite cells (Rhoads et al., 2013). Additionally, our lab has previously shown that VEGF concentration is significantly decreased in diaphragm tissue of 9-10 weeks-old *mdx/utrn*$^{+/-}$ mice (Gutpell et al., 2017). Thus, a prolonged elevation in Ang2 concentration may contribute to the detrimental vascular defects in DMD such as vessel regression, rather than supporting regenerating and inducing angiogenesis. As such, previously demonstrated administration of VEGF may help initiate angiogenesis and inhibit Ang2-mediated endothelial cell apoptosis and vessel regression within dystrophic tissue. Additional administration of Ang1 may skew the Ang1/Ang2 ratio towards Ang1 and allow for Tie2 activation and vessel maturation and stabilization.

Interestingly, neither of the aged 15-20 week-old *mdx/utrn*$^{+/+}$ mice nor the 15-20 week-old *mdx/utrn*$^{+/-}$ mice had significantly higher Ang2 concentrations compared to the WT. Qualitative analysis of H&E and Masson's Trichrome staining showed that chronic

inflammation and fibrosis were indeed profound in the diaphragm tissue of *mdx/utrn*$^{+/-}$ mice at this age, while similar symptoms present themselves in *mdx/utrn*$^{+/+}$ mice diaphragm as well. Previous serum analysis in Becker muscular dystrophy patients has also associated elevated Ang2 concentrations with higher degrees of skeletal myopathy (Kaese et al., 2017). Thus, we had initially hypothesized that Ang2 would be persistently upregulated in the DMD murine models at this age. When comparing Ang2 protein expression data between the two age cohorts, all three genotypes had an upwards trend in Ang2 concentration over time. Therefore, although no significant differences in Ang2 concentration were found in the mature age group, the level of Ang2 expression was sustained. This sustained increase in Ang2 coupled with a decrease in Ang1 expression results in an Ang1/Ang2 ratio that may shift away from Tie2 activation and vascular stability signalling to an inflamed endothelium phenotype.

5.4 Ang1/Ang2 ratio is skewed towards Ang2 in mature mdx/utrn+/- mice relative to the age-matched wild-type

Decreased Ang1/Ang2 ratios have been associated with several pathologies including sepsis, cancer, and metabolic disorders (David et al., 2012; Yeo et al., 2008). This is because the Ang1/Ang2 ratio can mediate Tie2 activation or inhibition. Thus, the Ang1/Ang2 ratio can be used as both a prognostic biomarker of endothelial activation and vascular permeability. However, there is a lack of information regarding Ang1/Ang2 ratio characterization in degenerative myopathies. To the best of our knowledge, this is the first study to examine the Ang1/Ang2 ratio in DMD. Here, we show that Ang1/Ang2 protein ratios were significantly lower in DMD murine models compared to the age-matched WT controls. This change in the ratio may reflect the inflammatory and ischemic conditions within the skeletal tissue of DMD mice. The decrease in Ang1/Ang2 ratio, and thus inhibition of Ang1 signalling, is required for the endothelium to exit from its quiescent state and move into an active state that can effectively respond to inflammatory and angiogenic signals. However, a chronically decreased Ang1/Ang2 ratio due to persistent Ang2 signalling and the resultant inability to return to a quiescent state partly mediated by a high Ang1/Ang2 ratio results in chronically leaky vasculature that cannot support functional perfusion, leading to tissue ischemia. This may explain why previous administration of VEGF alone into the similarly fibrotic

gastrocnemius tissue was unable to induce mature vessel formation. With the subsequent administration of Ang1, it may have acted to shift the Ang1/Ang2 ratio towards Ang1 and allow for Ang1-mediated Tie2 activation and the conclusion of the angiogenic cascade.

The shift from a low Ang1/Ang2 ratio to an elevated one is required in angiogenesis for the maturation of newly formed vessels. It is possible that the persistently low Ang1/Ang2 ratio in *mdx/utrn*$^{+/-}$ partially contributes to the reduced functional perfusion and angiogenic defects seen in its disease pathology. It is interesting to note that Ang1/Ang2 ratio was lower in the older age group for all genotypes. The decrease in Ang1/Ang2 ratio in *mdx/utrn*$^{+/-}$ appears to be mediated primarily by the decrease in Ang1 concentration while changes in *mdx/utrn*$^{+/+}$ and WT ratios appear to be due to increased Ang2. The decrease in Ang1 seen in *mdx/utrn*$^{+/-}$ mice may be due to the previously mentioned deficiency in Ang1 expressing cells. The increase in Ang2 seen in *mdx/utrn*$^{+/+}$ and WT mice may be due to increased tissue mass and vascularization in the mature mice. Protein analysis was done using whole-tissue lysates; thus, one limitation of this study is the inability to differentiate between Ang2 stored within Weibel-Palade bodies (WPB) and actively released Ang2. Lastly, Ang2 in physiological conditions can be a context-dependent Tie2 agonist and antagonist. Evidence has shown that although Ang2 inhibits Ang1-mediated Tie2 auto-phosphorylation, Ang2 itself can induce Tie2 phosphorylation and Akt phosphorylation (Yuan et al., 2009). However, in the context of inflammation, Ang2 signalling in Tie2 is antagonistic. The decrease in the Ang1/Ang2 ratio seen in the dystrophic diaphragm of *mdx/utrn*$^{+/-}$ mouse may result in Ang2-mediated Tie2 inhibition and vascular destabilization. Thus, it is necessary to quantify Tie2 and pTie2 levels to verify levels of vascular stability.

5.5 No significant differences in Tie2 expression

Tie2 phosphorylation in the quiescent endothelium helps to promote pro-survival signals through the downstream expression of survivin and eNOS, anti-inflammation through NFkB and FOXO1 inhibition, and inter-endothelial cell stability through VE-cadherin dephosphorylation (Daly et al., 2004; Fukuhara et al., 2010; Gavard et al., 2008; Tadros et al., 2003; Wong et al., 1997). From the Ang1/Ang2 data, we then hypothesized that pTie2 concentrations would be low relative to total Tie2 concentrations due to Ang2 mediated inhibition of Tie2 phosphorylation. Here we show that Tie2 mRNA was found to be

significantly lower in young *mdx/utrn*$^{+/-}$ mice relative to WT. However, when Tie2 protein concentration was assessed, *mdx/utrn*$^{+/-}$ mice had higher Tie2 protein concentration compared to WT. While Tie2 mRNA is upregulated during wound healing, it has been reported that Tie2 expression is reduced in conditions relating to severe vascular complications (Chandra et al., 2016). Tie2, upon Ang1 or Ang2 binding and activation, is also known to release the ligand, internalize, and then be targeted for degradation. Thus, it is possible that despite the reduction in Tie2 mRNA expression, Tie2 protein concentration remains elevated due to a high surface presentation of Tie2 in response to its inhibition by Ang2. Another factor may be the reduction of VEGF in DMD. Previous studies have shown that VEGF-induced sprouting angiogenesis is capable of inducing Tie2 cleavage and downregulating Tie2 mRNA expression in angiogenic endothelial cells (Findley et al., 2007). The decrease in Tie2 mRNA may be correlated with the level of sprouting angiogenesis occurring within the tissue of *mdx/utrn*$^{+/-}$ mice as endogenous muscle repair attempts to repair the damaged muscle fibers. However, our lab has previously shown a significant decrease in VEGF protein expression in the diaphragm tissue of 9-10 week-old *mdx/utrn*$^{+/-}$ mice. Therefore, it is also possible that in the absence of high VEGF concentrations, Tie2 ectodomain cleavage does not occur, resulting in higher Tie2 protein presentation. Analysis of Tie2 mRNA levels and protein expression in mature mice showed similar trends seen in younger mice. It is also important to note that while Tie2 is most prominently expressed on endothelial cells, it is also expressed on a variety of other cell types, including satellite cells, pericytes, macrophages, and fibroblasts. Thus, without being able to isolate endothelial Tie2 expression, changes in Tie2 concentration observed in this study must take into consideration changes in other cell populations.

5.6 Phosphorylated Tie2 expression and decreased pTie2/Tie2 ratio in mature mdx/utrn+/- mice

Due to Tie2's role in maintaining vascular quiescence and stability, Tie2 is constitutively activated in physiological conditions and inhibited in the context of inflammation. Tie2 phosphorylation is also required for differentiation between tip and stalk cells and vessel maturation during angiogenesis (Savant et al., 2015). Quantification of pTie2 in young mice revealed a non-significant decrease in phosphorylated protein concentration within the

diaphragm tissue of *mdx/utrn*$^{+/-}$ mice. This decrease did not correlate with the significant decrease in Ang1/Ang2 ratio shown previously. It is then possible that at 8-10 weeks of age, Tie2 phosphorylation, vascular stability, and angiogenic capabilities in *mdx/utrn*$^{+/-}$ mice are conserved. Young *mdx/utrn*$^{+/-}$ also demonstrated a slight decrease in mean pTie2 concentration, despite the significant change in Ang1/Ang2 protein concentrations. A possible explanation in which regenerative capabilities and angiogenesis are functional may also be applied to *mdx/utrn*$^{+/+}$ mice. Interestingly, when looking at pTie2 data in mature mice, all three genotypes had similar average pTie2 concentrations with large standard deviations. This variability in concentration was also seen with Tie2 concentration data for the mature mice. Although initially puzzling, when pTie2/total Tie2 analysis was performed, a significant trend towards decreased pTie2/Tie2 ratios was observed in *mdx/utrn*$^{+/-}$ mice compared to WT. A non-significant decreasing trend was also seen in *mdx/utrn*$^{+/+}$ mice. To eliminate the possibility of the decrease in pTie2/Tie2 ratio due to other inhibitory factors, VEPTP expression, a prominent endothelial cell-specific receptor tyrosine phosphatase, was also evaluated. No changes in VEPTP expression were observed between the different genotypes at 15-20 weeks of age. It is thus unlikely that the observed changed in the pTie2/Tie2 ratio is due to elevated expression of VEPTP. The decrease in pTie2/Tie2 ratio seen in the mature mice correlates more similarly with the decrease in Ang1/Ang2 ratio. As such, the significant decrease in Ang1/Ang2 ratios may result in continuous Ang2 inhibition of Ang1-mediated Tie2 phosphorylation in the diaphragm tissue of mature *mdx/utrn*$^{+/+}$ mice, leading to vascular instability and angiogenic dysfunction.

5.7 Dysregulated Akt Signalling

The second aim of this project was to evaluate changes in downstream signalling targets of Tie2 in DMD. One major target that was selected for analysis was Akt. PI3K-mediated Akt phosphorylation is a major downstream target of Tie2 and is known to contribute to cell survival, anti-inflammation, and maturation (Shiojima et al., 2002; Somanath et al., 2006). Elevated Akt is part of physiological muscle regeneration, and several-fold increases in both pAkt and total Akt protein concentrations in the skeletal muscle of mdx mouse and *mdx/utrn*$^{-/-}$ mouse, as well as young DMD patient biopsies, have previously been reported (Dogra et al., 2006). Additionally, conditional Akt overexpression in mdx mice has previously been

shown to enhance muscle mass and myofiber cross-sectional area (Kim et al., 2011). In this study, analysis of relative pAkt levels did not reveal any significant differences between WT, *mdx/utrn*$^{+/+}$, and *mdx/utrn*$^{+/-}$ mice diaphragms. Despite the indifferences in pAkt levels, total Akt protein expression was higher in mature 15-20 weeks-old *mdx/utrn*$^{+/-}$ mice diaphragms compared to the WT. Although Akt phosphorylation and total Akt expression have been actively cited to be elevated within the skeletal muscles of mdx mouse and DMD patients, the discrepancy between pAkt and total Akt levels has also been noted (Dogra et al., 2006; Peter et al., 2006). It has thus been hypothesized that Akt activation in DMD may be somewhat defective.

Akt signalling in endothelial cells is crucial in both established vasculature as well as vessels undergoing neovascularization. Studies have been shown Akt signalling to be non-essential in maintaining endothelial survival in established vessels, but rather, Akt-mediated activation of Notch signalling regulates the interactions between endothelial cells and mural cells such as pericytes and vascular smooth muscle cells (Kerr et al., 2016; Si et al., 2020). Specifically, Akt knockout has been shown to induce pericyte and smooth vascular cell death (Ha et al., 2019). It is possible then that Akt dysfunction in DMD may result in abnormal mural cell function or possibly a loss of mural cells. This may be further evidence that the decreased Ang1 concentration seen earlier may be due to a deficiency in mural cells. In immature angiogenic cells, however, Akt signalling is vital as it serves to induce an anti-apoptotic effect, promote VEGF expression, and regulating endothelial cell migration. Indeed, inhibition of Akt signalling severely attenuates ischemia-mediated blood flow recovery and angiogenesis (Ackah et al., 2005). As such, the apparent decrease in overall Akt phosphorylation may be a sign of reduced vascular stability as well as reduced angiogenesis. Aside from Ang1, several other cytokines such as insulin-like growth factor-1 (IGF-1), sphingosine-1-phosphate (S1P), reactive oxygen species (ROS), corticosteroids, and VEGF can activate PI3K mediated Akt signalling as well. Previous studies have implicated a reduction in autophagy due to altered Akt activation in DMD (De Palma et al., 2012). Autophagy has been shown to promote angiogenesis. As such, changes in Akt signalling may directly inhibit angiogenesis through decreased VEGF expression and reduced pro-survival signalling as well as indirectly inhibiting angiogenesis through Akt-mediated autophagy

dysfunction. Lastly, Akt signalling is active in myocytes associated with skeletal muscle growth and muscle regeneration as it regulates the compensatory muscular hypertrophy that is a hallmark of DMD (Peter et al., 2006). A large limitation of this study is the inability to delineate Akt expression and activation differences between myocytes and endothelial cells within the skeletal tissue. Thus, we aimed to analyze an endothelial cell-specific downstream target of Akt signalling as a means of characterizing Tie2-mediated Akt signaling.

5.8 No Significant Differences in eNOS Expression and Phosphorylation

One major target of Akt downstream signalling within endothelial cells is Akt mediated-eNOS expression, phosphorylation, and NO production. Previous studies have looked at eNOS expression in canine models of DMD and found reduced eNOS expression and reduced cyclic guanosine monophosphate (cGMP) concentrations, leading to increased vascular leakiness (Dabiré et al., 2011). The observed vascular defect was able to be resolved directly through the upregulation of eNOS. Indeed, elevations in Ang2 concentrations in sepsis are inversely proportional to NO-mediated microvascular reactivity (Davis et al., 2010). Interestingly, our results did not show any significant differences in either eNOS expression or eNOS phosphorylation between the DMD murine models and WT at neither 8-10 weeks of age nor 15-20 weeks of age. Ang1 induced beneficial effects have been shown to be partly mediated via eNOS phosphorylation and NOS production. It has been previously reported that Ang1 induced angiogenesis relies upon eNOS *in vitro*, as Ang1 induced capillary-like tube formation using HUVECs was abolished by the NO inhibitor L-NAME and $eNOS^{-/-}$ mice exhibited decreased neovascularization upon an Ang1 variant treatment compared to WT (Babaei et al., 2003). Conversely, Ang1 mediated NO production leads to increased vascular dilation and maintenance, upregulation of VE-cadherin, and inhibition of VE-cadherin phosphorylation, all functioning to promote stabilization of the endothelial barrier. As such, NO within endothelial cells appears to be important in both maintaining vascular stability as well as angiogenesis initiation. Due to the inflammatory and regenerative nature of the tissue, it is unlikely that eNOS activation and NO activity in the dystrophic tissue is strictly vascular maintenance. Rather, it most likely serves to promote the initiation of angiogenesis within DMD. As such, the indifference in eNOS expression and activation

may be a sign of dysregulated Akt signalling and dysregulated angiogenesis as eNOS activity has been positively correlated with ischemic angiogenesis, thus, it should be elevated within the dystrophic tissues. Causes for eNOS dysfunction may be due to a reduction in upstream signalling such as a reduction in VEGF, or as shown in this study, a reduction in Ang1 signalling. Thus, taking into account all the results from this study, it is possible that a significant decrease in Ang1 and increase in Ang2 inhibits Tie2 phosphorylation, thus altering Akt signalling and reducing eNOS expression and activation within the dystrophic diaphragm tissue of mature *mdx/utrn*$^{+/-}$ mice.

5.9 Limitations

This is the first study to use the *mdx/utrn*$^{+/-}$ mouse model to study the endogenous Ang1/Ang2 ratios present with the skeletal muscle of DMD. However, there are several limitations to this study that must be addressed. Firstly, this study only focused on the diaphragm tissue. It was chosen due to the high contractibility of the muscle and previous reports of degeneration and fibrosis present in this tissue. However, the hallmark of fibrosis is the displacement of myofibers and vasculature alike with collagen within the tissue. The difference in myofiber and vessel density may affect the RT-qPCR and proteomics results, leading to inaccuracies. As such, it represents a more dystrophic tissue that might not be representative of other tissues within the host. DMD is a systemic disease, and thus further serum analysis and other commonly damaged muscles such as the gastrocnemius should also be evaluated in the future.

Secondly, because the mRNA and protein data were collected from whole tissue lysates, it is impossible to differentiate the expression between different cell populations. As previously mentioned, Ang1, Tie2, and Akt are all expressed by several different cell types. As such, we are unable to differentiate the percentage of total Tie2 protein expressed by pericytes compared to endothelial cells. Thus, the reported pTie2/Tie2 ratio may not be representative of the actual ratio present on endothelial cells, resulting in a skewed perception of Tie2 signalling. Additionally, protein analysis of both Ang1 and Ang2 and the ratio between the two may not directly translate into their availability for Tie2 binding. One reason is due to the inability of Ang1 to bind to Tie2 as monomers. Instead, oligomerization and multimerization are required for Ang1-Tie2 binding (Kyung-Tae et al., 2005). However,

Ang1 monomers are present within the tissue and bind to integrins on myocytes, and promote pro-survival signalling pathways. Thus, total Ang1 protein analysis may reflect a higher concentration of Ang1 than is available for Tie2 activation. Another reason is due to Ang2 being stored within WPBs prior to their secretion. Because whole tissue lysate was assessed rather than serum, we cannot differentiate between secreted Ang2 which is actively able to bind to Tie2, and Ang2 stored in WPB that cannot contribute to signalling. Thus, Ang2 concentrations may be artificially inflated.

Thirdly, although Akt and eNOS are both major downstream signalling targets involved in Tie2 activation, they also have several different upstream kinase activators and different phosphorylation sites. As such, alterations in Akt signalling and eNOS activation reported in this study cannot be singularly attributed to changes in Tie2 activation. In addition, Protein analysis of Akt and eNOS, as well as their phosphorylation, were assessed using western blots. This may introduce inaccuracies due to western blots being only semi-quantitative and direct comparisons between different blots being unreliable, even if the blots were run in parallel.

Lastly, this study used both female and male murine models of DMD. DMD is an x-linked degenerative disease, thus, it typically affects males to a great degree than females. Indeed, at 12 months old, female *mdx* mice display higher vascular density and increased reperfusion after ischemic stress compared to their male counterparts (Guéniot et al. 2016). However, no vascular differences between sex at younger ages have been reported. The usage of a mixed-sex cohort is common in *mdx* mice literature. Due to the low sample size used in this study, statistical analysis did not factor in sex as a covariant.

5.10 Future Directions

This study, in combination with previous work from our lab, provides further evidence that Ang1 may be beneficial for vascular therapy in DMD. We have now shown tissue-specific reductions in Ang1 expression and upregulation in Ang2 expression. This leads to an Ang2-skewed Ang1/Ang2 ratio that promotes the inhibition of Tie2 signaling. Without Tie2 activation, vascular stability and angiogenic maturation are hindered. To promote angiogenesis and support endogenous muscle repair, activation of Ang1-mediated Tie2

signaling and downstream Akt activation and NO production is required. However, further investigation is required to determine cell-specific expression profiles. In this regard, future experiments should pursue the isolation of dystrophic endothelial cells and pericytes and evaluate Tie2 and Ang2 expression in endothelial cells and Tie2 and Ang1 expression in pericytes. This will allow us to paint a clearer picture in determining the source of the changes in the Ang1/Ang2 and pTie2/Tie2 ratios observed in this study. Furthermore, experiments involving the culturing of dystrophic endothelial cells and pericytes will allow for greater characterization of these populations within DMD. Evaluation of their angiogenic capabilities through quantification of Akt and eNOS phosphorylation as well as NO production in response to angiogenic factors such as Ang1 and VEGF as well as their response to proinflammatory serum isolated from dystrophic models would provide greater insight into the vascular defects within DMD. Additionally, we have briefly touched upon the hypothesis of pericyte deficiencies within DMD being a possible source of decreased Ang1 concentrations due to elevated Ang2 concentrations resulting in pericyte detachment and pericyte-myofibroblast differentiation. Thus, future experiments should evaluate pericyte coverage within dystrophic tissues using fluorescence-activated cell sorting or high-resolution fluorescence microscopy such as confocal and multiphoton microscopy. To this end, our lab has begun the investigation of utilizing immunofluorescence (Appendix B), immunohistochemistry (Appendix C), *ex vivo* micro-CT (Appendix D), and *ex vivo* multiphoton microscopy (Appendix E) to characterize endothelial cell and pericyte specific expression of Ang1, Ang2, and Tie2 as well as characterizing vasculature density, vasculature branching, and pericyte coverage in the microvasculature of dystrophic tissue. Unfortunately, due to health and safety precautions that were implemented in March 2020 in response to the COVID-19 pandemic, these key experiments, several of which required intensive inter-disciplinary collaborations, were halted at the proof-of-concept and antibody selection and validation stages. These experiments will resume following my MSc defence for publication purposes.

Taken together, characterization of the Ang1/Ang2 ratio and Tie2 activation opens another avenue of vascular therapy for DMD. Although our lab has shown that increasing Ang1 concentration, and possibly increasing the Ang1/Ang2 ratio may be beneficial in eliciting mature vasculature formation, it may also be beneficial to investigate anti-Ang2 therapies in

DMD. In the context of DMD, reducing free Ang2 may shift the Ang1/Ang2 back into an Ang1-favoured ratio that promotes Tie2 activation, maturation of the angiogenic cascade, and establishing a stabilized endothelium that can support functional perfusion and endogenous muscle repair.

Bibliography

Abbs, S., Tuffery-Giraud, S., Bakker, E., Ferlini, A., Sejersen, T., & Mueller, C. R. (2010). Best Practice Guidelines on molecular diagnostics in Duchenne/Becker muscular dystrophies. *Neuromuscular disorders : NMD, 20*(6), 422-427

Abou-Khalil, R., Le Grand, F., Pallafacchina, G., Valable, S., Authier, F.-J., Rudnicki, M. A., . . . Chazaud, B. (2009). Autocrine and Paracrine Angiopoietin 1/Tie-2 Signaling Promotes Muscle Satellite Cell Self-Renewal. *Cell stem cell, 5*(3), 298-309

Ackah, E., Yu, J., Zoellner, S., Iwakiri, Y., Skurk, C., Shibata, R., . . . Sessa, W. C. (2005). Akt1/protein kinase Bα is critical for ischemic and VEGF-mediated angiogenesis. *The Journal of clinical investigation, 115*(8), 2119-2127

Aguilera, K. Y., Aguilera, K. Y., Brekken, R. A., & Brekken, R. A. (2014). Recruitment and retention: factors that affect pericyte migration. *Cellular and molecular life sciences : CMLS, 71*(2), 299-309

Akwii, R. G., Sajib, M. S., Zahra, F. T., & Mikelis, C. M. (2019). Role of Angiopoietin-2 in Vascular Physiology and Pathophysiology. *Cells (Basel, Switzerland), 8*(5), 471

Arai, F., Hirao, A., Ohmura, M., Sato, H., Matsuoka, S., Takubo, K., . . . Suda, T. (2004). Tie2/Angiopoietin-1 Signaling Regulates Hematopoietic Stem Cell Quiescence in the Bone Marrow Niche. *Cell (Cambridge), 118*(2), 149-161

Armulik, A., Genové, G., & Betsholtz, C. (2011). Pericytes: Developmental, Physiological, and Pathological Perspectives, Problems, and Promises. *Developmental cell, 21*(2), 193-215

Armulik, A., Genove, G., Johansson, B. R., Betsholtz, C., MÄE, M., Nisancioglu, M. H., . . . Strittmatter, K. (2010). Pericytes regulate the blood-brain barrier. *Nature (London), 468*(7323), 557-561

Attwell, D., Mishra, A., Hall, C. N., O'Farrell, F. M., & Dalkara, T. (2016). What is a pericyte? *Journal of cerebral blood flow and metabolism : official journal of the International Society of Cerebral Blood Flow and Metabolism, 36*(2), 451-455

Avraamides, C. J., Varner, J. A., & Garmy-Susini, B. (2008). Integrins in angiogenesis and lymphangiogenesis. *Nature reviews. Cancer, 8*(8), 604-617

Babaei, S., Teichert-Kuliszewska, K., Zhang, Q., Jones, N., Dumont, D. J., & Stewart, D. J. (2003). Angiogenic actions of angiopoietin-1 require endothelium-derived nitric oxide. *The American journal of pathology, 162*(6), 1927-1936

Bach, J. R., & Martinez, D. (2011). Duchenne Muscular Dystrophy: Continuous Noninvasive Ventilatory Support Prolongs Survival. *Respiratory care, 56*(6), 744-750

Batra, A., Vohra, R. S., Chrzanowski, S. M., Hammers, D. W., Lott, D. J., Vandenborne, K., . . . Forbes, S. C. (2019). Effects of PDE5 inhibition on dystrophic muscle following an acute bout of downhill running and endurance training. *J Appl Physiol (1985), 126*(6), 1737-1745

Baum, O., Gübeli, J., Frese, S., Torchetti, E., Malik, C., Odriozola, A., . . . Tschanz, S. A. (2015). Angiogenesis-related ultrastructural changes to capillaries in human skeletal muscle in response to endurance exercise. *Journal of applied physiology (1985), 119*(10), 1118-1126

Belfall, B., Zubrzycka-Gaarn, E. E., Hodges, R. S., Worton, R. G., Ray, P. N., Talbot, J., . . . Karpati, G. (1988). The Duchenne muscular dystrophy gene product is localized in sarcolemma of human skeletal muscle. *Nature (London), 333*(6172), 466-469

Bergers, G., & Song, S. (2005). The role of pericytes in blood-vessel formation and maintenance. *Neuro-oncology, 7*(4), 452-464

Birbrair, A., Zhang, T., Wang, Z.-M., Messi, M. L., Enikolopov, G. N., Mintz, A., & Delbono, O. (2013). Skeletal muscle pericyte subtypes differ in their differentiation potential. *Stem cell research, 10*(1), 67-84

Blake, D. J., Tinsley, J. M., & Davies, K. E. (1996). Utrophin: a structural and functional comparison to dystrophin. *Brain Pathol, 6*(1), 37-47

Blanco, R., & Gerhardt, H. (2013). VEGF and Notch in tip and stalk cell selection. *Cold Spring Harbor perspectives in medicine, 3*(1), a006569-a006569

Bogdanovic, E., Nguyen, V. P., & Dumont, D. J. (2006). Activation of Tie2 by angiopoietin-1 and angiopoietin-2 results in their release and receptor internalization. *J Cell Sci, 119*(Pt 17), 3551-3560

Brenman, J. E., Chao, D. S., Xia, H., Aldape, K., & Bredt, D. S. (1995). Nitric oxide synthase complexed with dystrophin and absent from skeletal muscle sarcolemma in Duchenne muscular dystrophy. *Cell, 82*(5), 743-752

Brindle, N. P. J., Saharinen, P., & Alitalo, K. (2006). Signaling and functions of angiopoietin-1 in vascular protection. *Circulation research, 98*(8), 1014-1023

Brown, J. L., Cao, Z. A., Pinzon-Ortiz, M., Kendrew, J., Reimer, C., Wen, S., . . . Blakey, D. C. (2010). A human monoclonal anti-ANG2 antibody leads to broad antitumor activity in combination with VEGF inhibitors and chemotherapy agents in preclinical models. *Mol Cancer Ther, 9*(1), 145-156

Bushby, K. M. D., & Gardner-Medwin, D. (1993). The clinical, genetic and dystrophin characteristics of Becker muscular dystrophy: I. Natural history. *Journal of neurology, 240*(2), 98-104

Cai, J., Kehoe, O., Smith, G. M., Hykin, P., & Boulton, M. E. (2008). The Angiopoietin/Tie-2 System Regulates Pericyte Survival and Recruitment in Diabetic Retinopathy. *Investigative ophthalmology & visual science, 49*(5), 2163-2171

Campbell, K. P., Leveille, C. J., Ibraghimov-Beskrovnaya, O., Slaughter, C. A., Ervasti, J. M., & Sernett, S. W. (1992). Primary structure of dystrophin-associated glycoproteins linking dystrophin to the extracellular matrix. *Nature (London), 355*(6362), 696-702

Cappellari, O., Benedetti, S., Innocenzi, A., Tedesco, Francesco S., Moreno-Fortuny, A., Ugarte, G., . . . Cossu, G. (2013). Dll4 and PDGF-BB Convert Committed Skeletal Myoblasts to Pericytes without Erasing Their Myogenic Memory. *Developmental cell, 24*(6), 586-599

Carmeliet, P. (2000). VEGF gene therapy: stimulating angiogenesis or angioma-genesis? *Nat Med, 6*(10), 1102-1103

Chamberlain, J. S., Metzger, J., Reyes, M., Townsend, D., & Faulkner, J. A. (2007). Dystrophin-deficient mdx mice display a reduced life span and are susceptible to spontaneous rhabdomyosarcoma. *Faseb j, 21*(9), 2195-2204

Chandra, C. G., Sascha, D., Ruyang, Z., Anthony, B., Katelyn, M., Sarah, J. H., . . . Samir, M. P. (2016). Gene control of tyrosine kinase TIE2 and vascular manifestations of infections. *Proceedings of the National Academy of Sciences - PNAS, 113*(9), 2472-2477

Chang, N. C., Chevalier, F. P., & Rudnicki, M. A. (2016). Satellite Cells in Muscular Dystrophy – Lost in Polarity. *Trends in molecular medicine, 22*(6), 479-496

Chen, Y. T., Chang, F. C., Wu, C. F., Chou, Y. H., Hsu, H. L., Chiang, W. C., . . . Lin, S. L. (2011). Platelet-derived growth factor receptor signaling activates pericyte-myofibroblast transition in obstructive and post-ischemic kidney fibrosis. *Kidney Int, 80*(11), 1170-1181

Cho, C.-H., Kim, K. E., Byun, J., Jang, H.-S., Kim, D.-K., Baluk, P., . . . Koh, G. Y. (2005). Long-Term and Sustained COMP-Ang1 Induces Long-Lasting Vascular Enlargement and Enhanced Blood Flow. *Circulation research, 97*(1), 86-94

Choi, H.-J., Zhang, H., Park, H., Choi, K.-S., Lee, H.-W., Agrawal, V., . . . Kwon, Y.-G. (2015). Yes-associated protein regulates endothelial cell contact-mediated expression of angiopoietin-2. *Nature communications, 6*(1), 6943-6943

Ciafaloni, E., Fox, D. J., Pandya, S., Westfield, C. P., Puzhankara, S., Romitti, P. A., . . . Moxley, R. T. (2009). Delayed Diagnosis in Duchenne Muscular Dystrophy: Data from the Muscular Dystrophy Surveillance, Tracking, and Research Network (MD STARnet). *The Journal of Pediatrics, 155*(3), 380-385

Dabiré, H., Barthélémy, I., Blanchard-Gutton, N., Sambin, L., Sampedrano, C. C., Gouni, V., . . . Su, J. B. (2011). Vascular endothelial dysfunction in Duchenne muscular

dystrophy is restored by bradykinin through upregulation of eNOS and nNOS. *Basic Research in Cardiology, 107*(1), 240

Daly, C., Pasnikowski, E., Burova, E., Wong, V., Aldrich, T. H., Griffiths, J., . . . Rudge, J. S. (2006). Angiopoietin-2 functions as an autocrine protective factor in stressed endothelial cells. *Proc Natl Acad Sci U S A, 103*(42), 15491-15496

Daly, C., Wong, V., Burova, E., Wei, Y., Zabski, S., Griffiths, J., . . . Rudge, J. S. (2004). Angiopoietin-1 modulates endothelial cell function and gene expression via the transcription factor FKHR (FOXO1). *Genes & development, 18*(9), 1060-1071

Darras, B. T., Jones, J. H. R., Jr., Ryan, M. M., De Vivo, D. C., & De Vivo, D. C. (2014). *Neuromuscular Disorders of Infancy, Childhood, and Adolescence : A Clinician's Approach*. San Diego, UNITED STATES: Elsevier Science & Technology.

David, S., Ghosh, C. C., Mukherjee, A., & Parikh, S. M. (2011). Angiopoietin-1 requires IQGAP1 to activate Rac1 and promote endothelial barrier defense. *Arteriosclerosis, thrombosis, and vascular biology, 31*(11), 2643-2652

David, S., Mukherjee, A., Ghosh, C. C., Yano, M., Khankin, E. V., Wenger, J. B., . . . Parikh, S. M. (2012). Angiopoietin-2 may contribute to multiple organ dysfunction and death in sepsis*. *Critical care medicine, 40*(11), 3034-3041

Davis, J. S., Yeo, T. W., Piera, K. A., Woodberry, T., Celermajer, D. S., Stephens, D. P., & Anstey, N. M. (2010). Angiopoietin-2 is increased in sepsis and inversely associated with nitric oxide-dependent microvascular reactivity. *Critical care (London, England), 14*(3), R89-R89

De Palma, C., Morisi, F., Cheli, S., Pambianco, S., Cappello, V., Vezzoli, M., . . . Clementi, E. (2012). Autophagy as a new therapeutic target in Duchenne muscular dystrophy. *Cell Death & Disease, 3*(11), e418-e418

De Smet, F., Segura, I., De Bock, K., Hohensinner, P. J., & Carmeliet, P. (2009). Mechanisms of vessel branching: filopodia on endothelial tip cells lead the way. *Arterioscler Thromb Vasc Biol, 29*(5), 639-649

Deconinck, N. M. D. P., & Dan, B. M. D. P. (2007). Pathophysiology of Duchenne Muscular Dystrophy: Current Hypotheses. *Pediatric neurology, 36*(1), 1-7

del Gaudio, D., Yang, Y., Boggs, B. A., Schmitt, E. S., Lee, J. A., Sahoo, T., . . . Eng, C. M. (2008). Molecular diagnosis of Duchenne/Becker muscular dystrophy: enhanced detection of dystrophin gene rearrangements by oligonucleotide array-comparative genomic hybridization. *Hum Mutat, 29*(9), 1100-1107

Delaney, K., Kasprzycka, P., Ciemerych, M. A., & Zimowska, M. (2017). The role of TGF-β1 during skeletal muscle regeneration. *Cell biology international, 41*(7), 706-715

Dellavalle, A., Maroli, G., Covarello, D., Azzoni, E., Innocenzi, A., Perani, L., . . . Cossu, G. (2011). Pericytes resident in postnatal skeletal muscle differentiate into muscle fibres and generate satellite cells. *Nature communications, 2*(1), 499-499

Dellavalle, A., Sampaolesi, M., Tonlorenzi, R., Tagliafico, E., Sacchetti, B., Perani, L., . . . Cossu, G. (2007). Pericytes of human skeletal muscle are myogenic precursors distinct from satellite cells. *Nature cell biology, 9*, 255+

Derek, J. B., Andrew, W., Sarah, E. N., & Kay, E. D. (2002). Function and Genetics of Dystrophin and Dystrophin-Related Proteins in Muscle. *Physiological Reviews, 82*(2), 291-329

Desguerre, I., Arnold, L., Vignaud, A., Cuvellier, S., Yacoub-youssef, H., Gherardi, R. K., . . . Chazaud, B. (2012). A new model of experimental fibrosis in hindlimb skeletal muscle of adult mdx mouse mimicking muscular dystrophy. *Muscle & nerve, 45*(6), 803-814

Dogra, C., Changotra, H., Wergedal, J. E., & Kumar, A. (2006). Regulation of phosphatidylinositol 3-kinase (PI3K)/Akt and nuclear factor-kappa B signaling pathways in dystrophin-deficient skeletal muscle in response to mechanical stretch. *Journal of Cellular Physiology, 208*(3), 575-585

Duan, D. (2018). Micro-Dystrophin Gene Therapy Goes Systemic in Duchenne Muscular Dystrophy Patients. *Human gene therapy, 29*(7), 733-736

Dulauroy, S., Di Carlo, S. E., Langa, F., Eberl, G., & Peduto, L. (2012). Lineage tracing and genetic ablation of ADAM12(+) perivascular cells identify a major source of profibrotic cells during acute tissue injury. *Nat Med, 18*(8), 1262-1270

Dumont, N. A., Wang, Y. X., von Maltzahn, J., Pasut, A., Bentzinger, C. F., Brun, C. E., & Rudnicki, M. A. (2015). Dystrophin expression in muscle stem cells regulates their polarity and asymmetric division. *Nat Med, 21*(12), 1455-1463

Ennen, J. P., Verma, M., & Asakura, A. (2013). Vascular-targeted therapies for Duchenne muscular dystrophy. *Skelet Muscle, 3*(1), 9

Fagiani, E., & Christofori, G. (2013). Angiopoietins in angiogenesis. *Cancer Lett, 328*(1), 18-26

Fang, Y., Li, C., Shao, R., Yu, H., Zhang, Q., & Zhao, L. (2015). Prognostic significance of the angiopoietin-2/angiopoietin-1 and angiopoietin-1/Tie-2 ratios for early sepsis in an emergency department. *Critical Care, 19*(1), 367

Felcht, M., Luck, R., Schering, A., Seidel, P., Srivastava, K., Hu, J., . . . Augustin, H. G. (2012). Angiopoietin-2 differentially regulates angiogenesis through TIE2 and integrin signaling. *The Journal of clinical investigation, 122*(6), 1991-2005

Feron, O., & Balligand, J.-L. (2006). Caveolins and the regulation of endothelial nitric oxide synthase in the heart. *Cardiovascular Research, 69*(4), 788-797

Ferruccio, G., Daniela, V., Jeffrey, B. C., Maomi, L., Samson, W. F., Maofu, F., . . . Michael, P. L. (2000). Transgenic Overexpression of Caveolin-3 in Skeletal Muscle Fibers Induces a Duchenne-Like Muscular Dystrophy Phenotype. *Proceedings of the National Academy of Sciences - PNAS, 97*(17), 9689-9694

Fiedler, Reiss, Y., Scharpfenecker, M., Grunow, V., Koidl, S., Thurston, G., . . . Augustin, H. G. (2006). Angiopoietin-2 sensitizes endothelial cells to TNF-α and has a crucial role in the induction of inflammation. *Nat Med, 12*(2), 235-239

Fiedler, U., & Augustin, H. G. (2006). Angiopoietins: a link between angiogenesis and inflammation. *Trends Immunol, 27*(12), 552-558

Fiedler, U., Scharpfenecker, M., Koidl, S., Hegen, A., Grunow, V., Schmidt, J. M., . . . Augustin, H. G. (2004). The Tie-2 ligand Angiopoietin-2 is stored in and rapidly released upon stimulation from endothelial cell Weibel-Palade bodies. *Blood, 103*(11), 4150-4156

Fiedler, U., Vajkoczy, P., Preissner, K. T., Reiss, Y., Scharpfenecker, M., Augustin, H. G., . . . Thurston, G. (2006). Angiopoietin-2 sensitizes endothelial cells to TNF-α and has a crucial role in the induction of inflammation. *Nat Med, 12*(2), 235-239

Findley, C. M., Cudmore, M. J., Ahmed, A., & Kontos, C. D. (2007). VEGF Induces Tie2 Shedding via a Phosphoinositide 3-Kinase/Akt–Dependent Pathway to Modulate Tie2 Signaling. *Arteriosclerosis, thrombosis, and vascular biology, 27*(12), 2619-2626

Flanigan, K. M., Dunn, D. M., von Niederhausern, A., Soltanzadeh, P., Gappmaier, E., Howard, M. T., . . . Weiss, R. B. (2009). Mutational spectrum of DMD mutations in dystrophinopathy patients: application of modern diagnostic techniques to a large cohort. *Hum Mutat, 30*(12), 1657-1666

Fleming, I. (2010). Molecular mechanisms underlying the activation of eNOS. *Pflugers Arch, 459*(6), 793-806

Folkman, J., & Klagsbrun, M. (1987). Angiogenic factors. *Science, 235*, 442+

Fraser, H. M., & Wulff, C. (2003). Angiogenesis in the corpus luteum. *Reproductive biology and endocrinology : RB&E, 1*, 88-88

Frye, M., Dierkes, M., Küppers, V., Vockel, M., Tomm, J., Zeuschner, D., . . . Vestweber, D. (2015). Interfering with VE-PTP stabilizes endothelial junctions in vivo via Tie-2 in the absence of VE-cadherin. *The Journal of experimental medicine, 212*(13), 2267-2287

Fujisawa, T., Wang, K., Niu, X. L., Egginton, S., Ahmad, S., Hewett, P., . . . Ahmed, A. (2017). Angiopoietin-1 promotes atherosclerosis by increasing the proportion of circulating Gr1+ monocytes. *Cardiovasc Res, 113*(1), 81-89

Fukuhara, S., Sako, K., Noda, K., Zhang, J., Minami, M., & Mochizuki, N. (2010). Angiopoietin-1/Tie2 receptor signaling in vascular quiescence and angiogenesis. *Histol Histopathol, 25*(3), 387-396

Fuxe, J., Tabruyn, S., Colton, K., Zaid, H., Adams, A., Baluk, P., . . . McDonald, D. M. (2011). Pericyte requirement for anti-leak action of angiopoietin-1 and vascular remodeling in sustained inflammation. *The American journal of pathology, 178*(6), 2897-2909

Gail, D. T., Mikael, S., Kim, S. L., Paul, L. H., James, T. S., & Ronald, G. V. (1998). Impaired Metabolic Modulation of α -adrenergic Vasoconstriction in Dystrophin-Deficient Skeletal Muscle. *Proceedings of the National Academy of Sciences - PNAS, 95*(25), 15090-15095

Gao, Q. Q., & McNally, E. M. (2015). The Dystrophin Complex: Structure, Function, and Implications for Therapy. *Compr Physiol, 5*(3), 1223-1239

Gavard, J., Patel, V., & Gutkind, J. S. (2008). Angiopoietin-1 Prevents VEGF-Induced Endothelial Permeability by Sequestering Src through mDia. *Developmental cell, 14*(1), 25-36

Gerhardt, H., Golding, M., Fruttiger, M., Ruhrberg, C., Lundkvist, A., Abramsson, A., . . . Betsholtz, C. (2003). VEGF guides angiogenic sprouting utilizing endothelial tip cell filopodia. *The Journal of cell biology, 161*(6), 1163-1177

Gerli, M. F. M., Moyle, L. A., Benedetti, S., Ferrari, G., Ucuncu, E., Ragazzi, M., . . . Tedesco, F. S. (2019). Combined Notch and PDGF Signaling Enhances Migration and Expression of Stem Cell Markers while Inducing Perivascular Cell Features in Muscle Satellite Cells. *Stem cell reports, 12*(3), 461-473

Goudenege, S., Lebel, C., Huot, N. B., Dufour, C., Fujii, I., Gekas, J., . . . Tremblay, J. P. (2012). Myoblasts derived from normal hESCs and dystrophic hiPSCs efficiently fuse with existing muscle fibers following transplantation. *Molecular therapy : the journal of the American Society of Gene Therapy, 20*(11), 2153-2167

Grady, R. M., Teng, H., Nichol, M. C., Cunningham, J. C., Wilkinson, R. S., & Sanes, J. R. (1997). Skeletal and Cardiac Myopathies in Mice Lacking Utrophin and Dystrophin: A Model for Duchenne Muscular Dystrophy. *Cell (Cambridge), 90*(4), 729-738

Gutpell, K. M., Hrinivich, W. T., & Hoffman, L. M. (2015). Skeletal muscle fibrosis in the mdx/utrn+/- mouse validates its suitability as a murine model of Duchenne muscular dystrophy. *PloS one, 10*(1), e0117306-e0117306

Gutpell, K. M., Tasevski, N., Wong, B., Hrinivich, W. T., Su, F., Hadway, J., . . . Hoffman, L. M. (2017). ANG1 treatment reduces muscle pathology and prevents a decline in perfusion in DMD mice. *PloS one, 12*(3), e0174315-e0174315

Ha, J. M., Jin, S. Y., Lee, H. S., Vafaeinik, F., Jung, Y. J., Keum, H. J., . . . Bae, S. S. (2019). Vascular leakage caused by loss of Akt1 is associated with impaired mural cell coverage. *FEBS open bio, 9*(4), 801-813

Hakanpaa, L., Sipila, T., Leppanen, V.-M., Gautam, P., Nurmi, H., Jacquemet, G., . . . Saharinen, P. (2015). Endothelial destabilization by angiopoietin-2 via integrin β1 activation. *Nature communications, 6*(1), 5962-5962

Hathout, Y., Liang, C., Ogundele, M., Xu, G., Tawalbeh, S. M., Dang, U. J., . . . McDonald, C. (2019). Disease-specific and glucocorticoid-responsive serum biomarkers for Duchenne Muscular Dystrophy. *Scientific reports, 9*(1), 12167-12167

Hoffman, E. P., Fischbeck, K. H., Brown, R. H., Johnson, M., Medori, R., Loire, J. D., . . . Kunkel, L. M. (1988). Characterization of Dystrophin in Muscle-Biopsy Specimens from Patients with Duchenne's or Becker's Muscular Dystrophy. *The New England journal of medicine, 318*(21), 1363-1368

Holash, J., Maisonpierre, P. C., Compton, D., Boland, P., Alexander, C. R., Zagzag, D., . . . Wiegand, S. J. (1999). Vessel Cooption, Regression, and Growth in Tumors Mediated by Angiopoietins and VEGF. *Science (American Association for the Advancement of Science), 284*(5422), 1994-1998

Hu, B., & Cheng, S.-Y. (2009). Angiopoietin-2: development of inhibitors for cancer therapy. *Current oncology reports, 11*(2), 111-116

Hughes, D. P., Marron, M. B., & Brindle, N. P. (2003). The antiinflammatory endothelial tyrosine kinase Tie2 interacts with a novel nuclear factor-kappaB inhibitor ABIN-2. *Circulation research, 92*(6), 630-636

Ieronimakis, N., Hays, A., Prasad, A., Janebodin, K., Duffield, J. S., & Reyes, M. (2016). PDGFRα signalling promotes fibrogenic responses in collagen-producing cells in Duchenne muscular dystrophy. *J Pathol, 240*(4), 410-424

Iivanainen, E., Nelimarkka, L., Elenius, V., Heikkinen, S.-M., Junttila, T. T., Sihombing, L., . . . Elenius, K. (2003). Angiopoietin-regulated recruitment of vascular smooth muscle cells by endothelial-derived heparin binding EGF-like growth factor. *The FASEB journal, 17*(12), 1609-1621

Ilaria, C., Lucia, N., Fabrizio, M., Guido, S., & Federico, B. (2005). Stable Interaction between α5β1 Integrin and Tie2 Tyrosine Kinase Receptor Regulates Endothelial Cell Response to Ang-1. *The Journal of cell biology, 170*(6), 993-1004

Inna, N. R., Jitandrakumar, R. P., & James, M. E. (2000). The Dystrophin Complex Forms a Mechanically Strong Link between the Sarcolemma and Costameric Actin. *The Journal of cell biology, 150*(5), 1209-1214

Ivan, B. L., Peter, C. B., & Richard, A. L. (2002). Angiopoietin-2 Displays VEGF-Dependent Modulation of Capillary Structure and Endothelial Cell Survival in vivo. *Proceedings of the National Academy of Sciences - PNAS, 99*(17), 11205-11210

Jeansson, M., Gawlik, A., Anderson, G., Li, C., Kerjaschki, D., Henkelman, M., & Quaggin, S. E. (2011). Angiopoietin-1 is essential in mouse vasculature during development and in response to injury. *The Journal of clinical investigation, 121*(6), 2278-2289

Jones, N., Chen, S. H., Sturk, C., Master, Z., Tran, J., Kerbel, R. S., & Dumont, D. J. (2003). A unique autophosphorylation site on Tie2/Tek mediates Dok-R phosphotyrosine binding domain binding and function. *Mol Cell Biol, 23*(8), 2658-2668

Kaese, S., Lukasz, A., Bietenbeck, M., Florian, A., Frommeyer, G., Boegeholz, N., . . . Yilmaz, A. (2017). 4102Relation between serum values of angiopoietin-2 and vascular endothelial growth factor with the degree of cardiomyopathy and skeletal myopathy in patients with muscular dystrophy. *European Heart Journal, 38*(suppl_1)

Kerr, B. A., West, X. Z., Kim, Y.-W., Zhao, Y., Tischenko, M., Cull, R. M., . . . Byzova, T. V. (2016). Stability and function of adult vasculature is sustained by Akt/Jagged1 signalling axis in endothelium. *Nature communications, 7*(1), 10960-10960

Kim, M., Allen, B., Korhonen, E. A., Nitschké, M., Yang, H. W., Baluk, P., . . . McDonald, D. M. (2016). Opposing actions of angiopoietin-2 on Tie2 signaling and FOXO1 activation. *J Clin Invest, 126*(9), 3511-3525

Kim, M. H., Kay, D. I., Rudra, R. T., Chen, B. M., Hsu, N., Izumiya, Y., . . . Crosbie, R. H. (2011). Myogenic Akt signaling attenuates muscular degeneration, promotes myofiber regeneration and improves muscle function in dystrophin-deficient mdx mice. *Hum Mol Genet, 20*(7), 1324-1338

Kobayashi, H., Debusk, L. M., Babichev, Y. O., Dumont, D. J., & Lin, P. C. (2006). Hepatocyte growth factor mediates angiopoietin-induced smooth muscle cell recruitment. *Blood, 108*(4), 1260-1266

Kobayashi, H., & Lin, P. C. (2005). Angiopoietin/Tie2 signaling, tumor angiogenesis and inflammatory diseases. *Front Biosci, 10*, 666-674

Kodama, T., Takakura, N., Minami, T., Sako, K., Koh, G. Y., Fukuhara, S., . . . Kim, H. Z. (2008). Differential function of Tie2 at cell-cell contacts and cell-substratum contacts regulated by angiopoietin-1. *Nature cell biology, 10*(5), 513-526

Korhonen, E. A., Lampinen, A., Giri, H., Anisimov, A., Kim, M., Allen, B., . . . Saharinen, P. (2016). Tie1 controls angiopoietin function in vascular remodeling and inflammation. *J Clin Invest, 126*(9), 3495-3510

Kostallari, E., Baba-Amer, Y., Alonso-Martin, S., Ngoh, P., Relaix, F., Lafuste, P., & Gherardi, R. K. (2015). Pericytes in the myovascular niche promote post-natal myofiber growth and satellite cell quiescence. *Development (Cambridge), 142*(7), 1242-1253

Kupatt, C., Windisch, A., Moretti, A., Wolf, E., Wurst, W., & Walter, M. C. (2021). Genome editing for Duchenne muscular dystrophy: a glimpse of the future? *Gene therapy*

Kyung-Tae, K., Han-Ho, C., Michel, O. S., Bohumil, M., Richard, A. K., So Young, A., . . . Gou Young, K. (2005). Oligomerization and Multimerization Are Critical for Angiopoietin-1 to Bind and Phosphorylate Tie2. *The Journal of biological chemistry, 280*(20), 20126-20131

Lane, S. W., Williams, D. A., & Watt, F. M. (2014). Modulating the stem cell niche for tissue regeneration. *Nature biotechnology, 32*(8), 795-803

Latroche, C., Matot, B., Martins-Bach, A., Briand, D., Chazaud, B., Wary, C., . . . Jouvion, G. (2015). Structural and Functional Alterations of Skeletal Muscle Microvasculature in Dystrophin-Deficient mdx Mice. *The American journal of pathology, 185*(9), 2482-2494

Latroche, C., Weiss-Gayet, M., Muller, L., Gitiaux, C., Leblanc, P., Liot, S., . . . Chazaud, B. (2017). Coupling between Myogenesis and Angiogenesis during Skeletal Muscle Regeneration Is Stimulated by Restorative Macrophages. *Stem cell reports, 9*(6), 2018-2033

Lee, H. J., Cho, C.-H., Hwang, S.-J., Choi, H.-H., Kim, K.-T., Ahn, S. Y., . . . Koh, G. Y. (2004). Biological characterization of angiopoietin-3 and angiopoietin-4. *The FASEB journal, 18*(11), 1200-1208

Lee, J., Kim, K. E., Choi, D.-K., Jang, J. Y., Jung, J.-J., Kiyonari, H., . . . Koh, G. Y. (2013). Angiopoietin-1 guides directional angiogenesis through integrin αvβ5 signaling for recovery of ischemic retinopathy. *Science translational medicine, 5*(203), 203ra127-203ra127

Lee, O. H., Xu, J., Fueyo, J., Alonso, M. M., Liu, D., Martin, V., . . . Gomez-Manzano, C. (2008). Angiopoietin-2 decreases vascular endothelial growth factor expression by modulating HIF-1α levels in gliomas. *Oncogene, 27*(9), 1310-1314

Lee, R. J., Springer, M. L., Blanco-Bose, W. E., Shaw, R., Ursell, P. C., & Blau, H. M. (2000). VEGF gene delivery to myocardium: deleterious effects of unregulated expression. *Circulation, 102*(8), 898-901

Liu, Y., Beyer, A., & Aebersold, R. (2016). On the Dependency of Cellular Protein Levels on mRNA Abundance. *Cell, 165*(3), 535-550

Loufrani, L., Matrougui, K., Gorny, D., Duriez, M., Blanc, I., Lévy, B. I., & Henrion, D. (2001). Flow (shear stress)-induced endothelium-dependent dilation is altered in mice lacking the gene encoding for dystrophin. *Circulation, 103*(6), 864-870

Mann, C. J., Perdiguero, E., Kharraz, Y., Aguilar, S., Pessina, P., Serrano, A. L., & Muñoz-Cánoves, P. (2011). Aberrant repair and fibrosis development in skeletal muscle. *Skeletal muscle, 1*(1), 21-21

McCarthy, M. J., Crowther, M., Bell, P. R., & Brindle, N. P. (1998). The endothelial receptor tyrosine kinase tie-1 is upregulated by hypoxia and vascular endothelial growth factor. *FEBS Lett, 423*(3), 334-338

McGreevy, J. W., Hakim, C. H., McIntosh, M. A., & Duan, D. (2015). Animal models of Duchenne muscular dystrophy: from basic mechanisms to gene therapy. *Disease models & mechanisms, 8*(3), 195-213

Mercuri, E. M. D., & Muntoni, F. P. (2013). Muscular dystrophies. *The Lancet (British edition), 381*(9869), 845-860

Messina, S., Mazzeo, A., Bitto, A., Aguennouz, M., Migliorato, A., De Pasquale, M. G., . . . Vita, G. (2007). VEGF overexpression via adeno-associated virus gene transfer promotes skeletal muscle regeneration and enhances muscle function in mdx mice. *Faseb j, 21*(13), 3737-3746

Metheny-Barlow, L. J., & Li, L. Y. (2003). The enigmatic role of angiopoietin-1 in tumor angiogenesis. *Cell research, 13*(5), 309-317

Miike, T., Sugino, S., Ohtani, Y., Taku, K., & Yoshioka, K. (1987). Vascular endothelial cell injury and platelet embolism in Duchenne muscular dystrophy at the preclinical stage. *J Neurol Sci, 82*(1-3), 67-80

Mikael, S., Bahman, C., Shannon, A. H., Susan, T. I., James, T. S., Gail, D. T., & Ronald, G. V. (2000). Functional Muscle Ischemia in Neuronal Nitric Oxide Synthase-Deficient Skeletal Muscle of Children with Duchenne Muscular Dystrophy. *Proceedings of the National Academy of Sciences - PNAS, 97*(25), 13818-13823

Miyatake, S., Shimizu-Motohashi, Y., Takeda, S. i., & Aoki, Y. (2016). Anti-inflammatory drugs for Duchenne muscular dystrophy: focus on skeletal muscle-releasing factors. *Drug design, development and therapy, 10*, 2745-2758

Mofarrahi, M., & Hussain, S. N. A. (2011). Expression and functional roles of angiopoietin-2 in skeletal muscles. *PloS one, 6*(7), e22882-e22882

Mueller, S. B., & Kontos, C. D. (2016). Tie1: an orphan receptor provides context for angiopoietin-2/Tie2 signaling. *The Journal of clinical investigation, 126*(9), 3188-3191

Namba, T., Koike, H., Murakami, K., Aoki, M., Makino, H., Hashiya, N., . . . Morishita, R. (2003). Angiogenesis induced by endothelial nitric oxide synthase gene through vascular endothelial growth factor expression in a rat hindlimb ischemia model. *Circulation, 108*(18), 2250-2257

Nayak, L., Lin, Z., & Jain, M. K. (2011). "Go With the Flow": How Krüppel-Like Factor 2 Regulates the Vasoprotective Effects of Shear Stress. *Antioxidants & redox signaling, 15*(5), 1449-1461

Nelson, M. D., Rader, F., Tang, X., Tavyev, J., Nelson, S. F., Miceli, M. C., . . . Victor, R. G. (2014). PDE5 inhibition alleviates functional muscle ischemia in boys with Duchenne muscular dystrophy. *Neurology, 82*(23), 2085-2091

Ngok, S. P., Geyer, R., Liu, M., Kourtidis, A., Agrawal, S., Wu, C., . . . Anastasiadis, P. Z. (2012). VEGF and Angiopoietin-1 exert opposing effects on cell junctions by regulating the Rho GEF Syx. *The Journal of cell biology, 199*(7), 1103-1115

Ong, T., McClintock, D. E., Kallet, R. H., Ware, L. B., Matthay, M. A., & Liu, K. D. (2010). Ratio of angiopoietin-2 to angiopoietin-1 as a predictor of mortality in acute lung injury patients. *Critical care medicine, 38*(9), 1845-1851

Palladino, M., Gatto, I., Neri, V., Straino, S., Smith, R. C., Silver, M., . . . Pola, R. (2013). Angiogenic Impairment of the Vascular Endothelium: A Novel Mechanism and Potential Therapeutic Target in Muscular Dystrophy. *Arteriosclerosis, thrombosis, and vascular biology, 33*(12), 2867-2876

Pang, D., Wang, L., Dong, J., Lai, X., Huang, Q., Milner, R., & Li, L. (2018). Integrin α5β1-Ang1/Tie2 receptor cross-talk regulates brain endothelial cell responses following cerebral ischemia. *Experimental & molecular medicine, 50*(9), 1-12

Park, S. W., Yun, J. H., Kim, J. H., Kim, K. W., Cho, C. H., & Kim, J. H. (2014). Angiopoietin 2 induces pericyte apoptosis via α3β1 integrin signaling in diabetic retinopathy. *Diabetes, 63*(9), 3057-3068

Passamano, L., Taglia, A., Palladino, A., Viggiano, E., D'Ambrosio, P., Scutifero, M., . . . Politano, L. (2012). Improvement of survival in Duchenne Muscular Dystrophy: retrospective analysis of 835 patients. *Acta myologica : myopathies and cardiomyopathies : official journal of the Mediterranean Society of Myology, 31*(2), 121-125

Peter, A. K., & Crosbie, R. H. (2006). Hypertrophic response of Duchenne and limb-girdle muscular dystrophies is associated with activation of Akt pathway. *Experimental Cell Research, 312*(13), 2580-2591

Peter, C. M., Chitra, S., Pamela, F. J., Sona, B., Stanley, J. W., Czeslaw, R., . . . George, D. Y. (1997). Angiopoietin-2, a Natural Antagonist for Tie2 that Disrupts In vivo Angiogenesis. *Science (American Association for the Advancement of Science), 277*(5322), 55-60

Podkalicka, P., Mucha, O., Dulak, J., & Loboda, A. (2019). Targeting angiogenesis in Duchenne muscular dystrophy. *Cellular and molecular life sciences : CMLS, 76*(8), 1507-1528

Porter, J. D., Khanna, S., Kaminski, H. J., Rao, J. S., Merriam, A. P., Richmonds, C. R., . . . Andrade, F. H. (2002). A chronic inflammatory response dominates the skeletal muscle molecular signature in dystrophin-deficient mdx mice. *Hum Mol Genet, 11*(3), 263-272

Rafael, J. A., Tinsley, J. M., Potter, A. C., Deconinck, A. E., & Davies, K. E. (1998). Skeletal muscle-specific expression of a utrophin transgene rescues utrophin-dystrophin deficient mice. *Nat Genet, 19*(1), 79-82

Ramsauer, M., & D'Amore, P. A. (2007). Contextual role for angiopoietins and TGFbeta1 in blood vessel stabilization. *J Cell Sci, 120*(Pt 10), 1810-1817

Rhoads, R. P., Flann, K. L., Cardinal, T. R., Rathbone, C. R., Liu, X., & Allen, R. E. (2013). Satellite cells isolated from aged or dystrophic muscle exhibit a reduced capacity to promote angiogenesis in vitro. *Biochem Biophys Res Commun, 440*(3), 399-404

Rockey, D. C., Bell, P. D., & Hill, J. A. (2015). Fibrosis — A Common Pathway to Organ Injury and Failure. *The New England journal of medicine, 372*(12), 1138-1149

Saito, M., Hamasaki, M., & Shibuya, M. (2003). Induction of tube formation by angiopoietin-1 in endothelial cell/fibroblast co-culture is dependent on endogenous VEGF. *Cancer science, 94*(9), 782-790

Savant, S., La Porta, S., Budnik, A., Busch, K., Hu, J., Tisch, N., . . . Augustin, Hellmut G. (2015). The Orphan Receptor Tie1 Controls Angiogenesis and Vascular Remodeling by Differentially Regulating Tie2 in Tip and Stalk Cells. *Cell Reports, 12*(11), 1761-1773

Scharpfenecker, M., Fiedler, U., Reiss, Y., & Augustin, H. G. (2005). The Tie-2 ligand angiopoietin-2 destabilizes quiescent endothelium through an internal autocrine loop mechanism. *J Cell Sci, 118*(Pt 4), 771-780

Schnurch, H., & Risau, W. (1993). Expression of tie-2, a member of a novel family of receptor tyrosine kinases, in the endothelial cell lineage. *Development (Cambridge), 119*(3), 957-968

Scholz, A., Lang, V., Henschler, R., Czabanka, M., Vajkoczy, P., Chavakis, E., . . . Reiss, Y. (2011). Angiopoietin-2 promotes myeloid cell infiltration in a β_2-integrin-dependent manner. *Blood, 118*(18), 5050-5059

Seegar, T. C. M., Eller, B., Tzvetkova-Robev, D., Kolev, M. V., Henderson, S. C., Nikolov, D. B., & Barton, W. A. (2010). Tie1-Tie2 Interactions Mediate Functional Differences between Angiopoietin Ligands. *Molecular cell, 37*(5), 643-655

Shepro, D., & Morel, N. M. (1993). Pericyte physiology. *Faseb j, 7*(11), 1031-1038

Shiao, T., Fond, A., Deng, B., Wehling-Henricks, M., Adams, M. E., Froehner, S. C., & Tidball, J. G. (2004). Defects in neuromuscular junction structure in dystrophic muscle are corrected by expression of a NOS transgene in dystrophin-deficient muscles, but not in muscles lacking alpha- and beta1-syntrophins. *Hum Mol Genet, 13*(17), 1873-1884

Shimizu-Motohashi, Y., & Asakura, A. (2014). Angiogenesis as a novel therapeutic strategy for Duchenne muscular dystrophy through decreased ischemia and increased satellite cells. *Frontiers in physiology, 5*, 50-50

Shiojima, I., & Walsh, K. (2002). Role of Akt Signaling in Vascular Homeostasis and Angiogenesis. *Circulation research, 90*(12), 1243-1250

Si, Y., Huang, J., Li, X., Fu, Y., Xu, R., Du, Y., . . . Jiang, H. (2020). AKT/FOXO1 axis links cross-talking of endothelial cell and pericyte in TIE2-mutated venous malformations. *Cell communication and signaling, 18*(1), 139-139

Somanath, P. R., Razorenova, O. V., Chen, J., & Byzova, T. V. (2006). Akt1 in Endothelial Cell and Angiogenesis. *Cell cycle (Georgetown, Tex.), 5*(5), 512-518

Springer, M. L., Chen, A. S., Kraft, P. E., Bednarski, M., & Blau, H. M. (1998). VEGF Gene Delivery to Muscle: Potential Role for Vasculogenesis in Adults. *Molecular cell, 2*(5), 549-558

Stedman, H. H., Petrof, B., Leferovich, J. M., Kelly, A. M., Narusawa, M., Sladky, J. T., . . . Sweeney, H. L. (1991). The mdx mouse diaphragm reproduces the degenerative changes of Duchenne muscular dystrophy. *Nature (London), 352*(6335), 536-539

Straino, S., Germani, A., Di Carlo, A., Porcelli, D., De Mori, R., Mangoni, A., . . . Capogrossi, M. C. (2004). Enhanced arteriogenesis and wound repair in dystrophin-deficient mdx mice. *Circulation, 110*(21), 3341-3348

Stratman, A. N., Schwindt, A. E., Malotte, K. M., & Davis, G. E. (2010). Endothelial-derived PDGF-BB and HB-EGF coordinately regulate pericyte recruitment during vasculogenic tube assembly and stabilization. *Blood, 116*(22), 4720-4730

Stuppia, L., Antonucci, I., Palka, G., & Gatta, V. (2012). Use of the MLPA assay in the molecular diagnosis of gene copy number alterations in human genetic diseases. *International journal of molecular sciences, 13*(3), 3245-3276

Tabruyn, S. P., Colton, K., Morisada, T., Fuxe, J., Wiegand, S. J., Thurston, G., . . . McDonald, D. M. (2010). Angiopoietin-2-Driven Vascular Remodeling in Airway Inflammation. *The American journal of pathology, 177*(6), 3233-3244

Tadros, A., Hughes, D. P., Dunmore, B. J., & Brindle, N. P. J. (2003). ABIN-2 protects endothelial cells from death and has a role in the antiapoptotic effect of angiopoietin-1. *Blood, 102*(13), 4407-4409

Teichert, M., Milde, L., Holm, A., Stanicek, L., Gengenbacher, N., Savant, S., . . . Augustin, H. G. (2017). Pericyte-expressed Tie2 controls angiogenesis and vessel maturation. *Nature communications, 8*(1), 16106-16106

Tidball, J. G., & Wehling-Henricks, M. (2014). Nitric oxide synthase deficiency and the pathophysiology of muscular dystrophy. *J Physiol, 592*(21), 4627-4638

Tuffery-Giraud, S., Béroud, C., Leturcq, F., Yaou, R. B., Hamroun, D., Michel-Calemard, L., . . . Claustres, M. (2009). Genotype–phenotype analysis in 2,405 patients with a dystrophinopathy using the UMD–DMD database: a model of nationwide knowledgebase. *Hum Mutat, 30*(6), 934-945

Ugarte, G., Cappellari, O., Perani, L., Pistocchi, A., & Cossu, G. (2012). Noggin recruits mesoderm progenitors from the dorsal aorta to a skeletal myogenic fate. *Developmental biology, 365*(1), 91-100

Wang, Q., & Lash, G. E. (2017). Angiopoietin 2 in placentation and tumor biology: The yin and yang of vascular biology. *Placenta (Eastbourne), 56*, 73-78

Wehling, M., Spencer, M. J., & Tidball, J. G. (2001). A nitric oxide synthase transgene ameliorates muscular dystrophy in mdx mice. *The Journal of cell biology, 155*(1), 123-131

Whitehead, M., Osborne, A., Widdowson, P. S., Yu-Wai-Man, P., & Martin, K. R. (2019). Angiopoietins in Diabetic Retinopathy: Current Understanding and Therapeutic Potential. *Journal of diabetes research, 2019*, 1-9

Wong, A. L., Haroon, Z. A., Werner, S., Dewhirst, M. W., Greenberg, C. S., & Peters, K. G. (1997). Tie2 Expression and Phosphorylation in Angiogenic and Quiescent Adult Tissues. *Circulation research, 81*(4), 567-574

Xu, M., Xu, H.-H., Lin, Y., Sun, X., Wang, L.-J., Fang, Z.-P., . . . Zhou, W.-J. (2019). LECT2, a Ligand for Tie1, Plays a Crucial Role in Liver Fibrogenesis. *Cell (Cambridge), 178*(6), 1478-1492.e1420

Yamazaki, T., & Mukouyama, Y.-S. (2018). Tissue Specific Origin, Development, and Pathological Perspectives of Pericytes. *Frontiers in cardiovascular medicine, 5*, 78-78

Yamazaki, T., Nalbandian, A., Uchida, Y., Li, W., Arnold, T. D., Kubota, Y., . . . Mukouyama, Y.-s. (2017). Tissue Myeloid Progenitors Differentiate into Pericytes through TGF-β Signaling in Developing Skin Vasculature. *Cell reports (Cambridge), 18*(12), 2991-3004

Yang, P., Chen, N., Yang, D., Crane, J., Yang, S., Wang, H., . . . Wang, Z. (2017). The ratio of serum Angiopoietin-1 to Angiopoietin-2 in patients with cervical cancer is a valuable diagnostic and prognostic biomarker. *PeerJ (San Francisco, CA), 5*, e3387-e3387

Yeboah, K., Agyekum, J. A., Baafour, E. K., Antwi, D. A., Adjei, A. B., Boima, V., & Gyan, B. (2017). Circulating Angiogenic Growth Factors in Diabetes Patients with Peripheral Arterial Disease and Exertional Leg Pain in Ghana. *International journal of vascular medicine, 2017*, 2390174-2390177

Yeo, T. W., Lampah, D. A., Gitawati, R., Tjitra, E., Kenangalem, E., Piera, K., . . . Anstey, N. M. (2008). Angiopoietin-2 is associated with decreased endothelial nitric oxide and poor clinical outcome in severe falciparum malaria. *Proc Natl Acad Sci U S A, 105*(44), 17097-17102

Yin, H., Price, F., & Rudnicki, M. A. (2013). Satellite cells and the muscle stem cell niche. *Physiological Reviews, 93*(1), 23-67

Yiu, E. M., & Kornberg, A. J. (2015). Duchenne muscular dystrophy. *Journal of paediatrics and child health, 51*(8), 759-764

Yoshida, Y., Kabara, M., Kano, K., Horiuchi, K., Hayasaka, T., Tomita, Y., . . . Kawabe, J. I. (2020). Capillary-resident EphA7(+) pericytes are multipotent cells with anti-ischemic effects through capillary formation. *Stem Cells Transl Med, 9*(1), 120-130

Youn, S.-W., Lee, H.-C., Lee, S.-W., Lee, J., Jang, H., Lee, E. J., & Kim, H.-S. (2018). COMP-Angiopoietin-1 accelerates muscle regeneration through N-cadherin activation. *Scientific reports, 8*(1), 12323-12323

Young Koh, G., Augustin, H. G., Thurston, G., & Alitalo, K. (2009). Control of vascular morphogenesis and homeostasis through the angiopoietin-Tie system. *Nature reviews. Molecular cell biology, 10*(3), 165-177

Yuan, H. T., Khankin, E. V., Karumanchi, S. A., & Parikh, S. M. (2009). Angiopoietin 2 Is a Partial Agonist/Antagonist of Tie2 Signaling in the Endothelium. *Molecular and cellular biology, 29*(12), 3451-3451

Yun, J. H., Park, S. W., Kim, J. H., Park, Y. J., Cho, C. H., & Kim, J. H. (2016). Angiopoietin 2 induces astrocyte apoptosis via αvβ5-integrin signaling in diabetic retinopathy. *Cell Death & Disease, 7*(2), e2101-e2101

Zellweger, H., & Antonik, A. (1975). Newborn screening for Duchenne muscular dystrophy. *Pediatrics, 55*(1), 30-34

Zhang, J., Fukuhara, S., Sako, K., Takenouchi, T., Kitani, H., Kume, T., . . . Mochizuki, N. (2011). Angiopoietin-1/Tie2 Signal Augments Basal Notch Signal Controlling Vascular Quiescence by Inducing Delta-Like 4 Expression through AKT-mediated Activation of β-Catenin. *The Journal of biological chemistry, 286*(10), 8055-8066

Zhang, Y., Kontos, C. D., Annex, B. H., & Popel, A. S. (2019). Angiopoietin-Tie Signaling Pathway in Endothelial Cells: A Computational Model. *iScience*, *20*, 497-511

Zhang, Y., Li, H., Min, Y.-L., Sanchez-Ortiz, E., Huang, J., Mireault, A. A., . . . Olson, E. N. (2020). Enhanced CRISPR-Cas9 correction of Duchenne muscular dystrophy in mice by a self-complementary AAV delivery system. *Science advances*, *6*(8), eaay6812-eaay6812

Zhao, X., & Guan, J.-L. (2011). Focal adhesion kinase and its signaling pathways in cell migration and angiogenesis. *Advanced drug delivery reviews*, *63*(8), 610-615

Appendices

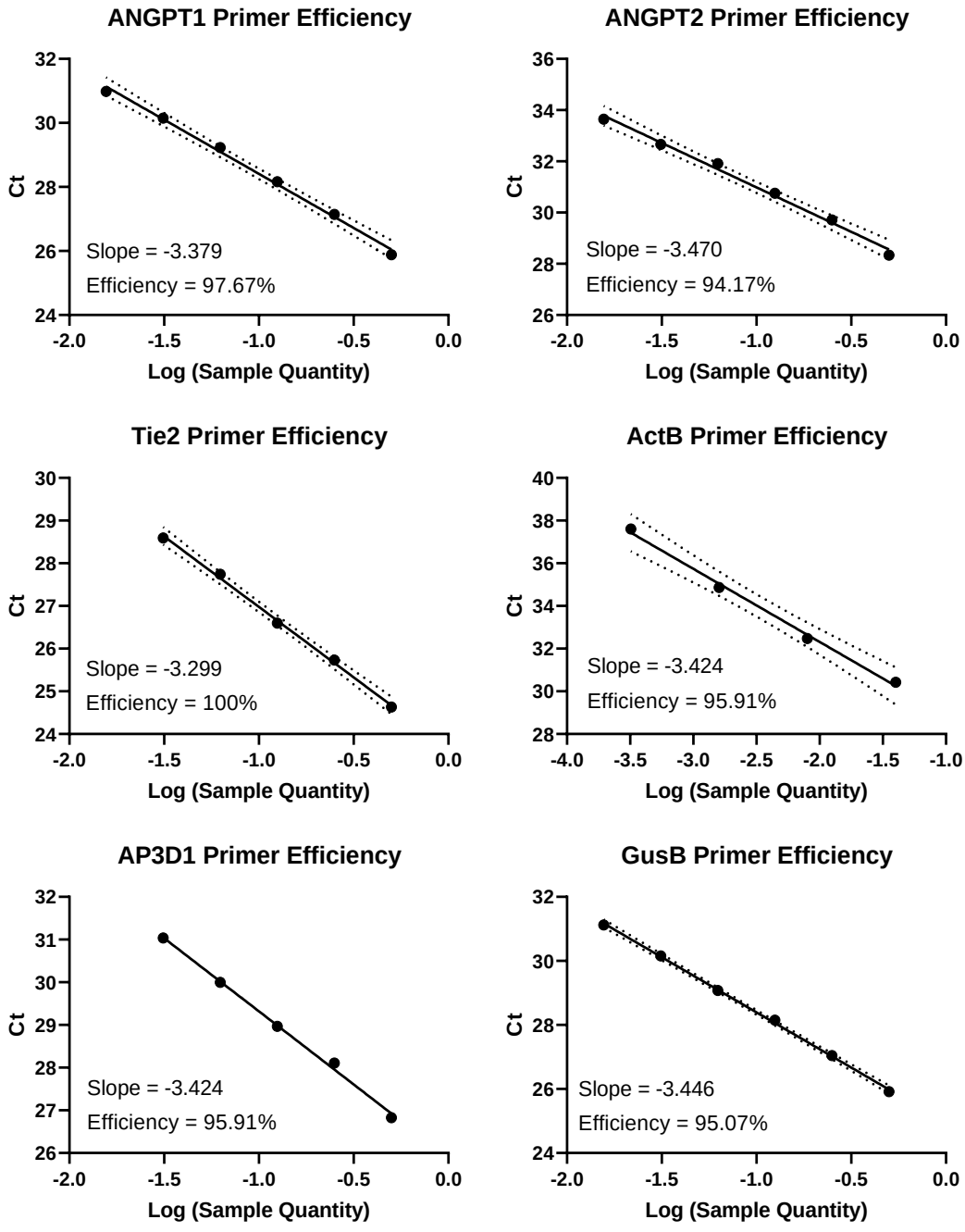

Appendix A: Primer Efficiency Validation.

Validation of primer efficiency for ANGPT1, ANGPT2, Tie2, ActB, AP3D1, and GusB.

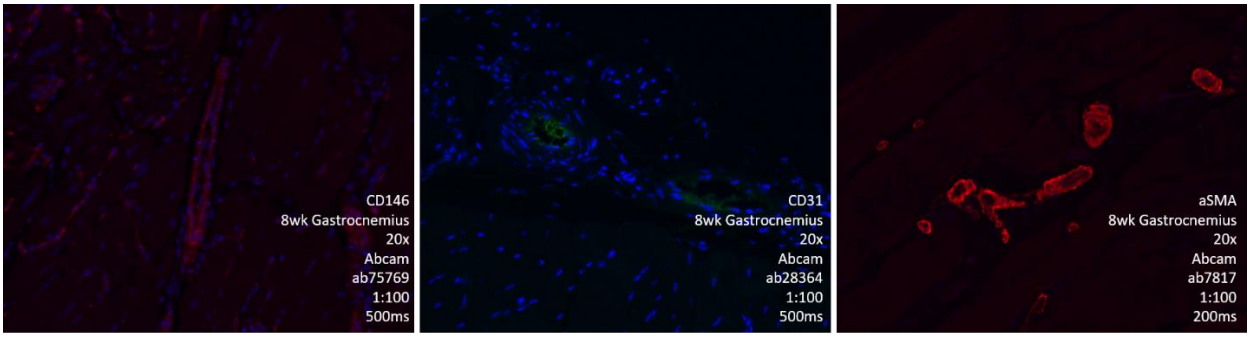

Appendix B: Immunofluorescence stain of endothelial cell marker and pericyte markers.

Paraffin sections were deparaffinized and rehydrated through a series of xylene and ethanol washes and ultimately PBS. Antigen retrieval was performed using Retriever 2100 (EMS). Sections were then rinsed with ddH2O and blocked via incubation with Background Sniper Blocking Reagent (Biocare Medical) for exactly 8 minutes. Sections were then incubated with CD31 (Abcam, ab28364, 1:100), CD146 (Abcam, ab75769, 1:100), and αSMA (Abcam, ab7817, 1:200) in 1% BSA PBS overnight at 4°C. After washes, slides were incubated with Goat Anti-Mouse (Alexa Fluro 647)(Abcam, ab150115, 1:500) or Donkey Anti-Rabbit (Alexa Fluro 647)(Abcam, ab150075, 1:500), or Goat Anti-Rabbit (Alexa Fluro 488)(Abcam, ab150077, 1:500) in 1% BSA PBS for 2 hours at room temperature. Tissue sections were then washed with PBS, treated with 100ul of Sudan Black for two minutes, and briefly rinsed with ethanol and PBS. Coverslips were mounted with gold anti-fade with DAPI (Life Technologies). Nail polish was ultimately used to seal the edges of the coverslip and allowed to dry for 15 minutes and stored at 4°C.

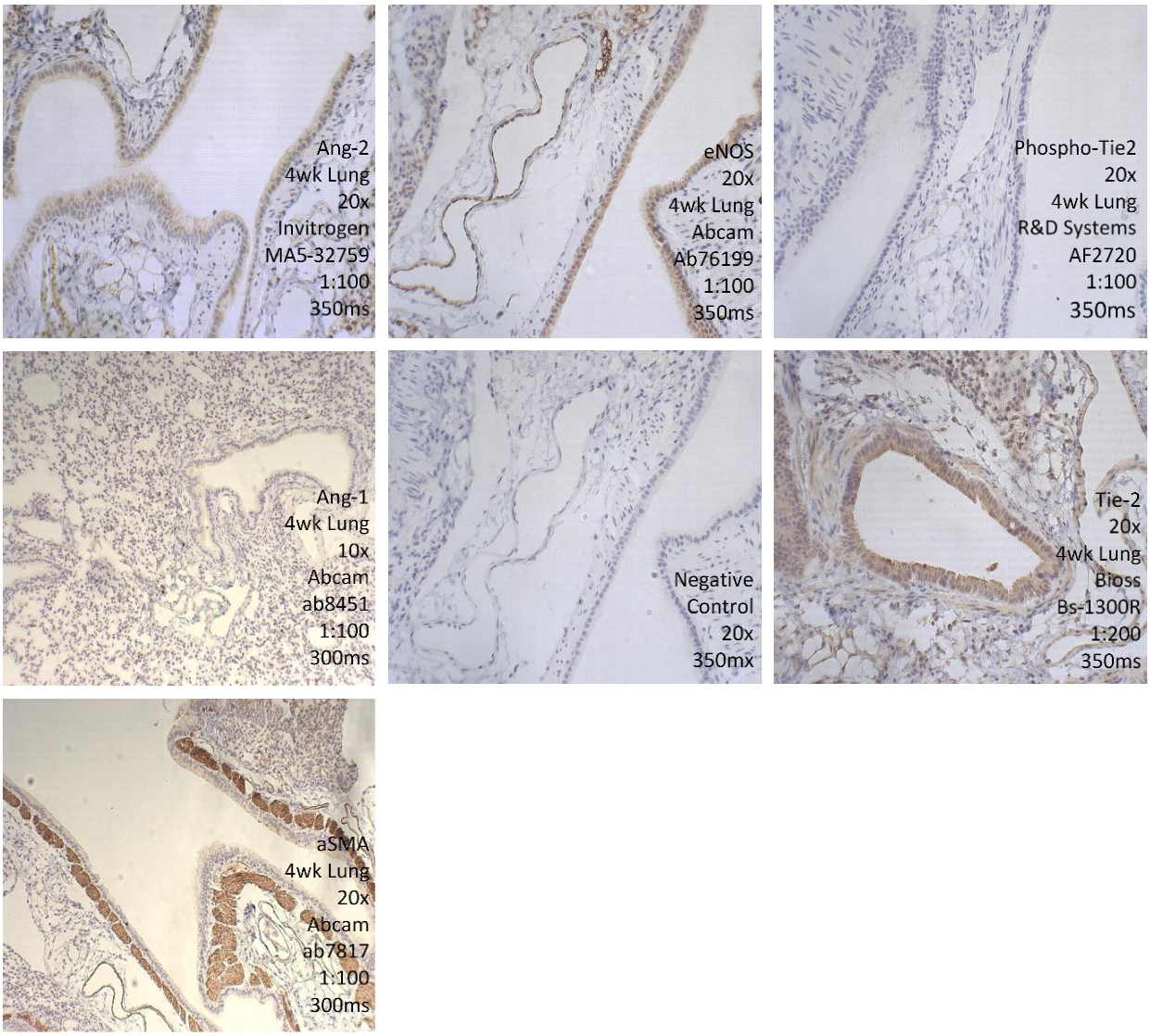

Appendix C: Immunohistochemical DAB substrate staining of paraffin-embedded 4-week-old WT Lung.

Tissue sections were deparaffinized and rehydrated via a series of xylene and ethanol washes and then washed with phosphate buffered saline (PBS) prior to antigen retrieval. Antigen retrieval was performed in citrate buffer with 0.5% Tween at 95°C for 20 minutes and allowed to cool at room temperature afterward. The citrate buffer was exchanged with PBS gradually during the cooling process. Tissue sections were placed in 3% H2O2 to inhibit endogenous peroxidase. Tissue sections were then incubated with Background Sniper Blocking Reagent (Biocare Medical) for exactly 8 minutes to prevent non-specific antibody binding. Tissue sections, excluding negative controls, were then incubated overnight at 4°C

with either Ang-1 (Abcam, ab8451, 1:100), Ang-2 (Invitrogen, PA5-27297, 1:100), Tie2 (Abcam, ab218051, 1:50), phospho-Tie2 (Y992)(R&D Systems, AF2720, 1:100), phospho-eNOS (Ser1177)(MyBioSource, MBS9601018, 1:100), PDGFRβ (Abcam, ab69506, 1:200), αSMA (Abcam, ab7817, 1:200), and NG2 (Abcam, ab129051, 1:100) in 1% BSA PBS. Tissue sections were washed with PBS the next day and incubated with biotinylated horse anti-mouse and biotinylated horse anti-rabbit secondaries for four hours. They were then incubated in streptavidin for one hour and followed by a DAB substrate kit (Abcam). Carazzi's hematoxylin was used to stain the nuclei. Ultimately, they were dehydrated and coverslip mounted using DAPI Prolong Gold.

a)

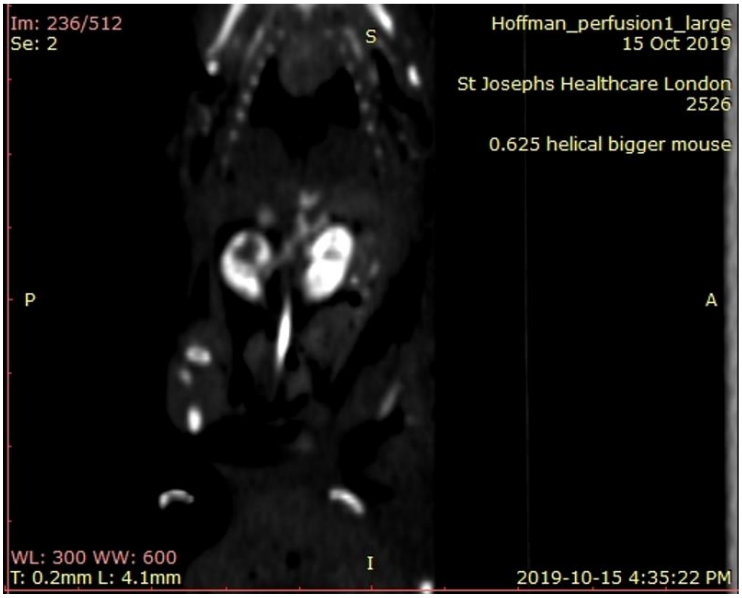

b)

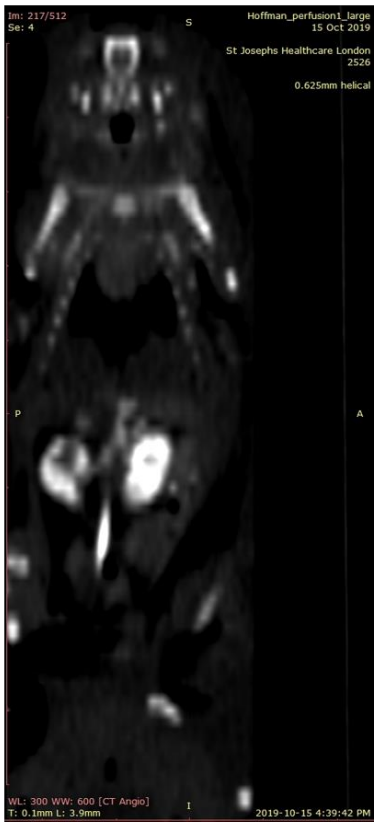

Appendix D: Ex vivo micro-CT with AlumHemFeI stain

Mice were sacrificed via gas euthanasia prior to tissue collection. Diaphragm and gastrocnemius (GM) muscles from the mice models were dissected and immediately fixed in formalin for 5 days. Samples were placed in 0.3% Triton X at room temperature for a 24-hour soak. Samples were then scanned on the scanner GR eXplore Locus scanner (20um) for pre-scan images. Samples were then placed into an AlumHemFeI stain or Eribium stain for 5 days and a final scan on GE eXplore Locus scanner (20um).

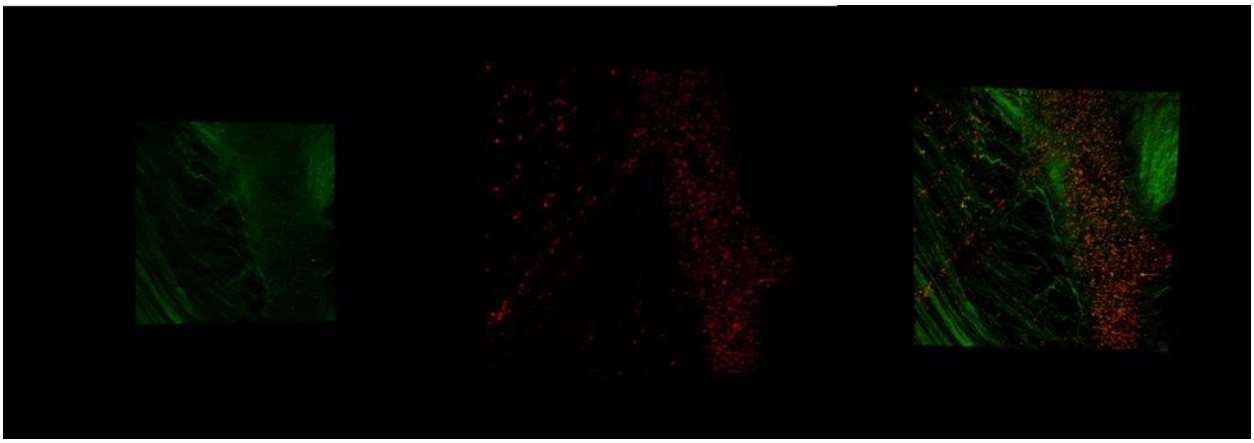

Appendix E: *Ex vivo* Multiphoton Microscopy

50µL of 2-5 µg of Alexa Fluro 647 anti-mouse CD31 (Red)(Biolegend, 102515) and Alexa Fluro 488 Anti-NG2 (Green)(Sigma-Aldrich, MAB5384A4) were intravenous injected via the tail vein into mdx mice. The antibodies were allowed to circulate for 15 minutes. Mice were then euthanized via gas-anesthesia and perfused with 4% paraformaldehyde and flushed with PBS. The diaphragm was extracted and placed into ice-cold PBS, onto an imaging apparatus, and imaged.

Curriculum Vitae

Yiming Lin

Education

Master of Science 2018-2021
Pathology and Laboratory Medicine
Schulich School of Medicine and Dentistry
Western University, London, ON

Bachelor of Medical Science 2014-2018
Honours Specialization in Microbiology and Immunology
Schulich School of Medicine and Dentistry
Western University, London, ON

Teaching and Mentoring

Mentor 2019 – 2020
Western Pathology Association
Western University, London, ON

Teaching Assistant September – December 2019
2500A Biology of Infection and Immunity
Western University, London, ON

Teaching Assistant September – December 2018
1033 Introduction to Multimedia and Communications
Western University, London, ON

Teaching Assistant Training Program August 2018
Western University, London, ON

Scholarships/Awards

Dr. Frederick Winnett Luney Graduate Scholarship
2020
Schulich School of Medicine and Dentistry
Western University London, London, ON

CHRI Trainee Scholarship 2019
2019
Lawson Health Research Institute
St. Joseph Health Care London, London, ON

Lawson Internal Research Fund Studentship Award 2019
2019
Lawson Health Research Institute
St. Joseph Health Care London, London, ON

Deans Honor List 2015-2018
Schulich School of Medicine and Dentistry
Western University, London, ON

Abstracts and Presentations

Lin Y, McClennan A, Hoffman LM. Characterization of Microvasculature Duchenne Muscular Dystrophy. Virtual Poster presented at the Canadian Bone & Joint Conference 2020; 2020 June 11-13; Virtual 2020

Lin Y, McClennan A, Hoffman LM. CT- based Characterization of Microvasculature Duchenne Muscular Dystrophy. Poster presented at the World Molecular Imaging Conference 2019; 2019 September 3-6; Montreal QC 2019

Lin Y, Kashyap N, Hakim S, McClennan A, Hoffman LM. Characterization of microvasculature in Duchenne Muscular Dystrophy. Poster presented at the 2019 Canadian Connective Tissue Conference 2019; 2019 May 29-31; Montreal QC 2019

Lin Y, Kashyap N, Hakim S, McClennan A, Hoffman LM. Characterization of microvasculature in Duchenne Muscular Dystrophy. Poster presented at the 019 Child Health Research Day; 2019 May 21; London ON 2019

Lin Y, Kashyap N, Hakim S, McClennan A, Hoffman 2019

LM. Characterization of microvasculature in Duchenne Muscular Dystrophy. Poster presented at the 2019 London Health Research Day; 2019 April 30; London ON

Lin Y, Kashyap N, Hakim S, McClennan A, Hoffman LM. Characterization of microvasculature in Duchenne Muscular Dystrophy. Poster presented at the 2019 PaLM Pathology Research Day; 2019 March 28; London ON 2019